TELOMERES AND THEIR ASSOCIATED FACTORS

IN *Arabidopsis thaliana*

A Dissertation

by

RACHEL A. IDOL

Submitted to the Office of Graduate Studies of
Texas A&M University
in partial fulfillment of the requirements for the degree of

DOCTOR OF PHILOSOPHY

August 2005

Major Subject: Biochemistry

TELOMERES AND THEIR ASSOCIATED FACTORS

IN *Arabidopsis thaliana*

A Dissertation

by

RACHEL A. IDOL

Submitted to the Office of Graduate Studies of
Texas A&M University
in partial fulfillment of the requirements for the degree of

DOCTOR OF PHILOSOPHY

Approved by:

Chair of Committee,	Dorothy E. Shippen
Committee Members,	James C. Hu
	Michael Polymenis
	Z. Jeffrey Chen
Head of Department,	Gregory D. Reinhart

August 2005

Major Subject: Biochemistry

ABSTRACT

Telomeres and Their Associated Factors in *Arabidopsis thaliana*. (August 2005)

Rachel A. Idol, B.S., Kansas State University

Chair of Advisory Committee: Dr. Dorothy E. Shippen

Telomeres are important protein-DNA structures at the ends of linear eukaryotic chromosomes that are necessary for genome integrity. Telomeres are maintained by intermittent action of telomerase. I explored the kinetics of telomere length homeostasis in the model plant *Arabidopsis thaliana* by crossing wild type plants to different generations of telomerase deficient plants, and then analyzing telomere length in the resulting progeny. Unexpectedly, I found plants lacking telomerase for seven generations can lengthen telomeres when telomerase is reintroduced, but one generation is not sufficient to reestablish the telomere set point.

Est1 is a non-catalytic component of the *Saccharomyces cerevisiae* *t*elomerase holoenzyme. To investigate the role of Est1 in higher eukaryotes, I identified two putative Est1 homologues in *Arabidopsis*, *AtEST1a* and *AtEST1b*. Plants deficient in *AtEST1a* displayed no vegetative or reproductive defects. However, plants deficient for *AtEST1b* were sterile and had severe vegetative and reproductive irregularities. Surprisingly, no defects in telomere maintenance were observed in any single or double mutant line. This suggests that the Est1-like proteins in plants have evolved new functions outside of telomere length maintenance and end protection.

One consequence of telomere dysfunction is end-to-end chromosome fusion. In mammals, telomere fusion is mediated through NHEJ and requires DNA Ligase IV (Lig4). Lig4 is an essential component of the NHEJ pathway along with the Ku70/Ku80 heterodimer and DNA-PK_{cs}. To address the mechanism of chromosome fusion in *Arabidopsis*, we investigated the role of Lig4 in mutant combinations lacking *TERT,* the catalytic subunit of telomerase, and Ku70. Surprisingly, telomere end-to-end fusions were observed in *ku70 tert lig4* triple mutants, suggesting that neither Lig4 nor Ku70 are required for the fusion of critically shortened telomeres in *Arabidopsis*. To investigate the origin of genome instability, terminal restriction fragment analysis was performed on triple mutants. Strikingly, telomeres diminished five to six-fold faster than in a *tert* single mutant. Moreover, in the triple mutants, telomere tracts were extremely heterogeneous, suggesting that the telomeres were exposed to catastophic nucleolytic attack. These data provide the first evidence that Lig4 contributes to telomere maintenance and chromosome end protection.

DEDICATION

I would like to extend my thanks to the following people: to my parents, whose constant love and support have allowed me to follow my dreams. Without this support I would not have been able to reach these dreams, and turn them into reality. To my friends, especially the incoming class of 1999, for all of the support and laughter you have brought into my life. I am extremely grateful for all you have done, thank you.

ACKNOWLEDGMENTS

First, I would like to thank Dr. Dorothy Shippen for all of her advice and support during my time in her lab. Her help and advice have allowed me to develop not only as a young scientist, but also as a member of a larger scientific community. She has also taught me how to critically analyze data and ask interesting questions. Her unwavering support both at work and in my personal life has encouraged me to always do my best. I am also thankful to Dr. Tom McKnight and Dr. Geoffrey Kapler for their suggestions, discussions and advice in our weekly lab meetings. Their guidance has helped me develop my projects and inspired me to do many of the experiments described here.

I also want to acknowledge Dr. Karel Riha for his numerous contributions to my work and development as a scientist. I learned everything I know about plant care and handling from him. He taught me how to design an experiment and think ahead to the next step. He always took time from his busy schedule to talk with me and think critically about my research. I know that the talks I had with him made a huge impact on how I do and look at science.

In addition, I want to acknowledge and thank the former and current members of the Shippen laboratory. Dr. Libin Wang helped me a great deal in my first years in the lab and taught me how to improve on lab protocols. Dr. Elizabeth Spangler, Dr. Eugene V. Shakirov, Dr. Laurent Vespa, and Dr. Zemfira Karamysheva provided a great deal of professional and technical advice in addition to help with experiments. I am also grateful to Jennifer Bullock, J. Matt

Watson, Michelle Heacock, Kalpana Kannan and Yulia Surovtseva for their valuable advice and input.

TABLE OF CONTENTS

CHAPTER Page

LIST OF FIGURES

LIST OF TABLES

CHAPTER I

INTRODUCTION

Telomeres are nucleic acid-protein complexes comprised of repeated DNA sequences and their associated proteins. These complexes cap the physical ends of eukaryotic chromosomes and are necessary for chromosomal stability and continued cell proliferation. Chromosomes lacking telomeres are detected as double strand breaks and result in activation of DNA damage checkpoints and cell cycle arrest.

The telomeric DNA sequence is specific for each organism, TTAGGG in vertebrates, TTTAGGG in plants, and $(TG)_{1-6}TG_{2-3}$ in *S. cerevisiae* (1). Telomere length is also species-specific. In budding yeast, telomeres are ~300bp, while in mammals telomeres range from 10-150kb. In the model plant *Arabidopsis thaliana,* telomeres span 2-8kb (2-4). Regardless of repeat sequence or length, all telomeres consist of a long double stranded region with a short single-stranded 3' overhang (Fig. 1). The double-stranded portion of the telomere is composed of a G-rich strand running 5'-3' towards the end of the chromosome, and a complementary C-rich strand which is shorter than the G-rich strand. The protrusion of the G-rich strand creates a single-stranded 3' overhang, or G-overhang at telomere ends.

Similar to the telomere length variation observed between organisms, the

---

This dissertation follows the style of *Proceedings of the National Academy of Science, USA.*

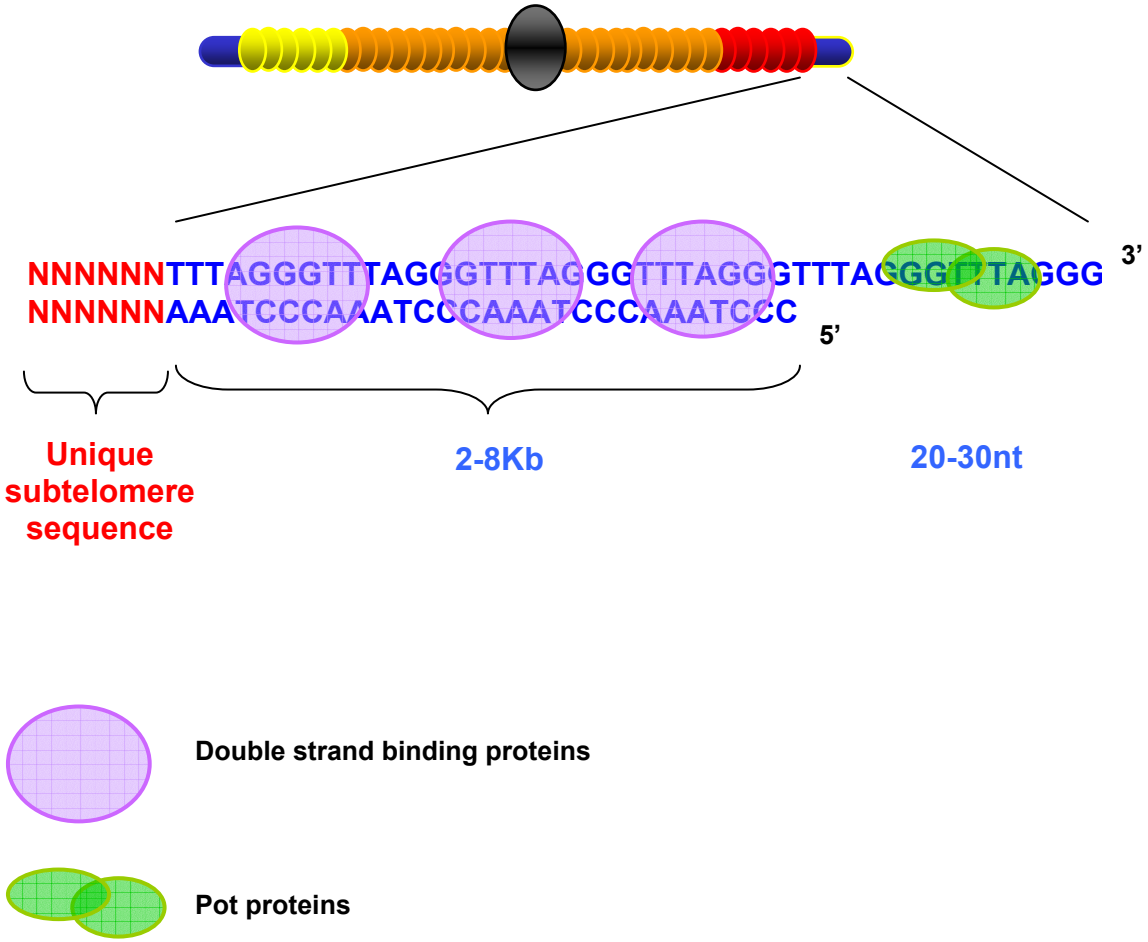

Fig. 1. The structure of telomeres in *Arabidopsis*. Putative double (purple) and single (green) stranded telomeric DNA binding proteins are shown.

of the G-overhang also varies. In the ciliate *Euplotes crassus*, G-overhangs are 14nt long, in humans 150nt in length, and in *Arabidopsis* a 25-30nt 3' overhang is present (5-7). The G-overhang is an essential feature of the telomere, as its loss is associated with end-to-end chromosome fusions (8). In humans, plants, ciliates and trypanosomes, the single-stranded region of the telomere loops back into the double-stranded portion, creating a structure called the t-loop, which is believed to help protect the telomere end *in vivo* (9-12). Although t-loops have only been found in a few organisms, it is probable that t-loops or similar structures are present at the telomeres in most organisms.

In wild type cells, telomere shortening is thought to occur primarily as a result of incomplete replication of the chromosome end due to the semi-conservative nature of DNA synthesis. Conventional DNA polymerases synthesize DNA in the 5' to 3' direction using a short RNA primer to initiate replication (Fig. 2). Removal of the most 5' RNA primer by the lagging strand machinery creates a short single-strand region that cannot be filled in by the conventional replication machinery. Failure to fill this gap leads to a small loss of DNA in each round of replication, and is known as the "end-replication problem" (13, 14). Telomere shortening is circumvented by telomerase, a unique DNA polymerase with reverse transcriptase activity (15).

TELOMERASE

Telomerase elongates the G-rich strand of the chromosome end by using a region within its integral RNA subunit as a template for the telomeric DNA

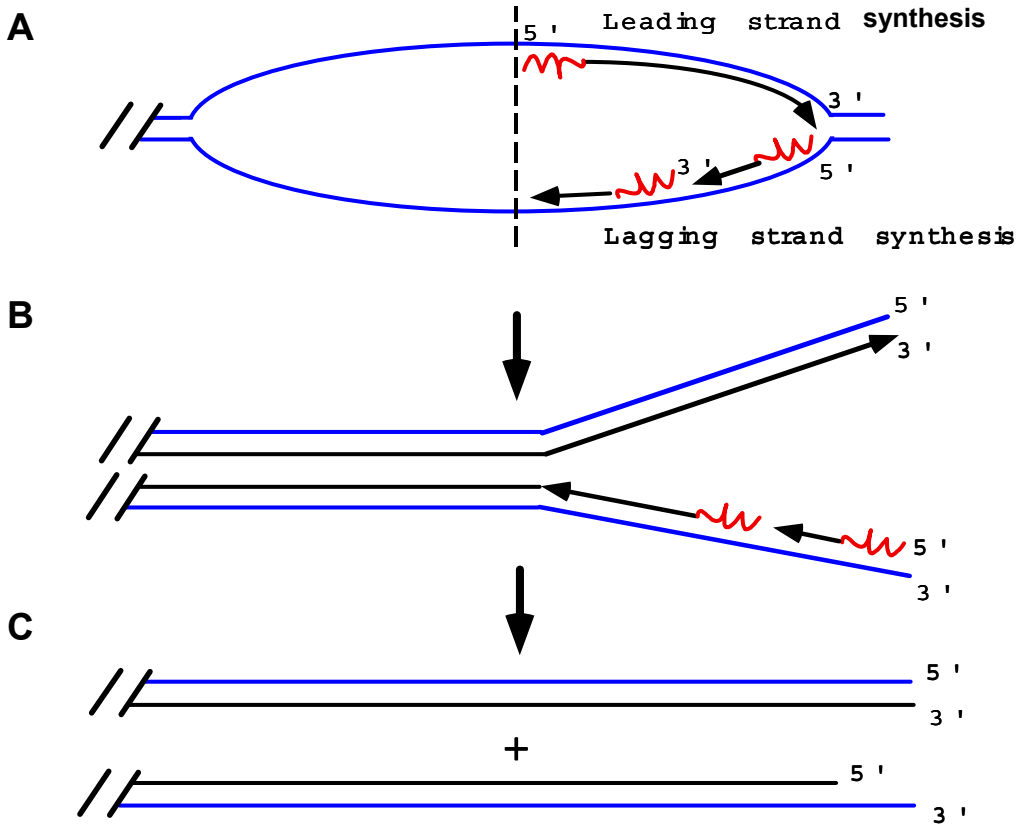

Fig. 2. The end replication problem. The semi-conservative nature of DNA replication does not allow replication of the extreme end of the chromosome. (*A* and *B*) DNA polymerases require a short RNA primer (red) to initiate synthesis, and when the final primer is removed, from the 5' end of the daughter strand, a gap remains (*C*).

addition (Fig. 3). Thus, the human telomerase RNA has the sequence 5' CUAACCCUA 3', which encodes TTAGGG repeats (16). The catalytic protein of telomerase is called TERT, for telomerase reverse transcriptase, and the integral RNA subunit is TR or telomerase RNA.

Reverse transcriptases contain seven characteristic sequence motifs (1, 2, A, B', C, D, and E), and these motifs are present in all TERTs identified (17). In addition, TERTs have another conserved N-terminal T-motif which is required for telomerase activity. TERTs from ciliates have a ciliated protozoa (CP) motif also in the N-terminus (18). The N-terminal half of TERT is necessary and sufficient for TR binding and is required for telomerase activity in *Tetrahymena*, *S. cerevisiae*, and humans (19-22). The C-terminus is required for telomerase activity in *Tetrahymena*, *S. cerevisiae*, and humans (19-22). So, while the central portion of telomerase contains the conserved reverse transcriptase domains, the N- and C- terminal regions are unique to telomerase.

Telomerase RNA subunits have been identified in many species including 23 ciliates (148-209nt in length), two yeasts (1300nt), mouse (327nt), human (451nt) and 33 other vertebrates (23). The telomerase RNA subunit has yet to be identified in any plant species. Although telomerase RNA subunits have a very low level of sequence conservation, several conserved features and a conserved secondary structure have been described (23). One of the conserved features is the telomere template sequence, complementary to the G-rich strand of the telomere, and located near the 5' end of the RNA. In addition, aligning vertebrate telomerase RNA subunits identified eight highly conserved regions

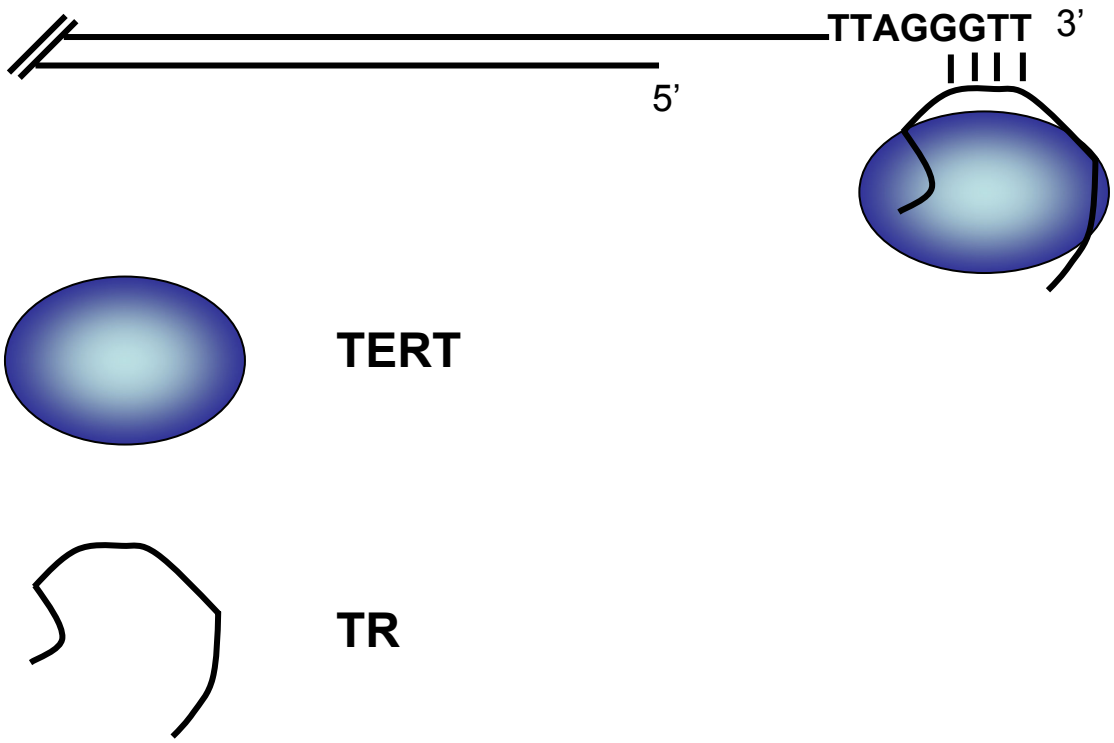

Fig. 3. Addition of telomeric DNA by telomerase. TERT, the catalytic subunit of telomerase, uses the template region within the telomerase RNA subunit (TR) to add telomeric repeats to the chromosome end.

(C1-8) (23), including a H/ACA RNA motif, which is composed of primary and secondary structure elements found at the 3' end of the RNA (24). The H/ACA motif is also found in small nucleolar (sno) RNAs and is required for both snoRNA and TR accumulation *in vivo (25)*.

TERT and TR are the only elements required for reconstitution of telomerase activity *in vitro* (26), although other proteins associate with the telomerase ribonucleoprotein and some of them are required for telomerase activity *in vivo* (27). In *S. cerevisiae*, genetic screens led to the identification of the reverse transcriptase subunit, *EST2* (ever shorter telomeres) (28) and the telomerase RNA subunit, *TLC1* (29). Three additional genes (*EST1*, *EST3* and *EST4*) encoding components of the yeast telomerase holoenzyme were also identified (28, 30). The functions of Est1p and Est4p in telomere biology have been well characterized (31), yet the role of Est3p, a stable component of the telomerase holoenzyme, remains unclear (32).

Est1p is a non-catalytic component of telomerase associated with the telomerase RNA subunit (33). Deletion of *EST1* leads to progressive telomere shortening and a senescence phenotype (30). Nucleic acid binding studies using recombinant Est1p indicate it is a single-stranded telomere end binding protein with non-specific RNA binding activity (34). Est1p also physically interacts with Est4p (Cdc13p, see below), another non-catalytic component of telomerase (35).

Cdc13p is a multifunctional telomere binding protein that recognizes the single-strand G-overhang (36). The interaction of the telomerase with telomeres

is mediated via the Est1p-Cdc13p interaction to recruit telomerase to the telomere (Fig. 4). Although Est1p was originally identified in yeast, homologues have been identified in many higher eukaryotes, including human, *Caenorhabditis elegans*, *Drosophila* and *Arabidopsis thaliana* (37, 38). Of the three Est1-like proteins found in humans, hEst1a is the best characterized. Human Est1a was found to have single-stranded telomeric DNA binding activity *in vitro* (38), and to directly interact with hTERT *in vitro (38)*. Additionally, immunoprecipitation experiments showed that hEst1a was associated with telomerase activity *in vivo* (37, 38).

One group found that overexpression of hEst1a induced chromosome fusions, without any alteration of telomere length (37). When telomeres are dysfunctional, they are recruited into chromosome fusion events involving other dysfunctional telomeres, creating end-to-end fusions and dicentric chromosomes. The other group reported that overexpression of hEst1a and hTERT lengthened telomeres, but did not detect chromosome fusion events (38). Together these results implicate hEst1a in telomerase recruitment and telomere capping. In Chapter III, I describe the characterization of two Est1-like proteins in *Arabidopsis*.

In addition to hEst1a, several auxiliary proteins of human telomerase have been identified. They include several heterogeneous nuclear ribonucleoproteins (hnRNPs) (39), snoRNA binding proteins (25), molecular chaperones (40), and TEP1 (telomerase-associated protein 1) (41). While the functions of most of these telomerase associated proteins are unknown, the snoRNA binding proteins

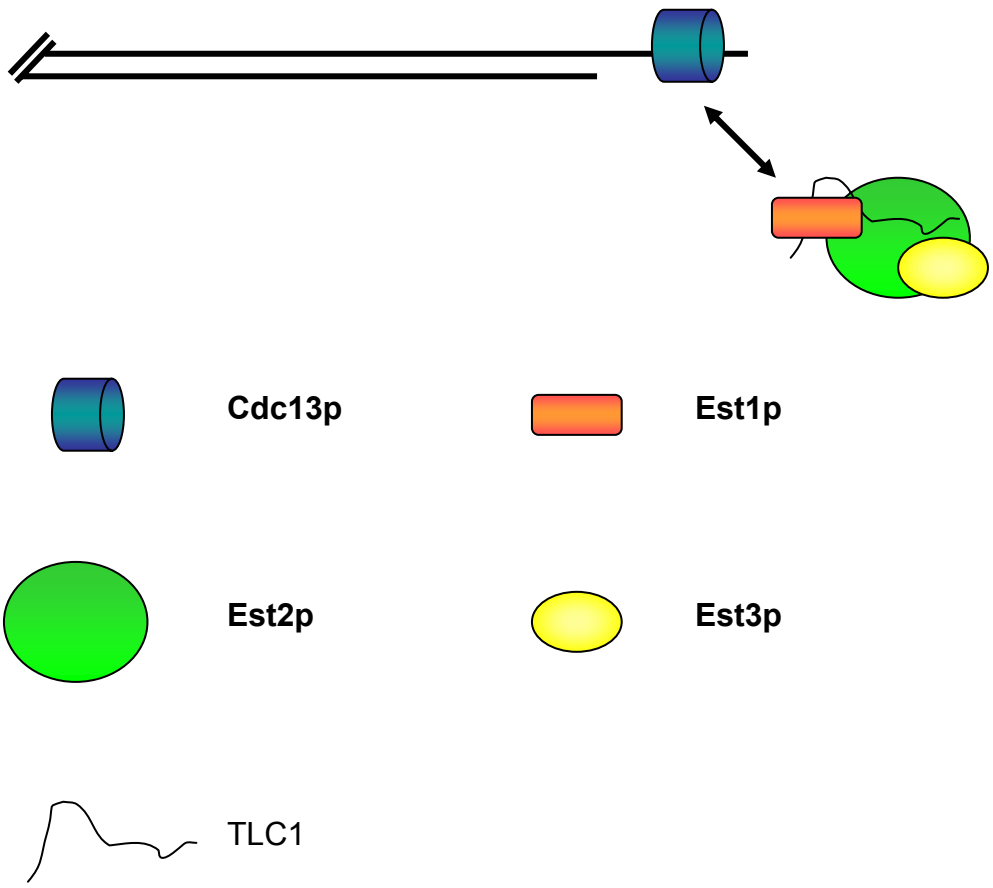

Fig. 4. The telomerase holoenzyme in *S. cerevisiae*. The telomerase holoenzyme consists of Est1p, Est2p, Est3p and TLC1. This complex is recruited to the end of the telomere through the Est1p-Cdc13p interaction.

are required for hTR accumulation and stability *in vivo* (24).

In many eukaryotes, expression of telomerase components and telomerase activity is regulated through development. In *Euplotes crassus*, higher order telomerase complexes with distinct biochemical properties arise during development (42). Programmed ribosomal frameshifting and a switch between telomerase catalytic subunits appear to contribute to this change (43).

In humans, telomerase activity is found in embryonic tissues and in rapidly dividing cells (germline, cancer cells), but not in most somatic cells (44). The presence of telomerase activity correlates with expression of *hTERT*, although *hTR* is ubiquitously expressed (45). The situation is very similar in *Arabidopsis*, where *AtTERT* expression and telomerase activity are detectable in embryonic tissue, reproductive and actively dividing cells (flowers, root tips and callus), but not in leaves where most cells are arrested in the G1 phase of the cell cycle (46-48). Telomerase activity in the embryo is believed to lengthen telomeres enough to provide the predominantly telomerase-negative somatic cells with a lifetime's worth of proliferative capacity. Additionally, post-embryonic regulation of telomerase activity in multicellular organisms is thought to offset telomere loss in the rapid cycles of proliferation necessary for tissue growth and differentiation (25).

Although telomerase is the primary mechanism for telomere lengthening in most eukaryotes, telomerase-independent mechanisms for telomere maintenance have been reported (49) (Fig. 5). In *Drosophila melanogaster*, telomeres are comprised of multiple copies of two retrotansposable elements,

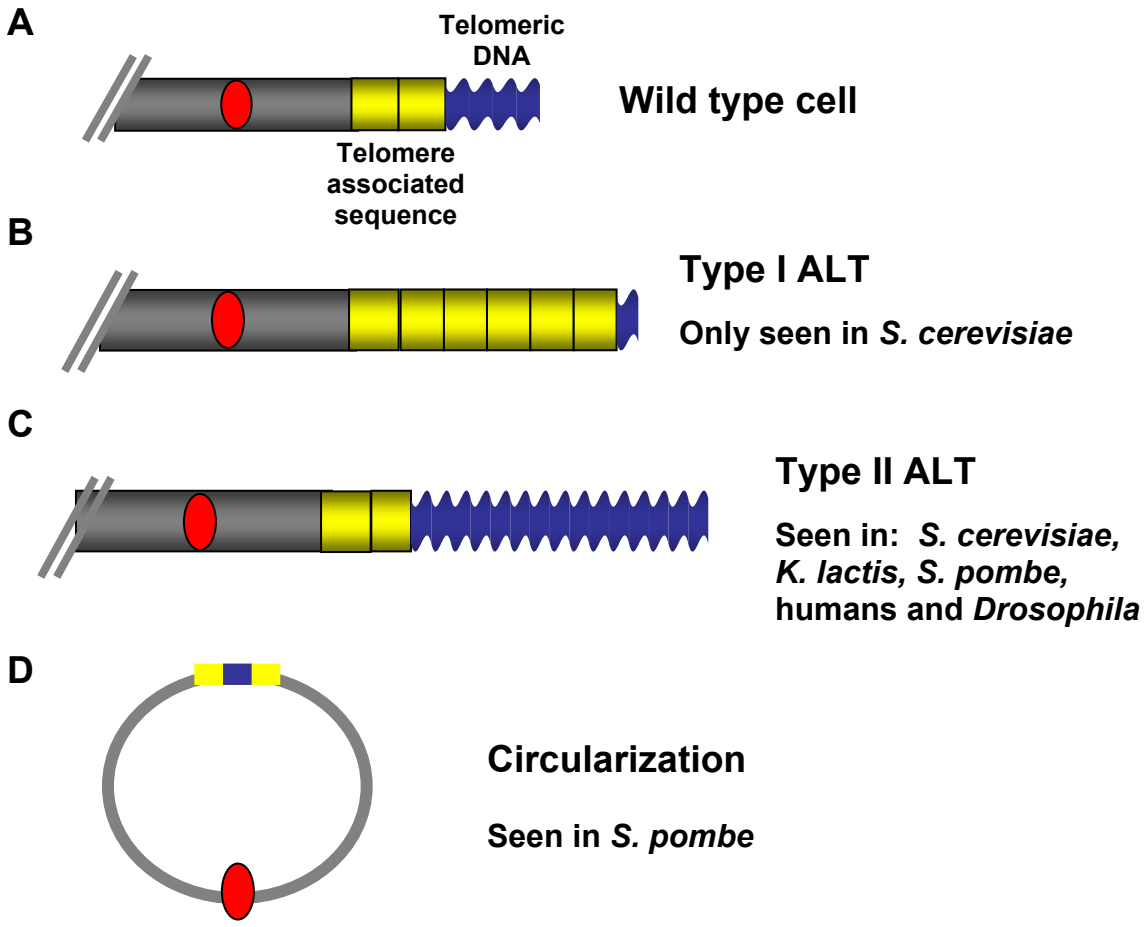

Fig. 5. Telomerase-independent mechanisms for telomere maintenance. (*A*) Telomeric DNA (blue) and telomere associated sequences (yellow) in a wild type cell. (*B*) Type I ALT. Telomeres are lengthened though extensive amplification of telomere associated sequences. (*C*) Type II ALT. Telomeres are lengthened by recombining with telomeric DNA on other chromosome ends. (*D*) Chromosome circularization. Chromosomes in *S. pombe* can be circularized to circumvent the need for telomerase.

HeT-A and TART. Transposition of these two elements creates arrays of repeats that are much larger and more irregular than the repeats added by telomerase (49). Some immortalized mammalian cell lines and tumors maintain or increase the overall length of their telomeres in the absence of telomerase activity by a mechanism known as alternative lengthening of telomeres (ALT) (Fig. 5C) (50). Telomeres in ALT cells are extremely heterogeneous in size, and telomere dynamics suggest a recombinational mechanism is responsible for this increase in telomere length (50). In telomerase negative budding or fission yeast, subpopulations of cells acquire the ability to maintain telomeres via a recombination mechanism (51-55) (Fig. 5B and 5C). Type I ALT in yeast involves extensive amplification of telomere-associated sequences (Fig. 5B), while Type II ALT is characterized by very long, heterogeneous telomere tracts (Fig. 5C) (56). Telomerase-deficient *S. pombe* cells can circularize their chromosomes, thus circumventing the need for telomerase or a recombination mechanism (Fig. 5D) (54). Surprisingly, telomerase-independent cell survival in *Arabidopsis* does not appear to utilize any of these known mechanisms, instead it may involve chromatin modification (Watson et al., in preparation).

For organisms maintaining telomere length via telomerase action, assays have been developed to detect and monitor telomerase activity *in vitro*. Telomerase activity can be assayed directly by incubating a single-stranded telomeric oligonucleotide with radio-labeled nucleotides and cellular extracts (15). A more sensitive assay, the telomere repeat amplification protocol (TRAP) (Fig. 6), uses PCR for telomerase detection (46, 57). In both the direct assay and

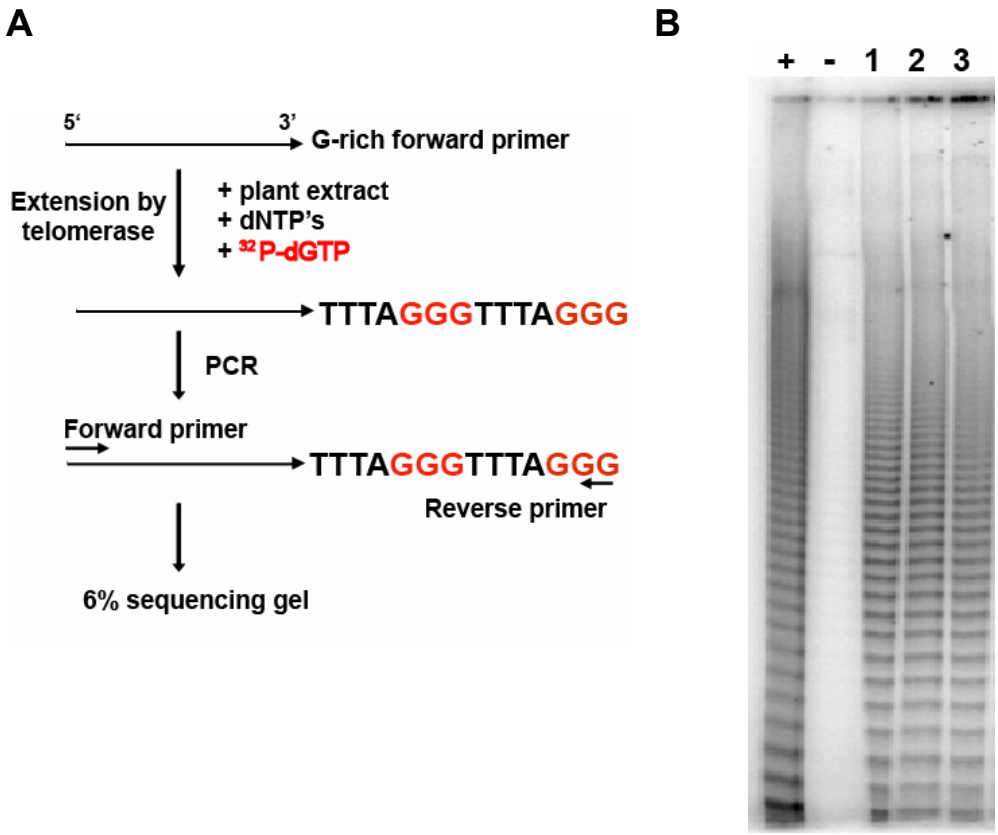

Fig. 6. The TRAP assay. (*A*) Schematic of the PCR based TRAP assay for telomerase activity in plants. (*B*) Typical results for the TRAP assay in Arabidopsis. Cauliflower extract was used as a positive control (+) and extract from wild type *Arabidopsis* leaves was used as the negative control (-). Lanes 1-3 show that three different extracts made from wild type *Arabidopsis* flowers have telomerase activity.

the TRAP assay, telomerase elongates the input oligonucleotide by adding one nucleotide at a time to generate tandem repeats of the telomeric sequence specified by the TR. The products can be resolved by PAGE, and generate a ladder of products whose periodicity corresponds to the telomere repeat sequence of each organism. Approximately 85% of human tumors have telomerase activity. Hence, checking suspicious tissue samples with the TRAP assay provides a useful tool for the diagnosis of cancer (58). The utility of the TRAP assay outside of basic research is one example of the contributions the telomerase field has made to improving human health.

TELOMERE LENGTH HOMEOSTASIS

Although telomere length varies between different eukaryotes, telomeres are strictly maintained at a species-specific set point. Regulation of this set point involves a large number of different genes: a genome wide screen for genes affecting telomere length in *S. cerevisiae* identified 173 genes whose deletion either increased or decreased telomere length (59). This screen illustrates the complex nature of maintaining the telomere set point in each cell.

Although the mechanisms controlling telomere size are not fully understood, telomeric DNA is subjected to both lengthening and shortening activities (60). The combined contributions of both types of activities maintain telomere length homeostasis. The primary cause of telomere shortening in wild type cells is thought to occur as a result of the end replication problem. In addition, more active processes may also lead to rapid loss of telomeric DNA.

These include Telomere Rapid Deletion (TRD) (61), a recombinational process that occurs on extremely long telomeres, deficiencies in proteins important for protection of the extreme terminus of the telomere (62), and exonuclease activity on uncapped telomeres (63). These telomere-shortening activities are circumvented through the action of telomerase. Taken as a whole, the combined contributions of lengthening and shortening activities at the telomere maintain telomere length homeostasis.

Despite the fact that telomere length is maintained at an equilibrium length for each species, this set point can vary within species of the same genus. In mice, telomeres in the established inbred mice strains are approximately 40kb, while in wild derived mice the length is much shorter, around 10-15kb (64). In the model plant, *Arabidopsis thaliana*, telomere length varies amongst different ecotypes, natural variants of *Arabidopsis* found in specific geographic locations. *Arabidopsis* plants can be divided into two distinct groups based on telomere length (3). In one group, telomeres ranged from 2-5kb, while in the other group telomeres ranged span 3.5-8kb. Thus, telomeres that range from 2-8kb are acceptable for *Arabidopsis* (3). Additionally, the species-specific telomere length is dependent on telomerase. In the absence of telomerase, telomere length is no longer maintained at the set point. In Chapter II I describe reestablishing the telomere set point in *Arabidopsis tert* mutants.

CONSEQUENCES OF TELOMERASE INACTIVATION

In unicellular organisms that express telomerase constitutively, loss of telomerase activity leads to an ever-shorter telomere (EST) phenotype (30) characterized by progressive shortening of telomeres and eventual loss of culture viability (1). Loss of telomerase activity in multicellular organisms such as plants or mice also causes a latent phenotype, which is only revealed when the telomeric DNA has been sufficiently eroded (65, 66). Ultimately, defects in cellular proliferation, and increasing genetic instability leads to failure of the germline (65-70).

Disruption of *TERT* in *Arabidopsis* causes a gradual shortening of the telomere, by ~250-500bp per plant generation (68). Telomerase-deficient plants are wild type in appearance until the sixth generation, and from then onward defects in cell proliferation become apparent (66). Such abnormalities include developmental defects in both vegetative and reproductive organs, such as alteration of leaf morphology (leaves become rough and misshapen) and grossly enlarged shoot apical meristems. Additionally, the number of cells per leaf decreases, while the cellular size increases (66). Seeds from late generation *tert* mutants have reduced germination efficiency, and many plants produce no seeds at all. All *tert* mutants ultimately arrest at a terminal vegetative state by the tenth generation (66).

When telomeres become dysfunctional, the cell recognizes them as a double strand break, and then “repairs” this break by fusion with another chromosome end to create dicentric chromosomes. Dicentric chromosomes feed

into a breakage/fusion/bridge cycle (BFB) cycle. In this cycle, dicentric chromosomes will be broken during anaphase and generate new unprotected ends that fuse again and reenter the BFB cycle (Fig. 7). The onset of the phenotypic changes in telomerase-deficient plants correlated with the onset of chromosome instabilities, visualized as anaphase bridges in mitotically dividing cells (66). The number of anaphases with end-to-end fusions increases with successive *tert* generations: when *tert* mutants arrest at the terminal state, up to 40% of the anaphases contain bridged chromosomes (66).

Cells respond to genome damage by cell cycle arrest and in mammals, apoptosis or senescence, which is mediated through p53 (67). However, programmed cell death is not the major response to telomere dysfunction in *Arabidopsis*. Late generation *tert* mutants cease growing, although they stay metabolically active long after wild type plants die (66). This is presumably due to their failure to induce developmentally programmed senescence by seed production (66).

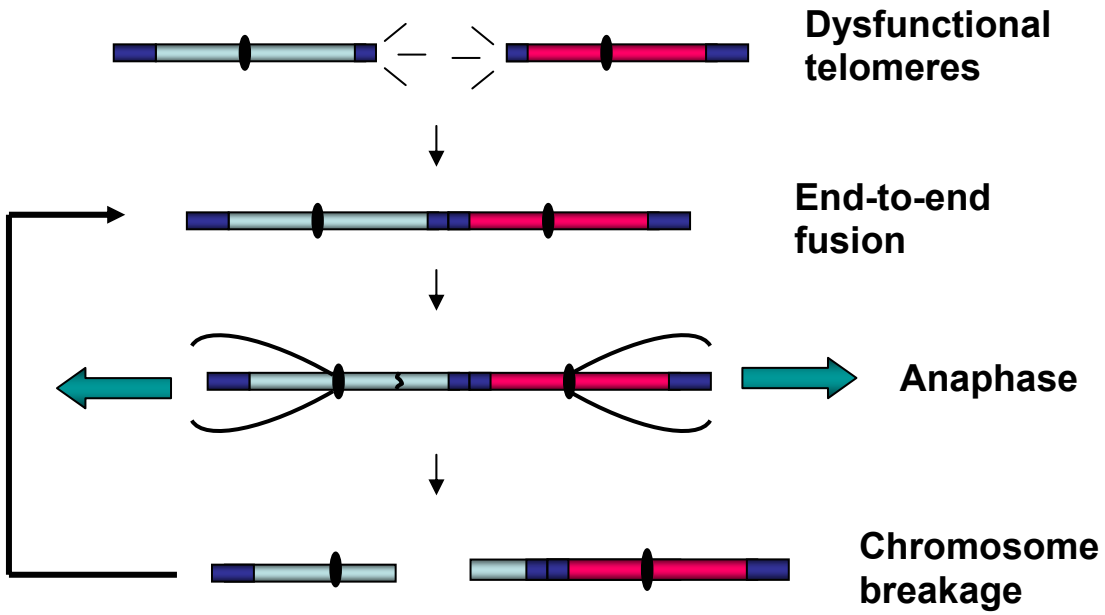

Fig. 7. The breakage/fusion/bridge (BFB) cycle. Dysfunctional telomeres are fused end-to-end creating a dicentric chromosome. During anaphase, the centromeres are pulled to opposite poles. Eventually this chromosome breaks and re-enters the BFB cycle.

TELOMERE BINDING PROTEINS

The terminal portion of telomeres exists in a non-nucleosomal DNA-protein complex (1). The interactions between telomeric DNA and the non-nucleosomal proteins form a protective cap at the ends of linear chromosomes. Telomeric binding proteins have been identified in many organisms, ranging from ciliates and yeast to humans (1). Telomere associated proteins can be divided into two groups, those that directly interact with double or single stranded telomeric DNA, and those brought to the telomere via protein-protein interactions with the telomeric DNA binding proteins.

Double-strand binding proteins

As their names suggest, double-stranded telomere binding proteins contact the duplex region of the telomere tract. They appear to be part of a length-sensing mechanism that can discriminate the number of telomeric repeats based on the number of duplex-binding proteins bound to the telomere (71). Counting the proteins provides negative regulation of the telomere by inhibiting access of telomerase through sequestration of the chromosome end (72). The most well characterized double-stranded telomere binding proteins are Rap1p from *S. cerevisiae* (71), Taz1 from *S. pombe* (73), and TRF1 and TRF2 from humans (74).

RAP1 (repressor/activator protein), is an essential gene that encodes the major double-strand telomere binding protein in *S. cerevisiae* (Fig. 8). Rap1p uses two central Myb-type DNA binding domain to bind a loosely-defined

recognition site that is present approximately 20 times on every yeast chromosome end (71). According to the protein-counting model of telomere length regulation, the number of telomere-bound Rap1p molecules determines whether a telomere is or is not acted upon by telomerase (75). Mutations within the C-terminus of Rap1p cause telomerase-dependent telomere lengthening (76). Two negative regulators of telomere length, Rif1 and Rif2 (Rap1p interacting factor) bind the C-terminus of Rap1 (77). Deletion of the nonessential Rif1 and Rif2 results in significant telomere elongation (77, 78). This same domain of Rap1p recruits the silencing proteins Sir3 and Sir4 (silent information regulator) (79). Sir3 and Sir4 form a complex with Sir2p to induce the transcriptional repression of subtelomeric genes (telomere silencing) (76). It is generally believed that Sir and Rif proteins bind the same portion of Rap1p C-terminus and antagonize each other *in vivo* by competing for Rap1p binding.

S. pombe contains a sequence homologue of Rap1p, but this protein does not directly bind telomeric DNA. Instead, SpRap1p associates with the telomere via a protein-protein interaction with Taz1p (telomere-associated in *Schizosaccharomyces pombe*), the major double-strand telomere binding protein in *S. pombe*. Taz1p was identified in a one-hybrid screen for genes encoding double-strand telomere binding proteins, and has been shown to be a negative regulator of telomere length (73). Taz1p contains a single Myb-like domain at its C-terminus, and binds fission yeast telomeric DNA in a sequence-dependent manner as a dimer (80). Taz1p recruits homologues of ScRap1p and ScRif1p to

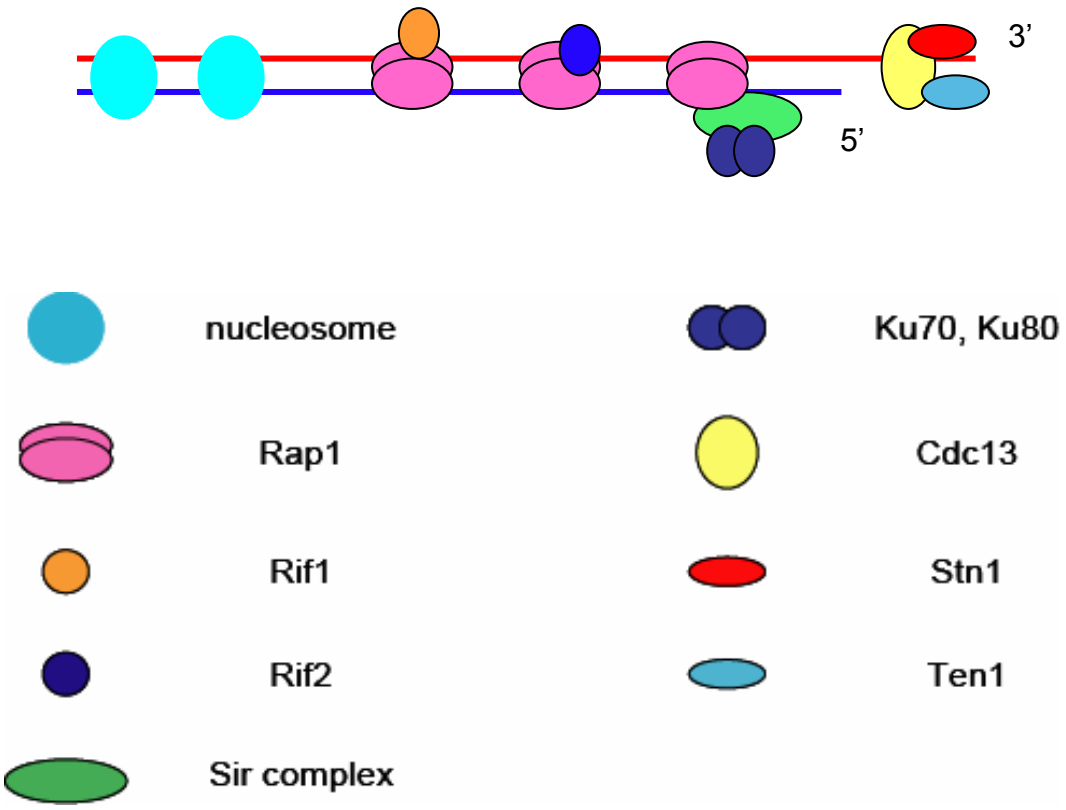

Fig. 8. Telomere binding proteins in *S. cerevisiae*. See text for detailed discussion of their functions and interactions.

telomeres in *S. pombe*. Deletion of SpRap1p or SpRif1p causes telomere elongation (81).

Loss of Taz1p leads to drastic alteration of both the single and double-stranded portions of the telomere (lengthening of both is observed), and disruption of the telomeric chromatin structure (73, 82). The long telomeres in the *taz1Δ* cells become entangled with each other at cold temperatures, leading to double strand breaks and chromosome missegregation (83). Treatments that arrest *S. pombe* cells in G1 lead to fusions between the elongated telomeres that are dependent on the non-homologous end joining (NHEJ) pathway components Ku and Lig4 (84). This suggests that in addition to its role as a negative regulator of telomere length, Taz1p contributes to the protective cap of the telomere and prevents the NHEJ machinery from detecting the telomere as a double stranded break.

In contrast to yeast, mammalian telomeres are bound by two major double-strand telomere binding proteins, TRF1 and TRF2 (TTAGGG repeat binding factor) (Fig. 9). TRF1 and TRF2 were identified on their ability to bind human telomeric oligonucleotides *in vivo* (74, 85). As with Rap1p and Taz1, TRF1 and TRF2 use a C-terminal Myb-like domain to bind telomeric DNA. TRF1/TRF2 bind telomeric DNA as homodimers, using a central domain for dimerization (86).

TRF1 behaves similarly to Rap1p, as a negative regulator of telomere length. Overexpression of a dominant negative TRF1 causes telomeres to elongate to a new equilibrium length (87). Two related proteins can inhibit the

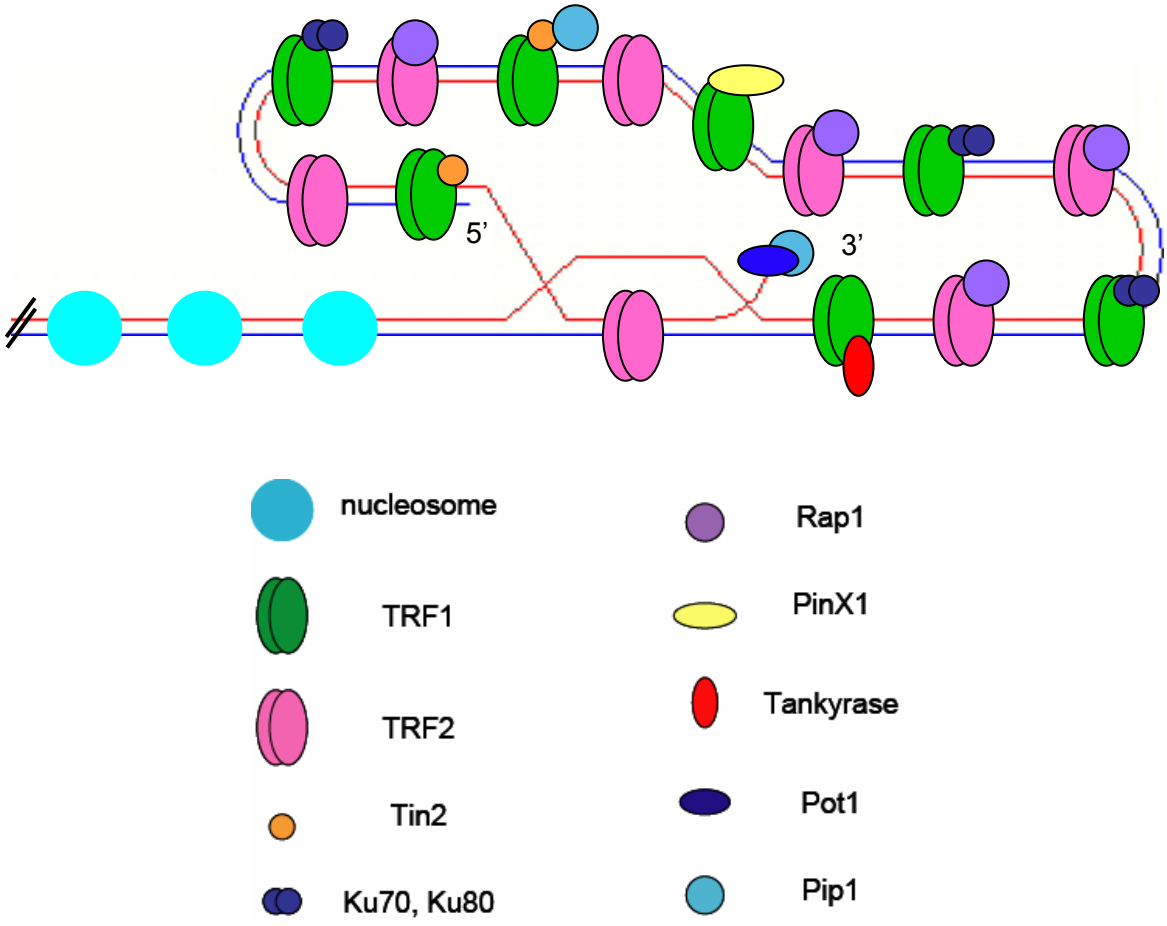

Fig. 9. Model of the human telomere**.** Telomere is drawn in the t-loop conformation, with associated proteins.

binding of TRF1 to telomeres, tankyrase 1 and 2. Tankyrases are poly (ADP-ribose) polymerases, and in addition to many non-telomeric cellular functions, can ADP-ribosylate TRF1 *in vitro*, thus decreasing TRF1's affinity for telomeric DNA (88). Overexpression of tankyrase causes telomere elongation by releasing TRF1 from the telomere, thereby allowing telomere elongation by telomerase (89).

TRF1 has another interacting partner, Tin2 (TRF1 interacting nuclear protein 2) (90). Tin2 is a small protein with no known domains beyond its C-terminal TRF1 binding domain. Tin2 also appears to be a negative regulator of telomere length; overexpression of a dominant negative Tin2 leads to telomerase dependent telomere elongation (90). Recently, a new binding partner for Tin2 was identified by mass spectrometry, Pip1 (Pot1 interacting protein) (91) (see below).

A fourth TRF1 interacting protein, PinX1, was identified in a yeast two-hybrid screen (92). Overexpression of PinX1 induces telomere shortening by inhibition of telomerase activity *in vivo* (93). PinX1 exerts its effect by sequestering TERT in an inactive complex in the nucleolus, which lacks the telomerase RNA (93). Therefore, PinX1 is the first known telomerase inhibitor *in vivo*.

TRF2, another major double strand binding protein in mammals, is also a negative regulator of telomere length (94). TRF2 binds along the double-stranded portion of the telomere with more than 100 protein molecules per chromosome end (74, 86). *In vitro*, TRF2 has the ability to create t-loops when

given a short stretch of duplex telomeric DNA that ends in a 3' overhang (10, 95). T-loop formation by TRF2 occurs at a low frequency, so *in vivo*, TRF2 is likely to be assisted by other factors in the process of t-loop formation (96).

Beyond its role in length regulation, TRF2 has emerged as the major telomere protection factor in human cells. Loss of endogenous TRF2 by overexpression of a dominant negative version of the protein results in activation of the Atm checkpoint kinase and induction of a p53 dependent cell-cycle arrest (8, 97). Loss of TRF2 creates an uncapped telomere, which is attacked by exonucleases that cleave off the G-overhang (98). After removal of the G-overhang, telomeres are immediately fused by the NHEJ pathway, thus preventing any significant loss of telomeric DNA at the fusion junction (99).

TRF2 also has an interacting partner, hRap1p. hRap1 was identified in a yeast two-hybrid screen using TRF2 as bait (100), and was also found by its sequence similarity to ScRap1p. Much like SpRap1, hRap1 does not bind telomeric DNA directly, but forms a complex with a double-strand telomere binding protein (Taz1p in *S. pombe*, TRF2 in humans). Overexpression of hRap1 causes gradual telomere shortening, consistent with its role as a negative regulator of telomere length (100).

Double-strand telomere binding proteins in plants are not as well characterized as those from yeast and mammals. When the *Arabidopsis* genome is queried for genes encoding proteins with similarity to TRF1 or TRF2, twelve genes are identified (101). All twelve proteins contain a C-terminal Myb-like domain similar to what is found in TRF1 and TRF2. Biochemical

characterization of these proteins identified two distinct gene families, named TRF-like (TRFL) family 1 and family 2. All proteins in family 1 contained a highly conserved region C-terminal to the Myb domain (Myb-extension). Recombinant proteins from family 1 formed homo- and heterodimers, and specifically bound double-stranded plant telomeric DNA *in vitro* (101). In contrast, family 2 members do not contain the Myb-extension, and do not dimerize or bind double-stranded plant telomeric DNA *in vitro* (101). Interestingly, when the Myb-extension from family 1 was introduced into the corresponding region of a family 2 member, telomeric DNA binding was observed (101). Thus, the Myb-extension is required for binding plant telomeric DNA and defines a novel class of proteins in *Arabidopsis* (101).

Another plant double-stranded telomere binding protein is NgTRF1 from tobacco (102, 103). *NgTRF1* was identified from a collection of cDNAs encoding Myb-containing proteins. Interestingly, *NgTRF1* displays an expression profile that is opposite to that of telomerase. The highest levels of *NgTRF1* expression are in non-proliferating cells (102). When NgTRF1 is over-expressed in cultured tobacco cells, telomeres shorten, yet when anti-sense NgTRF1 is expressed, telomeres lengthen (103). Cells over-expressing wild type or anti-sense NgTRF1 undergo apoptosis (103). This data suggests that NgTRF1 is important for telomere length regulation in tobacco, but also plays a role in maintaining genome stability.

The data discussed above illustrate the complex protein-protein and protein-nucleic acid interactions of double-strand telomere binding proteins.

Beyond the Myb-like DNA binding domain of these proteins, there is little to no sequence conservation of this class of proteins found in yeast, plants or mammals. However, their functional conservation through evolution demonstrates the necessity of protecting and regulating the double-stranded portion of the telomere.

Single-strand telomere binding proteins

Proteins that bind the single-stranded G-overhang also play important roles at the telomere, including protection against degradation and improper action of double strand break repair machinery, as well as recruitment of telomerase and other factors needed for proper telomere length maintenance (104). Proteins that specifically bind the G-overhang have been identified in almost every organism studied to date, but the best characterized are from ciliates, yeast and humans.

The first telomere end binding protein (TEBP) was identified in the ciliate *Oxytricha nova*. This protein consists of two subunits, α and β, that bind the G-overhang as a heterodimer (105, 106). Homologues of the α subunit have also been identified from other ciliates, including *Euplotes crassus*, *Oxytricha trifallax* and *Stylonychia mytilus* (107, 108). The α subunit binds telomeric DNA using a specialized DNA binding domain that folds into the oligosaccharide/ oligonucleotide (OB) fold (109). The α subunit uses four OB fold domains to bind single-stranded DNA (110). TEBP is predicted to stabilize the telomere by providing a cap at the chromosome end.

The *S. cerevisiae* Cdc13p is a sequence-specific, single-stranded telomeric DNA binding protein that also harbors an OB fold motif (111). Cdc13p localizes to telomeres *in vivo* (112) (Fig. 3). Although Cdc13p was originally identified as an essential gene involved in cell cycle control (113), in later screens Cdc13p was found as one of four genes that cause an EST phenotype (36). Further work demonstrated that Cdc13p was not required for telomerase activity *in vitro*, but certain alleles (*cdc13-2*) confer a telomerase-deficient phenotype (EST) that is characterized by telomere shortening and eventual cell death (36).

Cdc13p is a positive regulator of telomerase access to the telomere. This positive regulation depends on the physical interaction between Cdc13p and Est1p, a non-catalytic component of the yeast telomerase holoenzyme that binds the telomerase RNA subunit (35). The requirement of this protein-protein interaction can be bypassed if the DNA binding domain of Cdc13p is fused to Est1p in the absence of endogenous Cdc13p (114). This interaction brings telomerase to the extreme end of the chromosome to allow elongation of the telomeric DNA.

In addition to its positive role in promoting telomerase access, Cdc13p and its binding partners Stn1p and Ten1p are essential for protecting the chromosome ends from degradation. Stn1p was identified as a Cdc13p interacting protein by yeast two-hybrid screens (115). Deletion of Stn1p causes the accumulation of long G-overhangs and the *stn1-13* allele causes abnormally long telomeres (115). A genetic screen to find suppressors of temperature

sensitive *stn1* mutants lead to the identification of Ten1p, which physically interacts with both Cdc13p and Stn1p (116). Several *ten1* mutations have been shown to cause telomerase-dependent telomere lengthening, while other temperature sensitive mutants of *TEN1* accumulate single-stranded telomeric DNA (116). These three proteins, Cdc13p, Stn1p and Ten1p are proposed to form a protective cap at the telomere (Fig. 8) (72).

Surprisingly, Cdc13p can also act as a negative regulator of telomere length. Mutations in Cdc13p that lead to the EST phenotype also cause long G-overhangs (113). From this data, it was suggested that Cdc13p may promote C-strand synthesis by coordinating leading and lagging strand DNA synthesis machinery at the telomere. This idea was supported by mutations in lagging strand replication machinery that lead to similar telomere phenotypes (117) and evidence for a physical interaction between Cdc13p and the catalytic subunit of polymerase α *in vivo* (35). The current model for Cdc13p function suggests that Cdc13p first recruits telomerase to the telomere and then acts to limit telomerase action on the telomere in response to the lagging strand DNA synthesis by the DNA pol α-primase complex .

In *S. pombe* and humans, the predominant single-strand telomere binding protein is Pot1 (protection of telomeres). *POT1* genes were identified by their sequence similarity to the α subunit of TEBP from ciliates (118). Pot1 specifically binds single stranded G-rich DNA, and the loss of Pot1 leads to cell cycle arrest, end-to-end chromosome fusions and cell death (62, 118). In *S. pombe*, the few surviving cells have circularized all of their chromosomes (118). While SpPot1

uses a single OB fold to bind telomeric DNA, hPot1 has two tandem OB folds (110). The most N-terminal OB fold binds telomeric DNA and the other OB fold protects the 3' end of the single stranded DNA (119).

The hPot1 interacting factor, hPip1, binds both the human single strand telomere binding protein Pot1, and Tin2. This interaction tethers Pot1 to the TRF1 complex. Reduction of Pip1 or Pot1 levels with short hairpin RNAs led to telomere elongation, indicating that Pip1 contributes to telomere length control through recruitment of Pot1 (91). These physical interactions between Pot1, Pip1, TRF1, and Tin2 at the telomere may affect the loading of Pot1 onto the G-overhang, and modulate the ability of the telomere to transmit length information needed to positively or negatively regulate telomerase access at the telomere end.

Arabidopsis is the only organism to encode two Pot1-like proteins, AtPot1 and AtPot2. Recombinant AtPot1 and AtPot2 bind single-stranded plant telomeric DNA, and were able to form homo- and heterodimers *in vitro* (Shakirov et al., submitted). Overexpression of a truncated version of Pot1 lacking the DNA binding domain caused telomere shortening, suggesting that Pot1 is a positive regulator of telomere length. In contrast, overexpression of the DNA binding domain of Pot2 resulted in only moderate telomere shortening, yet these plants had severe growth defects, sterility and massive genome instability (Shakirov et al., submitted). The high level of genome instability in AtPot2 mutants implicates Pot2 in chromosome end protection (Shakirov et al., submitted).

Although the first single strand telomere binding protein was identified in *Oxytricha*, many higher eukaryotes have G-overhang binding proteins that have homology to the DNA binding domain of TEBP. Similar to what is seen for double strand binding proteins, G-overhang binding proteins from varied organisms are functional and possibly structural homologues not sequence homologues. Although these single strand telomere binding proteins are not as well characterized as their double strand telomere binding counterparts, the requirement of these proteins for end protection and recruitment of telomerase has been well established.

DNA DAMAGE RESPONSE PROTEINS AT THE TELOMERE

Double-strand breaks (DSBs) in DNA constitute a significant threat to the stability of cellular genomes. They can be generated through the physical impact of ionizing irradiation on DNA, but can also arise as a consequence of DNA metabolism such as DNA replication and repair processes. To protect against genome instability, a cell must differentiate between un-repaired DNA double strand breaks and the natural ends of the chromosomes, or telomeres. Surprisingly, telomere-binding proteins recruit DNA damage response (DDR) proteins, specifically those involved in DSB repair, and these DDR proteins play key roles in telomere maintenance.

Checkpoint PIKK proteins and telomeres

After DNA damage has occurred, it is detected by sensor proteins (DNA damage binding proteins) which then trigger the activation of a transduction system composed of protein kinases (120). Two large and highly conserved protein kinases of the PIKK (phosphatidyl inositol 3-kinase-like kinase) family amplify the original DNA damage signal and trigger a sundry of downstream effects. These two kinases go by many names. In humans they are called Atm and Atr, in budding yeast they are Tel1p and Mec1p, while in fission yeast they are named Tel1p and Rad3p (120). For simplification, I will refer to them as Atm and Atr.

Deletion of *ATM* in yeast or mammals leads to telomere shortening (121-127), and in yeast, deletion of *ATR* also leads to telomere shortening (121, 128). Yeast deficient for *ATM* and *ATR* are unable to maintain telomere length by telomerase, and this leads to progressive telomere shortening and eventual loss of proliferative capacity (127, 129). Parallel studies are not possible in mammals, as Atr is essential for cell viability (130).

Atm and Atr are both associated with the telomere in *S. cerevisiae*, albeit at different times during the cell cycle. The presence of Atr at the telomere peaks in S phase, whereas Atm is present during all other phases (131). The kinase activity of Atr governs these associations, and moreover, in the absence of Atm, Atr is associated with the telomere throughout the cell cycle (131).

In contrast to yeast and mammals, *Arabidopsis* null for *ATM* or *ATR* have wild type telomere lengths (Vespa et al., in preparation). In the *atm atr* double

mutants, chromosome end protection is compromised, as telomere-telomere fusions are observed (Vespa et al., in preparation). Deletion of *ATM* did not alter the rate of shortening in *tert* mutants. However, in the *atm tert* mutants, genome instabilities appeared three generations earlier than in *tert* single mutants (Vespa et al., in preparation). This is reminiscent of phenotypes observed in *atm tr* mice, with an early onset of chromosome fusions in the absence of accelerated telomere shortening (132). Strikingly, telomere shortening in *Arabidopsis atr tert* mutants was accelerated two-to-three fold in comparison to *tert* mutants. Taken together, these data imply that Atm functions in chromosome end protection while Atr acts synergistically with telomerase in the maintenance of telomeric DNA. These observations from *Arabidopsis* and yeast point out a crucial role for checkpoint PIKKs in telomere maintenance.

DNA repair proteins and telomeres

The two major DSB repair pathways are homologous recombination (HR) and non-homologous end joining (NHEJ) (Fig. 10). Both systems are highly conserved throughout eukaryotic evolution, but the preference for one system over another varies between higher and lower eukaryotes. In higher eukaryotes, NHEJ is the major pathway for DSB repair, whereas single-celled organisms such as yeast rely most heavily on HR (133, 134).

HR requires the RAD52 epistasis group and utilizes an undamaged homologous partner for repair. The DSB is first resected in the 5'-3' direction by an unknown nuclease whose activity is modulated by the MRN complex (Mre11,

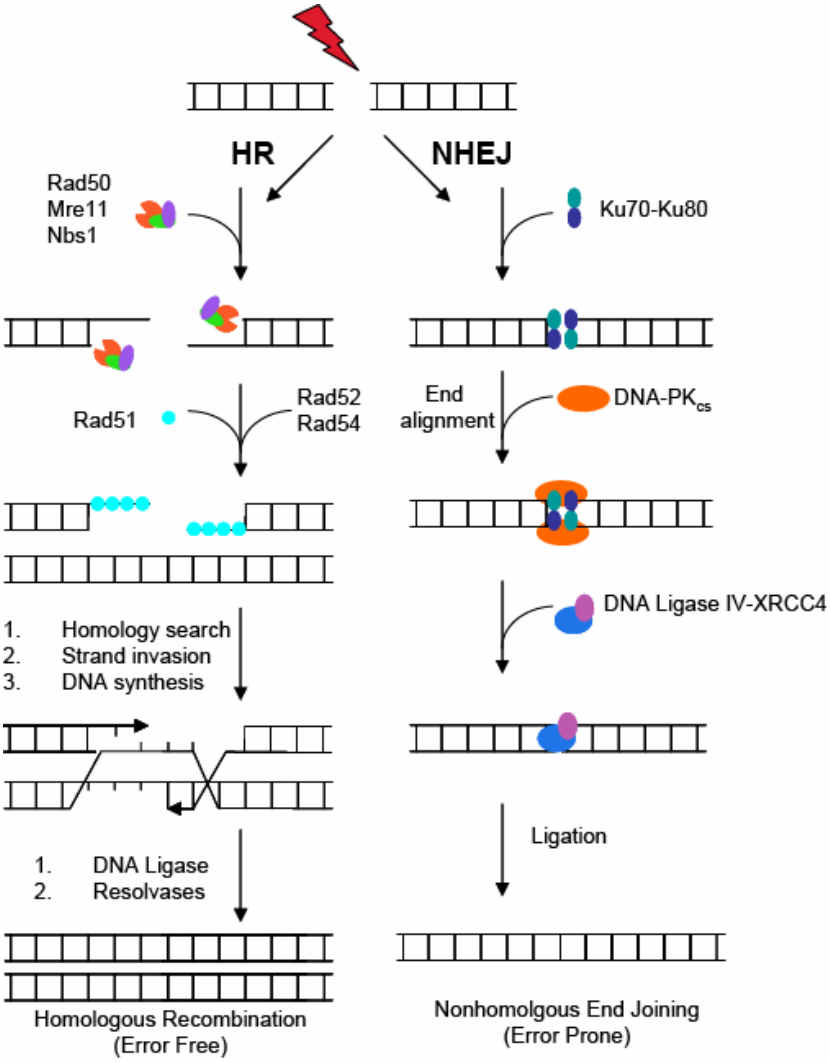

Fig. 10. DNA double strand break repair. After a double strand break has occurred, two pathways can be utilized to repair the break, homologous recombination (HR) or non-homologous end joining (NHEJ). In HR, the double strand break is resected by the MRN (Mre11, Rad50, Nbs1) complex, the single-stranded DNA is bound by Rad51, a homology search is instigated, followed by strand invasion and DNA synthesis. This leads to error-free repair of DNA double strand breaks. NHEJ is mediated by end alignment via the Ku70-Ku80 heterodimer. After the ends are aligned, DNA-PK_{cs} is recruited and followed by DNA Ligase IV-XRCC4. Using end alignment for repair makes NHEJ a more error prone process than HR.

Rad50 and Nbs1/Xrs2). This creates 3' overhangs, which are then bound by Rad51, and catalyzes a strand-exchange reaction with the homologous undamaged DNA partner. Finally, the 3' overhang of the damaged partner is extended by DNA polymerase, ligated, and the DNA crossovers are resolved (135).

The role of HR proteins at telomeres remains unclear. In *S.cerevisiae*, deletion of *RAD51* does not affect telomere length, but a double *rad51 tlc1* (*TLC1*, yeast telomerase RNA subunit) mutant cells senesce at a faster rate than the *tlc1* single mutants (52, 53). Deletion of *RAD51* in chicken cells increases the presence of G-overhangs (136), and *RAD54* knockout mice have shorter telomeres than their wild type siblings (137). These results suggest that the presence of HR proteins at the telomere is required for proper telomere maintenance.

Current models for the role of HR proteins at the telomere revolve around the t-loop. The t-loop resembles an intermediate in HR and t-loop formation can be promoted *in vitro* by TRF2, a telomeric protein implicated in t-loop formation (10). A mutant allele of TRF2 was recently identified that induced catastrophic deletions of telomeric DNA (138). The deletion events were stochastic and occurred rapidly, generating dramatically shortened telomeres that were accompanied by a DNA damage response and induction of senescence. Telomeric DNA deletions induced by this mutant allele were dependent on XRCC3 (x-ray cross complementing), a protein implicated in Holliday junction resolution (138). The amount of telomeric DNA deleted created t-loop-sized

telomeric circles *in vivo* (138), suggesting that t-loop deletion by HR proteins can influence the integrity of mammalian telomeres.

In stark contrast to HR, NHEJ does not require an undamaged partner for repair, and is capable of joining any two exposed double-stranded DNA ends. Key components in the NHEJ pathway are the Ku70/80 heterodimer, DNA ligase IV (Lig4), and Lig4's binding partner, XRCC4. In mammals, the catalytic subunit of DNA-dependent protein kinase (DNA-PK_{cs}), a member of the PIKK family, is also required for efficient NHEJ (133).

Once a DSB has been detected, the Ku heterodimer binds each end of the DSB and recruits DNA-PK_{cs}. The broken ends are then processed by a complex consisting of DNA-PK_{cs} and Artemis, which becomes an exonuclease after being phosphorylated by DNA-PK_{cs}. In the final step, the processed ends are ligated by the DNA ligase IV/XRCC4 complex (133).

The functions of these NHEJ components at telomeres are complicated by the fact that Ku and DNA-PKcs are important for both telomere length regulation and capping. Deletion of Ku in yeast causes telomere shortening and extension of the 3' overhang, but no chromosome fusions are observed (139-144). In the model plant, *Arabidopsis thaliana*, knocking out *KU70* causes telomerase-dependent telomere lengthening (145), but no telomere fusions (146). Interpreting the role of Ku at murine telomeres has been complicated as both telomere lengthening (147) and shortening (148) have been reported. However, deletion of Ku in mice does lead to chromosome fusions, thereby demonstrating a role in telomere capping (147, 148). Deletion of DNA-PKcs leads to gradual

telomere shortening and chromosome fusions in mice (149-151) and interestingly, the kinase activity of DNA-PK_{cs} is required to prevent the end-to-end fusions (152).

Knocking out either DNA Ligase IV or XRCC4 has not been shown to alter telomere length or cause chromosome fusions in yeast, mammals or plants (153-155). Although deletion of *LIG4* or *XRCC4* leads to embryonic lethality in mice (156-158), Lig4 is not an essential gene in yeast or *Arabidopsis* (139, 153-155). In Chapter IV, I present an analysis of the role of Lig4 at *Arabidopsis* telomeres.

The convergence of DSB repair proteins and telomeres is intriguing. One of the major functions of the telomere is to prevent the chromosome end from being detected as a DSB, yet many of the same proteins that facilitate DSB repair are also necessary for proper telomere integrity. Interestingly, dysfunctional telomeres elicit extensive checkpoint responses, and the DSB repair machinery plays a major role in responding to these "damaged" telomeres. Consolidating the seemingly antagonizing functions of DSB repair proteins at and on telomeres is one of the major enigmas in the telomere field today.

ARABIDOPSIS AS A MODEL FOR TELOMERE BIOLOGY

Arabidopsis thaliana is a small flowering plant, and a member of the mustard family, that is widely used as a model organism in plant biology. Although it is not of agronomic significance, *Arabidopsis* offers important advantages for basic research in genetics and molecular biology. It has a small, sequenced genome (125 Mb over 5 chromosomes) and extensive genetic and

physical maps. A rapid life cycle (6-8 weeks per generation), easy cultivation and a prolific production of seeds make *Arabidopsis* an excellent model plant. It also has efficient transformation methods, and a large number of mutant lines and genomic resources are readily available (www.arabidopsis.org).

Arabidopsis telomeres are short, ranging from 2-8kb and do not fluctuate during plant development (68, 159). These properties facilitate the identification of mutations that alter telomere length through simple Southern blotting techniques. Additionally, the presence of unique sequences immediately adjacent to the telomere on eight out of ten chromosome arms facilitates the examination of individual telomeres. The only telomeres that lack unique sub-telomeric sequences are the short arm of chromosome 2 and 4 which each contains rRNA gene clusters (160). Nevertheless, unique sub-telomeric sequences have allowed the development of two PCR based assays to precisely measure the length of individual chromosome arms and detect fusions between dysfunctional telomeres (161).

In the past several years *Arabidopsis thaliana* has emerged as an excellent model system to study telomere biology. The genome sequencing project was finished in 2000, and this allowed the identification of many genes encoding proteins that are homologous to known telomere proteins from other systems (*Arabidopsis* Genome Initiative, 2000).

This small weed shows extreme tolerance to genome instability and major stresses such as DNA damage, chromosome fusions and telomere deregulation (66). Many of the genes involved in sensing and repairing these abnormalities

are essential in other higher eukaryotes, making a detailed analysis of their functions difficult or impossible. In striking contrast, mutations or deletions in many *Arabidopsis* genes encoding functional homologues are often not lethal and allow comprehensive analysis of their functions. Examples include Atr (see above) and DNA Ligase IV (see above). Deletion of either gene is lethal in mammals, yet *Arabidopsis* plants deficient for either are viable (154, 155, 162).

Arabidopsis is a genetically tractable organism. Double and triple mutant combinations can be created by simple genetic crosses, this allows a detailed analysis of multiple phenotypes to decipher the function of each gene, and the function of each gene within a complex pathway or network can be determined. Finally, the strong correlation between many aspects of telomere biology in *Arabidopsis* and mammals suggests that information gained from the study of telomeres in *Arabidopsis* will be applicable to a wide range of organisms besides plants.

In this dissertation, I will first examine the consequences of reestablishing the telomere set point in *tert* mutants, and demonstrate that one generation is not enough to return short telomeres to the *Arabidopsis* set point. Secondly, I present the characterization of two Est1-like proteins in *Arabidopsis*, and show that these two proteins do not function in telomere length regulation. Finally, I address the role of DNA Ligase IV at *Arabidopsis* telomeres and demonstrate that while Lig4 is not required for the fusion of critically shortened telomeres, it is required for telomere length regulation and end protection.

CHAPTER II

REESTABLISHING THE TELOMERE LENGTH SET POINT IN *tert* MUTANTS

INTRODUCTION

Telomeres are the DNA-protein complexes that cap the linear ends of eukaryotic chromosomes. These complexes protect the chromosome end from degradation and prevent fusions with other chromosome ends. Although telomere length varies between different eukaryotes, telomeres are strictly maintained at a species-specific set point. Regulation of this set point involves a large number of different genes: a genome wide screen for genes affecting telomere length in *S. cerevisiae* identified 173 genes whose deletion either increased or decreased telomere length (59). Of the genes identified, 150 were previously unknown to alter telomere length. Moreover, the genes identified function in a multitude of processes, including DNA and RNA metabolism, protein modification, translation, nutrient metabolism and chromatin remodeling (59). This screen illustrates the complex nature of maintaining the telomere set point in each cell.

Although the mechanisms controlling telomere size are not fully understood, telomeric DNA is subjected to both lengthening and shortening activities (60). The combined contributions of both types of activities maintain telomere length homeostasis. In wild type cells, the primary shortening is

thought to occur as a result of incomplete replication of the chromosome end. In this process, known as the end replication problem, a few nucleotides are lost from the 5' end of the daughter strand synthesized by the lagging strand machinery each time a cell divides. Recently, more active processes have been identified that can lead to rapid loss of telomeric DNA. These include Telomere Rapid Deletion (TRD) (61), a recombinational process that occurs on extremely long telomeres, deficiencies in proteins important for protection of the extreme terminus of the telomere (62) and exonuclease activity on uncapped telomeres (63). These telomere-shortening activities are circumvented through the action of telomerase. Telomerase, a unique RNA-dependent DNA polymerase, uses its integral RNA subunit to direct the addition of a species specific repeat to the chromosome ends, thereby compensating for the loss of telomeric DNA. Telomerase is comprised by two essential components; the telomerase reverse transcriptase (TERT), and the telomerase RNA subunit (TR) (1).

Despite the fact that telomere length is maintained at an equilibrium length for each species, this "set point" can vary within species of the same genus. In mice, telomeres in the established inbred mice strains are approximately 40kb, while in wild derived mice the length is much shorter, around 10-15kb (64). In the model plant, *Arabidopsis thaliana*, telomere length varies amongst different

ecotypes, which can be divided into two distinct groups based on telomere length (3). In one group, telomeres ranged from 2-5kb and in the other group telomeres ranged from 3.5-8kb; thus, telomeres that range from 2-8kb are acceptable for *Arabidopsis* (3).

When crosses are made between mice with long telomeres and mice with short telomeres, a new telomere length set point is established in the F1 progeny (163). The new telomere length is intermediate relative to the short and long telomere parents. Telomeres from the short telomere parent are lengthened, but the long telomeres from the long parent are not acted upon and may shorten slightly (163). This observation suggests that telomere elongation by telomerase is limited to the shortest telomeres. Similar to what is seen in mice, crosses between plants with long and short telomeres result in an intermediate telomere length in the F1 progeny (3). This species-specific telomere length is dependent on telomerase; in the absence of telomerase telomere length is no longer maintained at the set point.

Disruption of telomerase activity leads to progressive telomere shortening, defects in cellular proliferation, and an increase in genome instability and infertility (65-70, 164). Although telomeric DNA is lost over successive generations, in mice, phenotypic defects are not observed until the fourth generation (G_4) (65, 164) and the sixth generation (G_6) in *Arabidopsis (66)*.

Telomerase-deficient mice and *Arabidopsis* ultimately reach a terminal phenotype, characterized by severe genome instability and sterility, which occurs by G_6 in mice and G_9 in plants (65, 66).

Interestingly, the damage to chromosome ends in telomerase-deficient mice is reversible. By re-introducing one copy of the TR, telomeres are elongated and progeny show no defects in growth or proliferation (163, 165). In this study we investigated the dynamics of reestablishing the telomere length set point in *Arabidopsis*. Our approach was to cross wild type plants to different generations of telomerase-deficient plants (*TERT*$^{-/-}$) and analyze the telomeres in the F1 progeny from these crosses. Unexpectedly, we found plants lacking telomerase for seven generations can lengthen telomeres when telomerase is reintroduced, but one generation was not sufficient to reestablish the telomere set point.

RESULTS

Generation of plants heterozygous for *TERT*

In the absence of telomerase, *Arabidopsis* telomeres shorten 250-500bp per generation (66). Restoring telomerase activity to plants with short telomeres allowed us to investigate the dynamics of telomeres reestablishing telomere length homeostasis. Although telomeres progressively shorten through successive generations, *tert* mutants are wild type in appearance until $G_{6,}$ when slight decreases in fertility and minor alterations in leaf morphology are observed (66). The onset of phenotypic changes correlates with the onset of chromosome instability, a hallmark of telomere dysfunction. Therefore, we sought to restore the telomere set point in *tert* mutants before, during and after the predicted onset of chromosome instability. Accordingly, we crossed wild type plants to G_5, G_6, and G_7 *tert* mutants.

Of the twenty-eight crosses that were attempted, twelve were successful and produced seeds (Table 1). The crosses were numbered sequentially, and one, two or three siliques, or seed pods, were harvested from each cross. If more than one silique was harvested per cross, they were differentiated by the letter: A, B or C. The overall scheme for the initial characterization of the F1 plants generated is illustrated in Fig. 11A. The resulting F1 seeds were planted and PCR was used to genotype each plant (66), and to verify that they were heterozygous for the T-DNA insertion in *TERT*. As expected, we found that F1 progeny plants were heterozygous for the T-DNA insertion in *TERT* (data not shown).

Table 1. Summary of *tert*-back crosses

Cross #	Mother (♀)	Father (♂)	# of Siliques
1	$G_5$96-17	WT 9	2 (A, B)
5	$G_5$96-15	WT 19	1
9	$G_6$96-4	WT 10	2 (A, B)
12	$G_6$96-4	WT 9	3 (A, B, C)
17	WT 11	$G_6$96-1	1
18	WT 9	$G_5$96-1	1
19	WT 10	$G_6$96-2	1
22	$G_7$96-1	WT 18	1
23	$G_7$96-2	WT 4	2 (A, B)
26	WT 19	$G_5$96-3	2 (A, B)
27	WT 20	$G_5$96-5	2 (A, B)
28	WT 17	$G_7$96-4	3 (A, B, C)

F1 plants have telomerase activity

Previous work has shown that plants heterozygous for a T-DNA insertion in the *TERT* gene have telomerase activity (68). To verify telomerase activity is retained in the F1 progeny of the crosses, telomere repeat amplification protocol (TRAP) assays were performed on one plant from each cross (Fig. 11B and 11C). If more than one silique was harvested, one plant from each silique of that cross was analyzed (Fig. 11C, lanes 6 and 7). As expected, all plants had telomerase activity (Fig. 11C and data not shown).

Telomere length in the F1 progeny

To examine telomere length in the F1 progeny, a terminal restriction fragment (TRF) analysis was carried out on parent plants and their progeny. Prior to creating the crosses, tissue was harvested from each parent and genomic DNA was extracted. Tissue was also harvested from several of the F1 plants, and genomic DNA was extracted. In Fig. 12, the TRF analysis of cross #1 is shown: the mother is a G_5 *tert* mutant with telomeres ranging from 0.65-1.6kb (lane 1) and the father is wild type, with telomeres in the 2-5kb range (Fig. 12, lane 9). Three progeny from two siliques were analyzed. In all progeny, while the bulk of the telomeres were within the 2-5kb range, a long smear of telomeric DNA can be seen trailing from the wild type range down to the shortest telomeres of the G_5 parent (Fig. 12, lanes 2-7). The longest telomeres in the wild type parent were 6kb. However, in the progeny, the longest telomeres were now

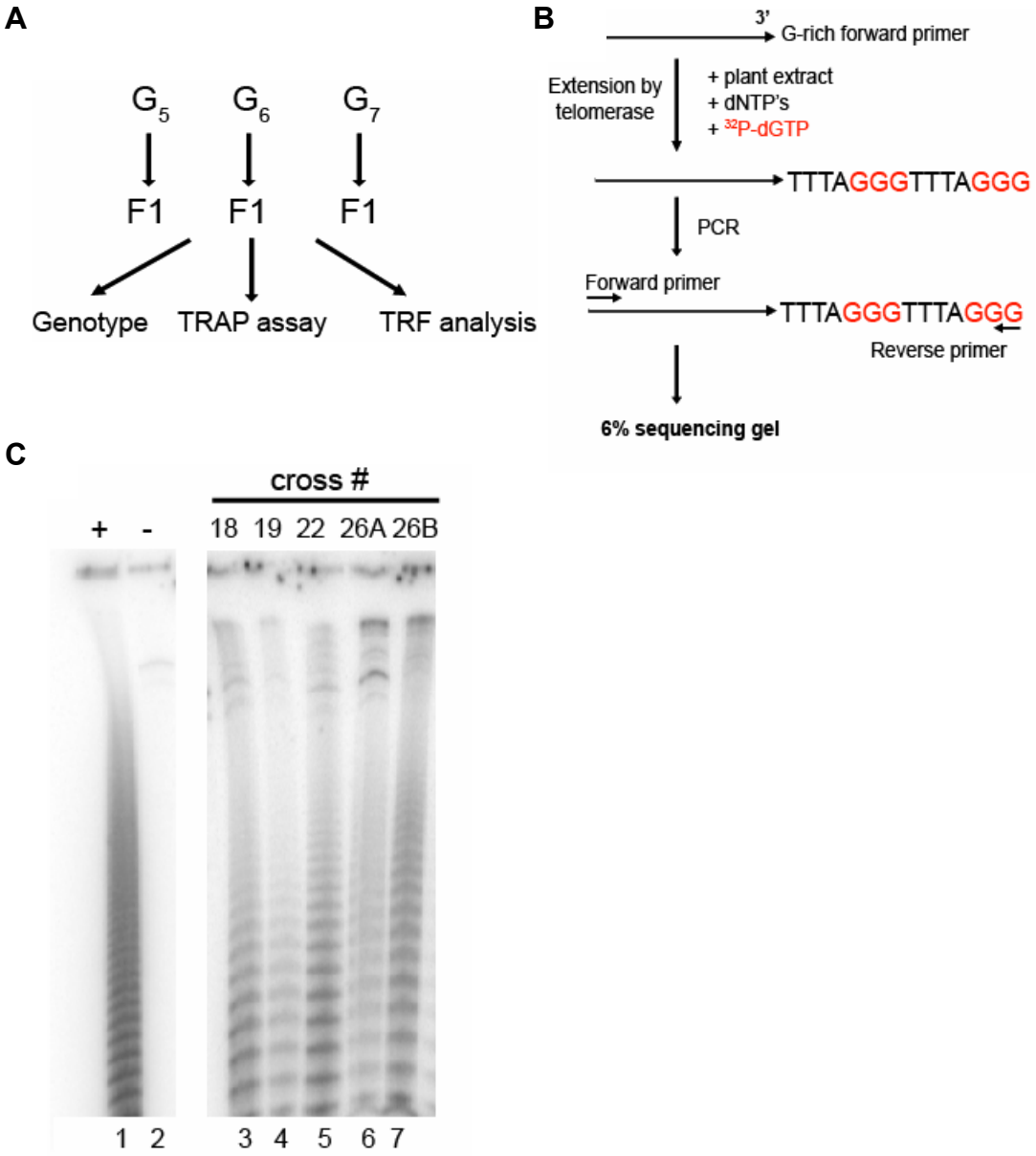

Fig. 11. Characterization of *TERT* heterozygotes. (*A*) Scheme for generation and characterization of progeny from different generations of *tert* mutants and wild type plants. (*B*) Schematic of the TRAP assay. (*C*) TRAP assay, results for several of the F1 progeny of the back crosses.

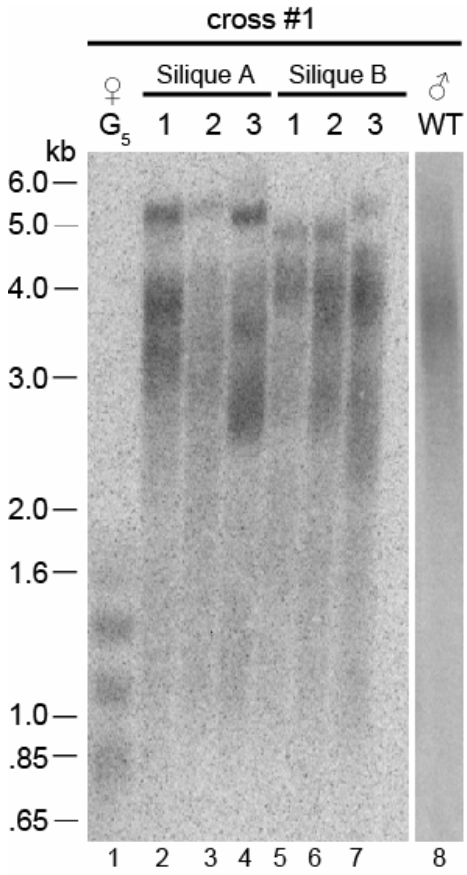

Fig. 12. TRF analysis of cross #1. TRF analysis was performed on genomic DNA from both parental plants (mother, lane 1 and father, lane 8), and three siblings each from two siliques (lanes 2-8).

5.5kb. The loss of 500bp from the longest telomeres is consistent with the complete absence of telomerase action on these chromosome ends (3, 68). These data indicate that not all telomeres are acted upon by telomerase in a plant generation, and suggests that only the shortest telomeres are efficiently extended. Disruption of *TERT* in *Arabidopsis* causes a decrease in the heterogeneity of the TRF profile (66, 68). Instead of a smear of telomeric DNA typical of wild type plants, telomeres in *tert* mutants appeared as sharp bands (Fig. 12, compare lanes 1 and 8). In the F1 progeny of all crosses analyzed, telomeres appeared as long smears, implying that telomerase was re-engaged in maintaining telomere length heterogeneity in these plants.

The shortest telomeres are lengthened relative to the maternal or paternal parent

To investigate whether there were differences in the contribution of the maternal or paternal parent in lengthening of the shortest telomeres, we used G_5 *tert* plants as either the mother or the father in two crosses with one wild type plant. In cross # 5, the wild type plant was the father, while in cross #26 the same wild type plant was the mother (Fig. 13). In both crosses, we see the same result was obtained: the bulk telomeres were within the wild type range, although there was a long smear down to the range of each G_5 parent. Strikingly, a decrease of approximately 500bp was again observed in the longest telomeres of the progeny when compared to the wild type parent. When this experiment was repeated using G_6 instead of G_5, very similar results were obtained (Fig. 14).

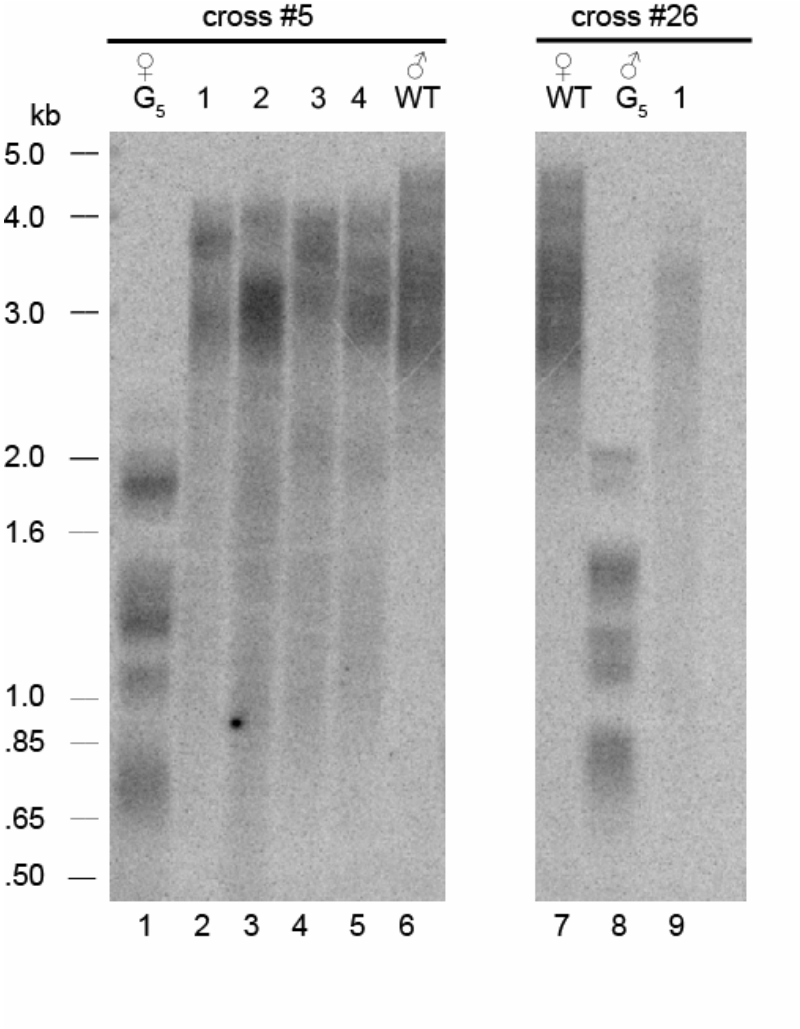

Fig. 13. Telomeres are elongated regardless of which parent contributes the shortest telomeres. TRF analysis of two crosses between one wild type (lanes 6 and 7) and two different G_5 *tert* mutants (lanes 1 and 7). For cross #5, mother is in lane 1, father in lane 6. For cross #26, mother is in lane 7, father is in lane 8. Telomere lengths of the F1 progeny from cross #5 (lanes 2-5) and cross #26 (lane 9) are shown.

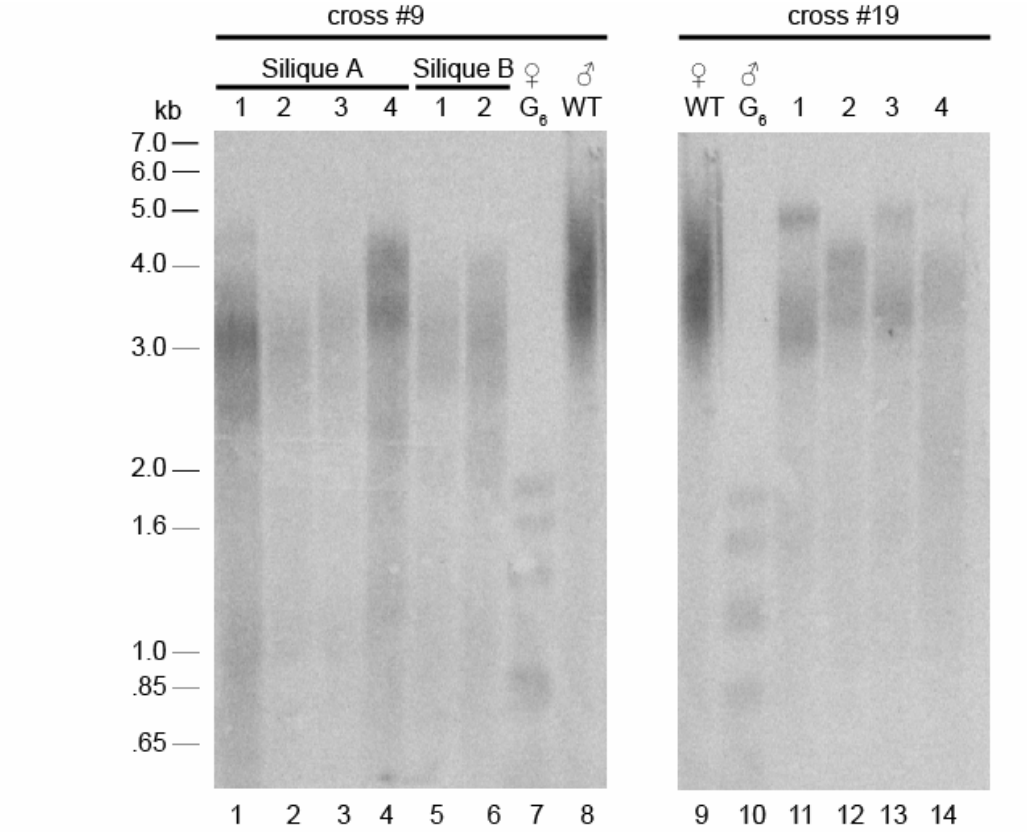

Fig. 14. Telomere length analysis of two G_6 crosses. One wild type plant (lane 8) was crossed to two individual G_6 plants (lanes 7 and 10). For cross #9 (mother in lane 7, father in lane 8), four progeny from silique A (lanes 1-4) and two progeny from silique B (lanes 5 and 6) were analyzed. Four F1 progeny from cross #19 (mother in lane 9, father in lane 10) are shown in lanes 11-14.

These data argue that the shortest telomeres are preferentially lengthened, regardless of whether they come from the mother or the father.

Analysis of individual telomere arms in F1 progeny

To better gauge the dynamics of telomere length regulation, we followed the fate of individual telomeres in the F1 progeny by performing a parent-progeny TRF analysis of three chromosome arms. For comparison, a TRF analysis was performed on all the telomeres from two crosses, cross #22 (G_7 *tert* mother, wild type father) and cross #27 (wild type mother, G_5 *tert* father). Again for the G_5 cross, the longest telomeres from the wild type parent shortened slightly, while the shortest telomeres from the G_5 parent were lengthened (Fig. 15, lanes 5-12).

A different result was obtained for the G_7 cross. In these progeny, while the shortest telomeres were lengthened, the longest telomeres were much shorter than in the wild type parent (Fig. 15, compare lane 2 with lanes 3 and 4). This was also true for another G_7 cross, cross #28 (data not shown). The rate of shortening on the longest telomeres was greater than expected for no telomerase action (66, 68). Occasionally, telomeres in wild type plants undergo a dramatic loss in length. Whether this behavior represents a TRD event similar to what is seen in mammals and yeast (61) remains to be determined.

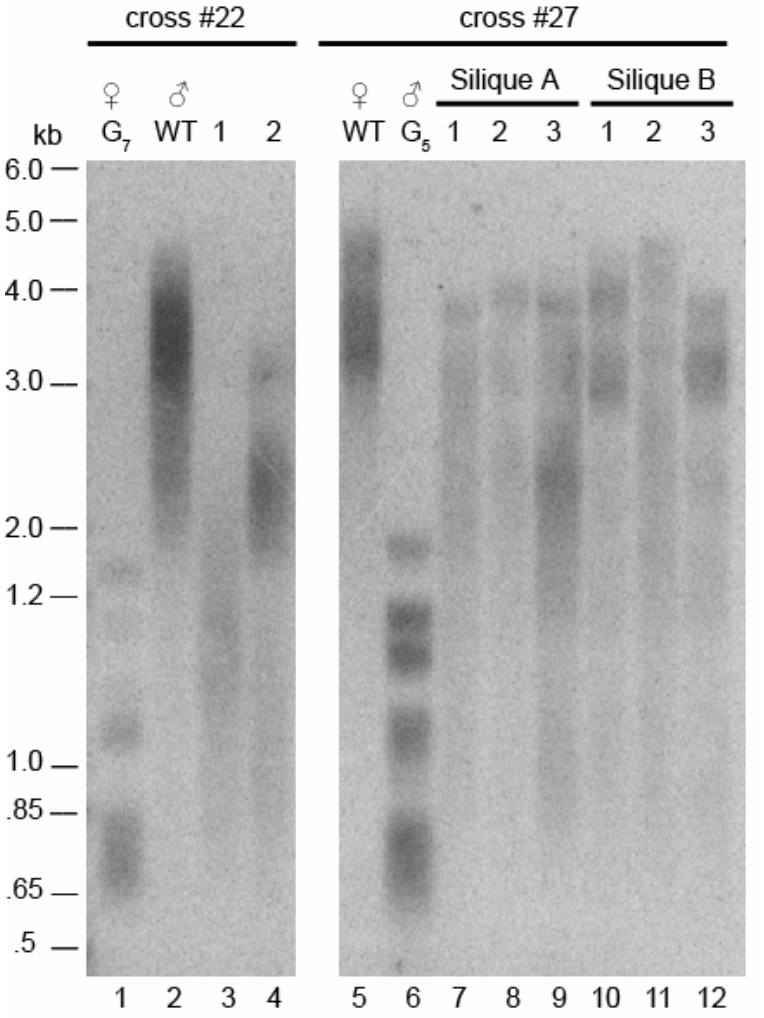

Fig. 15. TRF analysis of cross #22 and cross #27. For cross #22, a G_7 *tert* plant (mother, lane 1) was crossed to a wild type plant (father, lane 2). Two F1 progeny are shown (lanes 3 and 4). For cross #27, a wild type plant (mother, lane 5) was crossed to a G_5 *tert* plant (father, lane 6). Three progeny from two siliques are shown (Silique A, lanes 7-9; Silique B, lanes 10-12).

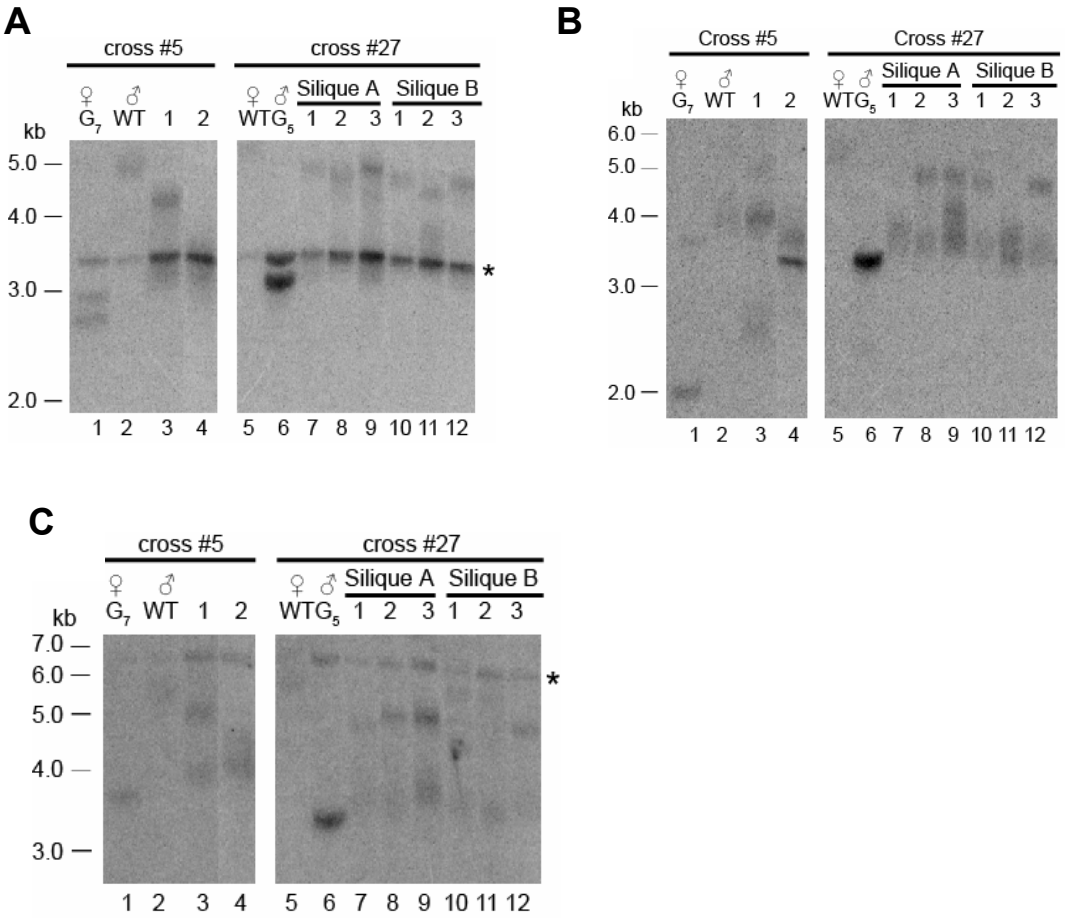

Fig. 16. TRF analysis of individual chromosome arms in the F1 progeny. Parent-progeny TRF analysis of DNA from cross #22 and cross #27 using probes specific for 2R (*A*), 5L (*B*) and 5R (*C)*. Asterisk indicates interstitial band cross-hybridizing to the 2R or 5R probe.

To monitor individual telomere tracts, DNA from the same plants was digested for TRF analysis on three individual telomere arms (Fig. 16), the south arm of chromosome 2 (2R) (Fig. 16A), the north arm of chromosome 5 (5L) (Fig. 16B) and the south arm of chromosome 5 (5R) (Fig. 16C). The data generated for 2R was difficult to interpret due to the presence of an interstial band running approximately in the range of the telomeres for the F1 progeny. This blot was stripped and re-probed for 5R and then 5L. Analysis of each arm showed that telomeres in the F1 progeny fell within the range of the wild type and *tert* mutant parents. In some progeny two distinct bands were seen (Fig. 16C, lanes 3, 7, 8 and 9), while in others only one broad band (Fig. 16B, lanes 7 and 11) were observed. These findings confirm the bulk telomere analysis, and support the idea that telomerase acts on the shortest telomeres. Longer telomeres are refractory to telomerase action, and shorten slightly.

DISCUSSION

Telomeres are not static structures. Instead, they are dynamic and fluctuate in length. Each cell establishes an equilibrium between telomere shortening and lengthening events, thus creating a species-specific telomere length set point (166). In *tert* mutants, telomere length homeostasis is disrupted as the primary mechanism for telomere lengthening has been removed. In this study we explored the kinetics of reestablishing the telomere length set point.

The telomere length set point is not immediately reestablished

The work shown here supports previous data from mice where restoring telomerase activity to telomerase deficient mice allows the preferential lengthening of short telomeres. In one generation, not all telomeres were returned to the murine set point (165). Similarly, in *Arabidopsis*, although the shortest telomeres were lengthened in the F1 progeny, one generation of *TERT* heterozygosity was not enough to immediately return all telomeres to the set point of 2-5kb. Previous work from our lab has shown that *Arabidopsis* telomerase is able to lengthen telomeres up to 4kb in one generation; telomeres in a G_1 *ku70* mutant extend from 2-8kb to 6-12kb (146). We did not see this degree of lengthening in the F1 progeny, the shortest telomeres were only

elongated by approximately 250bp. This suggests that in the presence of very short telomeres, telomerase cannot lengthen telomeres to this extent. Alternatively, the presence of Ku70 at the telomere may suppress lengthening to some degree.

In yeast, telomerase extends telomeres in late S phase (167). However, telomerase does not act at all telomeres in a single cell cycle (168). Interestingly, telomere elongation of an abnormally shortened telomere in yeast returns this telomere to the set point within 50 generations (169). Normal human fibroblasts lack telomerase activity, and telomeres progressively shorten with increased population doublings (PD) (170). However, restoring telomerase activity to these cells 10-15 PDs before they reach senescence restores telomeres to the human set point within 30 PDs (171). This data suggest that multiple cell divisions are required to restore shortened telomeres to the species specific set point.

The number of cellular divisions required to form a mature *Arabidopsis* plant is not known. Perhaps the number of cellular divisions in one plant generation, and thus the amount of time telomeres are accessible to telomerase is not enough to fully restore all telomeres to the *Arabidopsis* set point. This hypothesis would explain why mice are also unable to return all telomeres to the set point in one generation after reinstating telomerase activity. Propagating the

F1 progeny will allow the wild type *TERT* allele to segregate, giving rise to wild type, heterozygous and homozygous *tert* mutant plants. The resulting wild type and heterozygous *tert* mutants will have additional cellular divisions in the presence of telomerase activity, allowing further extension of any telomeres below the set point. Repeating the TRF analysis on these F2 plants will address the number of plant generations needed to reestablish the telomere length set point.

Chromosome instability in the presence of telomerase

When telomerase activity is restored to late generation *tr* mice, in addition to elongating short telomeres, chromosome instability and premature aging are prevented (165). All plants used for crosses in these experiments appeared wild type with none of the phenotypic changes associated with late generation *tert* mutants (66). Previous characterization of *tert* mutants demonstrated only mild phenotypic changes in G_6 and G_7, but very severe phenotypes in G_8 (66). Following the F1 population for successive generations will allow us to test whether re-activating telomerase is sufficient to prevent the phenotypic changes associated with telomerase deficiency.

In this study we did not examine the F1 progeny for the presence or absence of chromosome instability. Typically, dysfunctional telomeres are recruited into end-to-end fusions and can be visualized as anaphase bridges in mitotically dividing cells. It would be very interesting to ask whether these F1 plants have ongoing genome instability, even in the presence of telomerase activity. *Arabidopsis* telomeres have unique sequences adjacent to the telomeric repeats (sub-telomeric sequences), thereby allowing the capture of fusion events by PCR (fusion PCR) and sequence analysis of the fusion junctions (161). A careful parent-progeny analysis using fusion PCR would let us identify any fusion events in the F1 progeny, and allow us to ask several interesting questions. First, are there telomere fusions in the F1 progeny, and secondly, if there are fusions in the F1 progeny, do they persist in the F2 population? Finally, have any fusion events been “healed” by the addition of telomeric DNA, and are they propagated in successive generations?

MATERIALS AND METHODS

Plant material

Plants were grown at 23°C in an environmental chamber under a 16/18-hr light/dark photoperiod. *tert* mutants used in this study were derived from the previously characterized telomerase-deficient line 96 (66). Wild type, *tert* mutants and F1 progeny were genotyped as described previously (66).

Preparation of telomerase extracts and TRAP assays

Protein extracts were prepared from F1 progeny, and TRAP assays were performed as previously described (46). Samples were run on a 6% sequencing gel, dried and subjected to a phophorimager screen overnight. TRAP signals were detected using a STORM PhosphorImager (Molecular Dynamics) and the data were analyzed using IMAGEQUANT software (Molecular Dynamics).

DNA isolation and TRF analysis

DNA from individual plants was extracted as described (66). TRF analysis was performed with *Tru*1I (Fermentas) restriction enzyme and ^{32}P 5' end labeled $(TTTAGGG)_4$ oligonucleotide as a probe (68). Single telomere analysis for the south arm of chromosome 2 (2R), north or left arm of chromosome 5 (5L) and south or right arm of chromosome 5 (5R) was performed as follows: 1μg of

genomic DNA was digested with *Pvu*II and *Spe*I, DNA was separated by electrophoresis in a 0.8% agarose gel and blotted onto a nylon membrane. Telomere adjacent DNA sequences were amplified with primers PAT5l-5 (CAACATGGCCCATTTAA GATTGAACG) and PAT5l-3 (CACATATATGTTTGTTGAGTGTCGC) for the 2R probe; TAS5R-F1 (TACGGTTTAGATGTTTAGGGT) and TAS5R-R1 (CGCTCTCATTGCGAGTGGTA) for the 5R probe; TAS5L-F2 (TGAGTTTGCA TAAAGCGTCACG) and TAS5L-R2 (CGACAACGACGACGAATGACAC) for the 5L probe, and were used for hybridization. Signals were detected using a STORM PhosphorImager (Molecular Dynamics) and the data were analyzed using IMAGEQUANT software (Molecular Dynamics).

CHAPTER III

IDENTIFICATION AND ANALYSIS OF TWO *EST1* SEQUENCE HOMOLOGUES FROM *Arabidopsis thaliana*

INTRODUCTION

In *S. cerevisiae*, five genes encoding components of the telomerase holoenzyme have been identified: *EST1-4* (ever shorter telomeres) (28, 30), and the telomerase RNA subunit, *TLC1 (29)*. *EST1*, the first gene identified, was found using a linear plasmid stability assay (30). This assay takes advantage of the fact that a circular plasmid containing inverted telomeric repeats can be resolved into a linear molecule, which requires telomere formation at the ends for stable maintenance in yeast. The *EST2-4* genes were identified from mutants that could not maintain the linear plasmid (28, 30).

Est1p is a non-catalytic component of telomerase associated with the telomerase RNA subunit (33). Deletion of *EST1* leads to progressive telomere shortening and a senescence phenotype (30). Nucleic acid binding studies using recombinant Est1p indicate it is a single-stranded telomere end binding protein with non-specific RNA binding activity (34). Est1p also physically interacts with Est4p (Cdc13p), another non-catalytic component of telomerase (35). Cdc13p is a multifunctional telomere binding protein that recognizes the single-strand G-overhang. Although both Est1p and Cdc13p bind single stranded telomeric DNA, Cdc13p has almost a 100-fold higher affinity for DNA than Est1p (34, 36).

Additionally, Est1p requires a free 3'end for binding single stranded DNA, while Cdc13p is able to bind single stranded DNA without a free 3' end (34, 36).
The recruitment model for the role of Est1p in yeast telomere maintenance, (Fig. 17A), proposes that in late S phase, Est1p recruits telomerase to telomeres through its interactions with Cdc13p and *TLC1* (27). Chromatin immunoprecipitation (ChIP) experiments performed on synchronized cells found that Est1p, Est2p (TERT) and Cdc13p are telomere-associated during late S phase, supporting the recruitment model (172). However, these ChIP experiments also found that Est2p, but not Est1p, was associated with telomeres prior to late S phase, which led to the activation model for Est1p function. In the activation model (Fig. 17B), telomerase is bound at the telomere in an inactive state. In late S phase, the association of Est1p with Cdc13p and *TLC1* converts telomerase to an active form that allows for telomere elongation (172). More recently, a third model, the sequestration model (Fig. 17C) was proposed based on protein tethering experiments (173) and ChIP experiments (174). In this model, the Ku heterodimer recruits telomerase to telomeres in G1 via its interaction with TLC1 and this renders telomerase inactive. In late S phase, Est1p becomes telomere-associated and recruits telomerase to the telomere end by interaction with both *TLC1* and Cdc13p, promoting telomere elongation (173, 175).

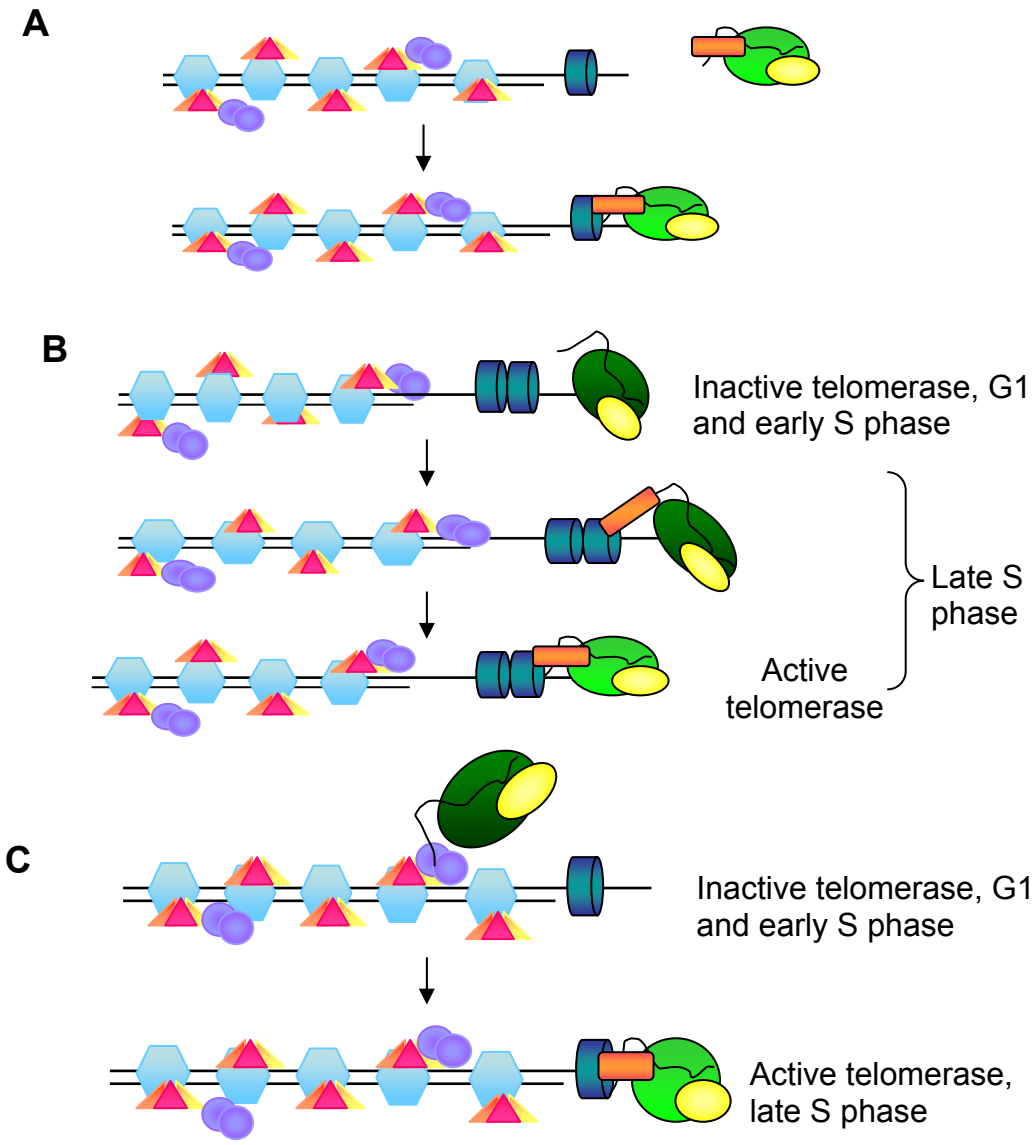

Fig. 17. Models for Est1p's role in telomere elongation. (*A*) Recruitment model. Est1p recruits telomerase to the telomere through interactions with TLC and Cdc13p. (*B*) Activation model. Inactive telomerase is bound at telomeres. Upon association of Est1p with the inactive, telomere-bound telomerase and Cdc13p, telomerase is converted to an active form. (*C*) Sequestration model. Ku70p sequesters telomerase at an internal telomeric location. Activation of telomerase occurs upon association of Est1p-Cdc13p, whereby telomerase is translocated to the end of the telomere.

Although Est1p was originally identified in yeast, homologues have been identified in many higher eukaryotes, including humans, *Caenorhabditis elegans*, *Drosophila* and *Arabidopsis thaliana*. Most of these higher eukaryotes have more than one ScEst1p sequence homologue (37, 38). Alignment of all sequence homologues of Sc Est1p allowed the identification of conserved domains (Fig. 18). These include an EST1 domain located at the N-terminus, a tetratricopeptide (TPR) domain implicated in protein-protein interactions that is located slightly C-terminal to the EST1 domain, and the PilT (PIN) domain, found in enzymes that ligate divalent cations. The PIN domain is located in the C-terminus of several Est1 sequence homologues, but not all (Fig. 18) (37).

Of the three Est1-like proteins found in humans, hEst1a is the best characterized. Human Est1a was found to have single-stranded telomeric DNA binding activity *in vitro* (38), and to directly interact with TERT *in vitro* (38). Immunoprecipitation experiments showed that hEst1a was associated with telomerase activity *in vivo* (37, 38).

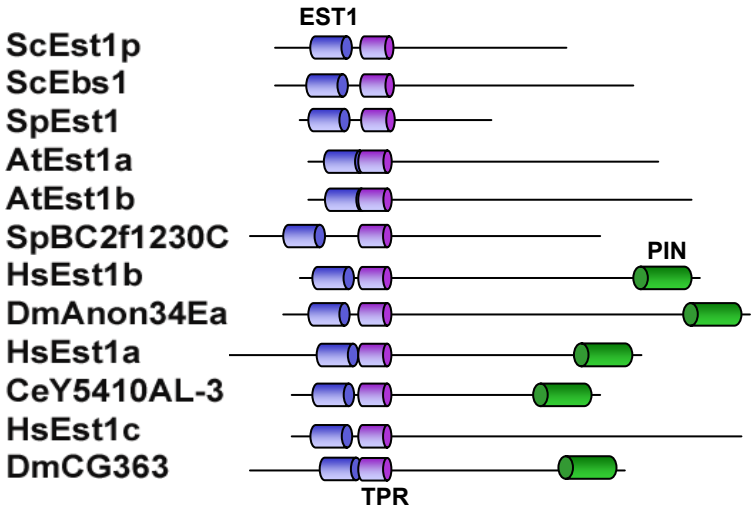

Fig. 18. Alignment of Est1 sequence homologues. The EST1 domain is in blue, the TPR domain in purple and the PIN domain in green. Sc-*Saccharomyces cerevisiae*, Sp- *S. pombe*, DmAnon-*A. gambiae*, Dm-*Drosophila*, Hs- *Homo sapiens*, Ce-*C. elegans*, At-*Arabidopsis thaliana*.

When telomeres are dysfunctional, they are recruited into chromosome fusion events involving other dysfunctional telomeres, creating end-to-end fusions and dicentric chromosomes. Such chromosomes then enter the breakage/fusion/bridge (B/F/B) cycle which involves the repeated fusion, bridge and breakage of chromosomes. Covalently fused chromosomes can be visualized as anaphase bridges during mitosis when the centromeres on dicentric chromosomes are pulled to opposite poles. Although one group found that overexpression of hEst1a induced anaphase bridges, but did not significantly perturb telomere length (37), another group reported that overexpression of hEst1a and hTERT lengthened telomeres (38). Together these results implicate hEst1a in telomerase recruitment and telomere capping.

Within the Est1 protein family are two predicted proteins from *Arabidopsis thaliana* (Fig. 18) (37, 38). To determine whether one or both of theses proteins are the *Arabidopsis* Est1 homologue, we examined the role of both proteins at telomeres in *Arabidopsis.*

RESULTS

Identification of *EST1a* and *EST1b* in *Arabidopsis thaliana*

The genes encoding putative Est1 orthologs from *Arabidopsis* (Fig. 19B) were identified in a Position Specific Iterated (PSI) –BLAST search (www.ncbi.nlm.nih.gov/blast/Blast). PSI- BLAST is the most sensitive of all BLAST searches and is used to identify distantly related proteins. Using amino acids 100-300 of the *K. lactis* Est1 (AAG49579) as the query against the non-redundant (nr) database, the first iteration of PSI-BLAST identified ScEst1p, ScEbs1p and SpEst1p. All three were added to the *K. lactis* sequence to create a position-specific scoring matrix (PSSM), which was then used to search the nr database. In the second iteration, a human protein (BAA344521) and *Arabidopsis* protein (AAF98429) were identified. The *Arabidopsis* protein was used as a query in a BLAST search against the *Arabidopsis* database. This search identified a protein that was 28% identical to the query sequence (Fig. 19B). These genes were named *AtEST1a* (At1g28260) and *AtEST1b* (At5g19400). When a phylogenetic tree of the Est1-like proteins was created (Fig. 19A) the *Arabidopsis* Est1 homologues are most closely related to hEst1c. There is currently nothing known about the function of hEst1c. All of the yeast Est1-like proteins cluster together as do all Est1-like proteins from higher eukaryotes.

Full-length cDNAs for both AtEst1a and AtEst1b were obtained by RT-PCR using primers directed to the predicted start and stop codons. *AtEST1a* has

A

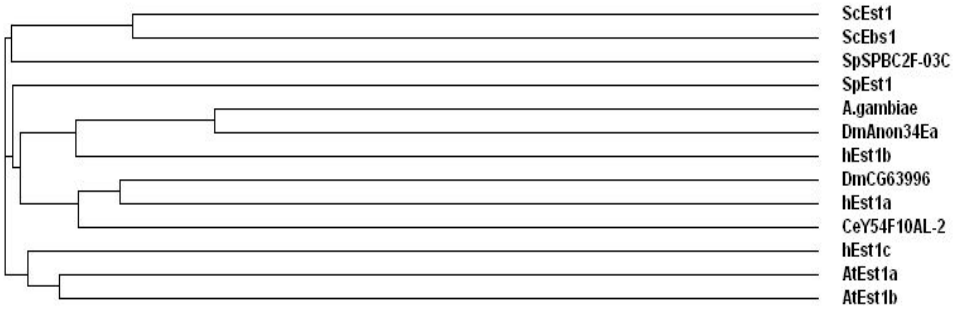

B

```
          10        20        30        40        50        60        70        80        90       100       110       120       130
          |--------+---------+---------+---------+---------+---------+---------+---------+---------+---------+---------+---------|
Est1a     MEANSADQKQKPNFLVEVNNIEKQLWTLIHSKTILHTDVS-ELYAKAGSTYEQIFKSNLQHEELQEVEFCLWKLHYKHIDEFRKGLK------TNDHAKHMKA-------------FKLFLSKAAEFYQN
Est1b      MTLQMDKTTASSSWERAKSIYDEIAELANKRQKAGNPPDPNLLQLLREKYEAILESHTFSEQHNIEIPLWQLHYKRIEYFRLHINRVLASSTSTAAQNVKGPSKAEQIAQLKLQFRTFLSEATGFYHD

          131       140       150       160       170       180       190       200       210       220       230       240       250       260
          |--------+---------+---------+---------+---------+---------+---------+---------+---------+---------+---------+---------|
Est1a     LISKVRGYY-------------HRLSEESGE-----QKSRFLCHRFYICLGDLQRYQEQYLKAHEHPN-WSTAATYYLEAAKSWPDSGNPHNQLAVLATYVSDELLALYHCVRSLAVKEPFPGASNNLLL
Est1b     MILKIRSKYGLPLGSFSEDQQSQNLSDKDGKELAEVQKALKSCHRCLIYLGDLARYKGMYAEGDSRSRQYASASSYYLQAASLWPASGNPHHQLAIVASYSRDEFVTTYRYFRSLAVEYPFPTARDNLIV

          261       270       280       290       300       310       320       330       340       350       360       370       380       390
          |--------+---------+---------+---------+---------+---------+---------+---------+---------+---------+---------+---------|
Est1a     LFEKNRSS--PLQSLSTDAEFNYLNPSEKK-VSVKERDLSKAKGELVAGIDLWPLVVRTTSFFFLKSSFDEFGRAFASTIRELDAAFAADDRNLEAMLESYQF---MDTARKGPYKILQIVAVFIYIFHN
Est1b     AFDKNRQSYEKLFVPSKDSSKRLTGKGRGKGADISLKDATLVAGPEKDKVTIANEMLKAFSIRFVHLNGILFTRTSLETFFDVLASTSSSLREVISLGSAKELTLGIDTSDSALFIVRVVTMLIFSVHNS

          391       400       410       420       430       440       450       460       470       480       490       500       510       520
          |--------+---------+---------+---------+---------+---------+---------+---------+---------+---------+---------+---------|
Est1a     LAEANGSDIVK--EEVKLTNLALTMVFIVMGRVVERCLKTTPLDSCPLLPALLVFLDYL---PFLLDKVEEEEEECRFDEKSKSAISYFFGKLVDILNQL--KVKDKNC----------PAKTLLALWED
Est1b     KKETEGQSYAEIVQRVEPARNSLTASFELLGLVIEKCVQLGDPSSSYFLPGVLVFVEWLACCPDIALGSDPDDRQTAVRNSFWNQFVVFFNQVLSLGPTFIDDVEDETCFSNMSLYDERETENRLALWED

          521       530       540       550       560       570       580       590       600       610       620       630       640       650
          |--------+---------+---------+---------+---------+---------+---------+---------+---------+---------+---------+---------|
Est1a     HELKSLAPLAPIHALLDFSSNMDLRESFDRGKELRLQRIISSAIDITTRQKKGSQKWLFFDNQRTHFYT----TSGELQSNGELFHGNGEGRNRKCVTIGPVEIIPLENERSVPVEEE--EVILLKPLV-
Est1b     YELRGFLPLLPAQTILNFSRKHSFGTEGPKEKKARIKRIFAAGKALTSVIKV-DQNHVYFDSKKKKFLVGVKPADDFLDSHSSPPKACNALQDNQVMIDHNSPIMQLDQQIYMGEEDDDEVIVFKPLVT

          651       660       670       680       690       700       710       720       730       740       750       760       770       780
          |--------+---------+---------+---------+---------+---------+---------+---------+---------+---------+---------+---------|
Est1a     --RCQSAPIYSSGIAAKPLSSDCTTSGNQTTTSNDSL----RRTLSLIGSESFSFTQGL---------KDTDPQHLHLEEGTVSGRPPS------LSAWVVDKNKEKGRLGLSKPNGLGPIDETGPVSAF
Est1b     EKRKEASDQIYVPSGGFRKSDQVTTMGDFKALSGSDVAFHENQILQARGNASIQVPASVGANLLGPLQPSTQSQAMHMQQVQTQVQVPASVGANLLGLLLTSTQSQAMHMQQVQTQAVNP-QPAQSLAAS

          781       790       800       810       820       830       840       850       860       870       880       890       900       910
          |--------+---------+---------+---------+---------+---------+---------+---------+---------+---------+---------+---------|
Est1a     DSLSINSSTEHPASSYSPPTPSAPLLPEDASWFHNDASTNKAESFYDQTRYMELPGIMKPYTNPPFVGISSSEWLRRYRESRNLGPAYSYQAQGTNNLRNFMAHGSSKFSLLARYGTPNDSSQNSTFHPQ
Est1b     RLQPIQSQVAQPLPSRVVHFQQTQAQVSHVSPAHSQSTSFGGGSKWSPEEAASLASSLSGFAQLGNGHVMRNEMQGNHGVSYYPAHSLPVHQSYNGNGMGGMPYSQSRTPEAVFPPKIDPVLSSGVVADG

          911       920       930       940       950       960       970       980       990      1000      1010      1020      1030      1040
          |--------+---------+---------+---------+---------+---------+---------+---------+---------+---------+---------+---------|
Est1a     LYMEDHESRGEKLGNVQQSTTNPYGFSDDPGPFLRFLREKEWLNENGQRLRGPPPPAYMNN
Est1b     LGVQSSLAKKNPISRAFRHLGPPPGFNSVPAKLQKEPAPGSELSGNNH-LPVDDYSWLDGYQAQSSRGVGLNSSLNYATSGKPEHLGSTGNGLNGPANFPFPGKQVPTSQVQADFPYFQNPQKDNFVDKN

          1041  1050      1060      1070      1080      1090  1096
          |--------+---------+---------+---------+---------+-----|
Est1a
Est1b     HQSTQLPEQYQGQSTWSSRHFDTAHVGEEICGNKNEWFCGIDRSKVPFSCYLRWRC
```

Fig. 19. Alignment and phylogenetic tree of the *Arabidopsis* Est1-like proteins. (*A*) Phylogenetic tree of Est1 sequence homologues. This tree was calculated with ClustalW (http://www.ebi.ac.uk/clustalw/) from the alignment shown above. AtEst1a and AtEst1b are most closely related to hEst1c. Additionally, all yeast Est1 like proteins cluster together, as do all Est1-like proteins from higher eukaryotes. (*B*) Alignment of predicted AtEst1a and AtEst1b proteins. Identical/similar residues are shown in red.

five exons (Fig. 20A) and encodes a protein of 880 amino acids (100 kDa), while *AtEST1b* has six exons (Fig. 20B) and encodes a protein of 1093 amino acids (120 kDa). To determine whether these genes are expressed, RT-PCR was performed on several *Arabidopsis* tissues. *AtEST1a* and *AtEST1b* were expressed in all tissues examined (Fig. 20C). The AtEst1a and AtEst1 b expression profile differs from that of the telomerase catalytic subunit, which is only expressed in rapidly dividing tissues (46).

Expression of recombinant proteins

The full-length *AtEST1a* and *AtEST1b* cDNAs were cloned to yield proteins, 100kDa and 120kDa, respectively, with an N-terminal T7-tag and a C-terminal 6X His-tag (Fig. 21B, lanes 1 and 2). We also cloned the 3' 1.6Kb of the *AtEST1a* cDNA (AtEst1a-Cterm), and expression of this clone yielded the predicted 53kDa protein with a N-terminal T7-tag and C-terminal 6X His-tag (Fig. 21A). To facilitate its expression, the *AtTERT* cDNA was cloned in three overlapping fragments: N-TERT (amino acids 1-513), M-TERT (amino acids 328-670), and C-TERT (amino acids 519-1124) (Fig. 21B, lanes 3-5). Expression of AtEst1a and AtEst1a-Ct in *E. coli* was verified by western blots analysis on *E. coli* extracts (Fig. 21C). Only the C-terminal fragment of AtEst1a was expressed in *E. coli*, but this polypeptide was soluble (Fig. 21C, lane 5). AtEst1a-Ct was purified by Ni-NTA affinity chromatography, and the fractions checked by SDS-PAGE for the presence of AtEst1a-Ct (Fig. 21D). Although

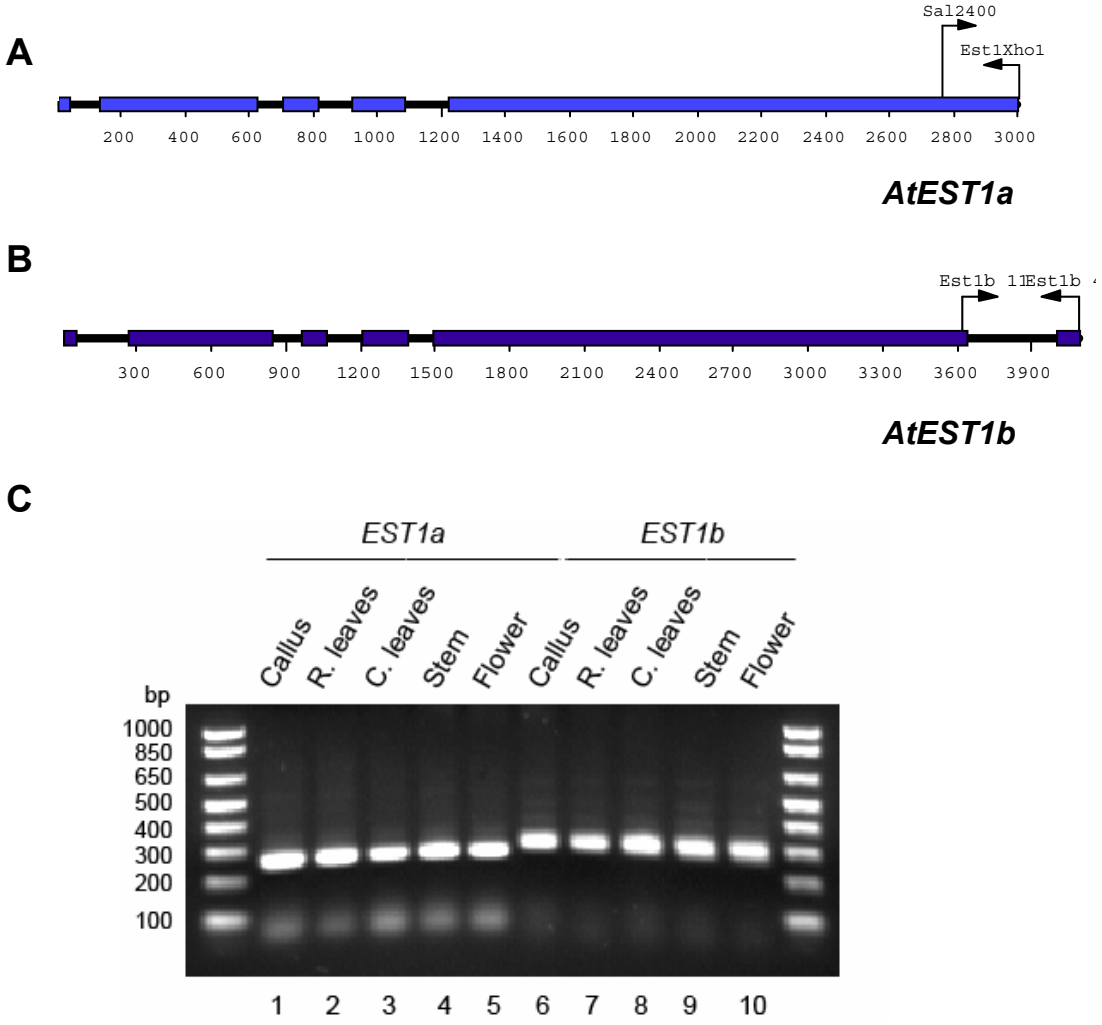

Fig. 20. Gene structure and expression of *AtEST1a* and *AtEST1b*. (*A*) Gene structure of *AtEST1a,* blue boxes represent exons. Primers used for RT-PCR are shown. (*B*) Gene structure of *AtEST1b*, blue boxes represent exons. Primers used for RT-PCR are shown. (*C*) RT-PCR analysis of *AtEST1a* and *AtEST1b* expression in *Arabidopsis*. First strand was generated using 1μg total RNA and oligo dT, followed by 40 cycles of PCR using gene specific primers. Control primers, flanking an intron-exon border for *AtKU70*, were used to verify there was no genomic DNA contamination (data not shown). Both *AtEST1a* and *AtEST1b* are expressed in all tissues examined.

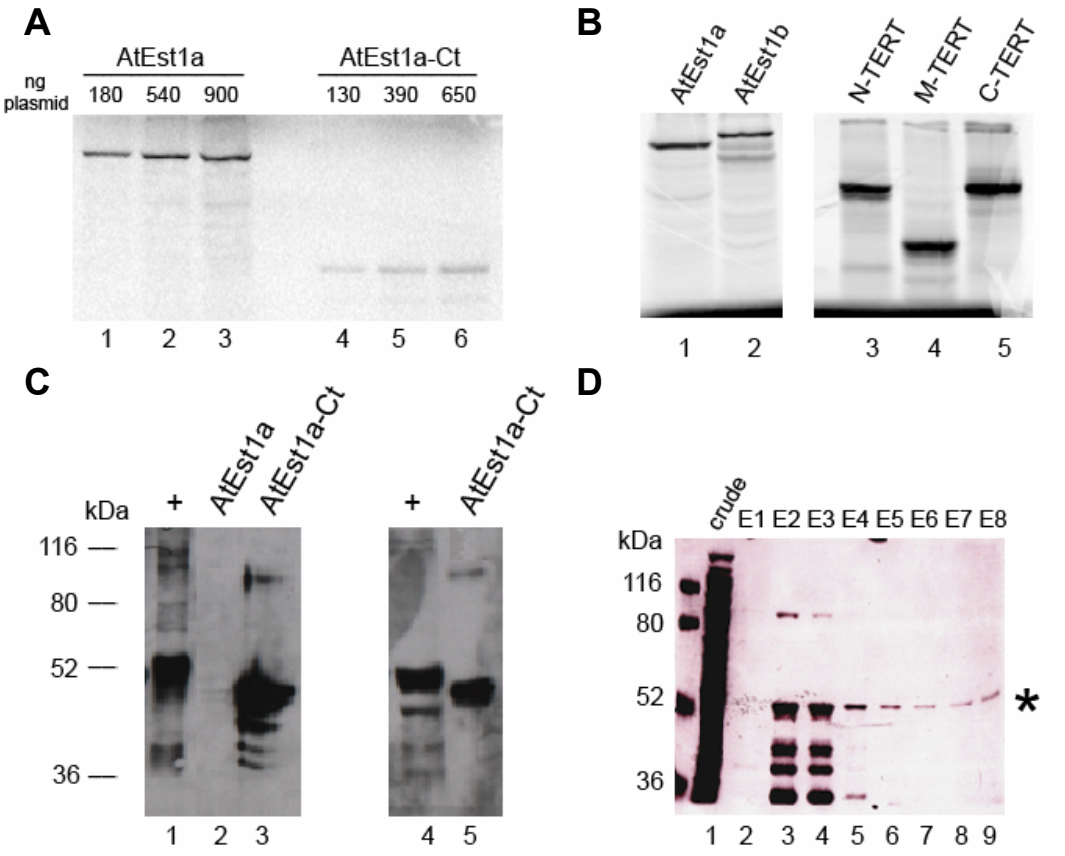

Fig. 21. Expression of recombinant proteins**.** (*A*) Expression of AtEst1a and AtEst1a-Cterm in rabbit reticulocyte lysate (RRL) using increasing amounts of plasmid. Proteins were labeled with ^{35}S-methionine. (*B*) Expression of proteins in RRL for use in coimmunoprecipitation experiments. Proteins were labeled with ^{35}S-methionine; full length AtEst1a (lane 1), full length AtEst1b (lane 2), N-TERT (lane 3), M-TERT (lane 4) and C-TERT (lane 5). (*C*) Western blot. Crude extracts from cells containing either AtEst1a or AtEst1a-Cterm constructs were run on a 10% SDS-PAGE and subjected to immunoblotting analysis using T7-tag antibodies (Novagen), lanes 2-3. AtPot2 (+) was used as a positive control for the Western blot (Shakirov *et. al.* unpublished data), lanes 1 and 4. Cells expressing AtEst1a-Cterm were harvested, spun down and sonicated. The crude extract was spun and the supernatant run on a 10% SDS-PAGE and immunobloted. Products were detected using a T7-tag antibody (Novagen). (*D*) Purification of AtEst1a-Cterm on a Ni-NTA column. Crude extract and eluted fractions (E1-E8) are shown. Asterisk indicates position of AtEst1a-Ct.

AtEst1a-Ct eluted in fractions 2-8, the first three fractions had a large amount of contaminating proteins. Therefore, these fractions were excluded and only fractions 5-8 were combined (Fig. 21C, lanes 6-9) and concentrated. Protein concentration was determined by a Bradford assay and the purified AtEst1a-Cterm fragment was used in electrophoretic mobility shift assays (EMSAs).

Nucleic acid binding properties of AtEst1a-Ct

Since DNA binding activity was observed with *S. cerevisiae* Est1p C-terminal fragments (34), we examined AtEst1a-Ct for DNA binding activity. AtEst1a-Cterm bound single-stranded *Arabidopsis* telomeric repeat DNA $(TTTAGGG)_n$ (Fig. 22). A minimum of five repeats was needed to detect binding, although binding was best when six repeats were used (Fig. 22 and data not shown). The protein failed to bind double stranded telomeric DNA, or a complementary telomeric C-strand oligonucleotide $(CCCTAAA)_6$ (data not shown). Two protein-nucleic acid complexes were observed (Fig. 22, lanes 2 and 3). Formation of the complexes appears to be specific as binding was competed by a 100-fold excess of cold telomeric oligonucleotide (Figure 22 lanes 3, 4 and 5), but required a 550-fold excess of a non-telomeric oligonucleotide to compete to the same extent (Fig. 23, compare lanes 3 and 6). Six repeats of the human telomeric sequence, TTAGGG, competed almost as well as six repeats of *Arabidopsis* telomeric DNA. Suggesting that the AtEst1a C-terminus has a relaxed specificity for G-rich telomeric DNA.

The ScEst1p displays non-specific binding to large RNA's (34).

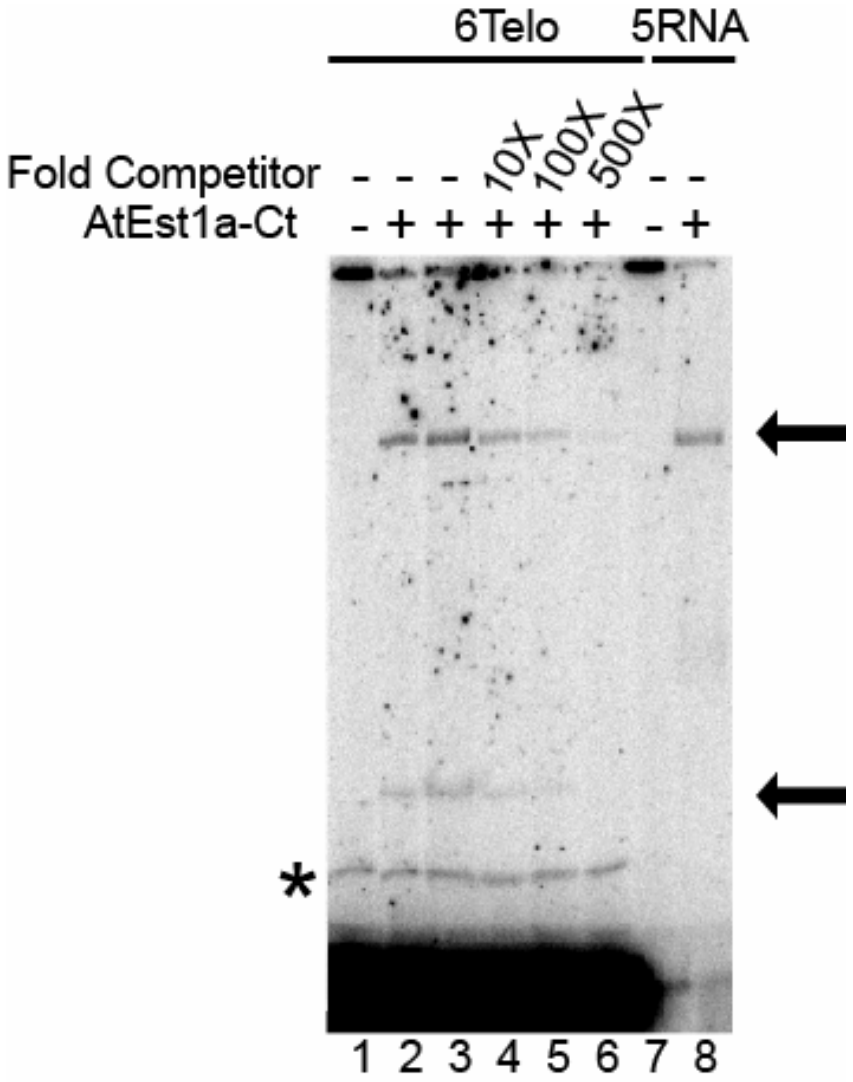

Fig. 22. Nucleic acid binding properties of recombinant AtEst1a-Cterm. Electrophoretic mobility shift assays (EMSAs) were performed with protein expressed in *E. coli*. Input 5' end-labeled probe was incubated in the presence or absence of Est1a-Cterm. Oligonucleotides used were 6Telo $(TTTAGGG)_6$ (lanes 1-6) and 5RNA $(UUUAGGG)_5$ (lanes 7-8). Arrows indicate specific complexes and the asterisk denotes a non-specific complex.

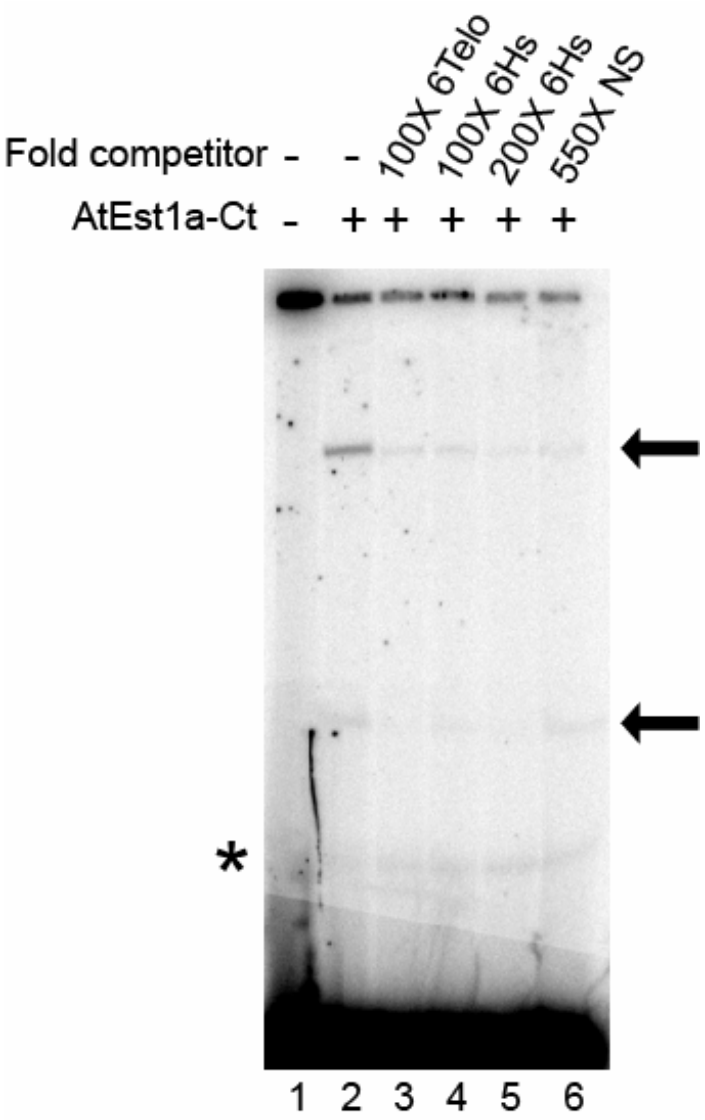

Fig. 23. The binding of AtEst1a-Cterm to single-stranded telomeric DNA can be competed by *Arabidopsis* and human telomeric DNA. EMSAs were performed with protein expressed in *E. coli*. Input 5' ^{32}P labeled probe was incubated in the presence or absence of AtEst1a-Cterm. Oligonucleotides used were 6Telo $(TTTAGGG)_6$ (lanes 1-6), 6Hs $(TTAGGG)_6$ (lanes 4-5), and NS (45 bases of non-telomeric DNA, land 6). Arrows indicate specific complexes and the asterisk denotes a non-specific complex.

Similarly, we found that AtEst1a-Cterm bound single stranded RNA oligonucleotide containing a sequence complementary to five *Arabidopsis* telomeric repeats (Fig. 22, lanes 7 and 8), as well as the *Euplotes crassus* telomerase RNA (data not shown). Therefore, AtEst1a-Cterm displays similar nucleic acid binding properties as ScEst1p.

Physical interactions of AtEst1a and AtEst1b

Human Est1a physically interacts with hTERT, and unlike Sc Est1p, this interaction does not require the telomerase RNA subunit (38). To determine whether *Arabidopsis* Est1a or Est1b bind AtTERT we performed a coimmunoprecipitation experiment using proteins expressed in RRL (Fig. 21A and 21B). In this experiment if the T7 tagged protein interacts with the ^{35S}Met labeled protein, both proteins are brought down in the pull-down with the T7-antibody conjugated beads (pellet, P) (Fig. 24A). If there is no interaction, the ^{35S}Met labeled protein will remain in the supernatant (S) and will not pellet with the beads. As controls, *Arabidopsis* Ku70 and Ku80 were used (43). T7-Ku70 was incubated with either Ku70 or Ku80 (synthesized in the presence of ^{35}S-Met, asterisk), and subjected to coimmunoprecipitation using T7 antibody agarose beads. As expected, Ku70 did not homodimerize with Ku70 (Fig. 24B, lanes 1 and 2), but did interact with Ku80 (Fig. 24B, lanes 3 and 4). To verify there were no non-specific interactions between the recombinant proteins and the beads, labeled proteins were added to T7 antibody beads and subjected to coimmunoprecipitation.

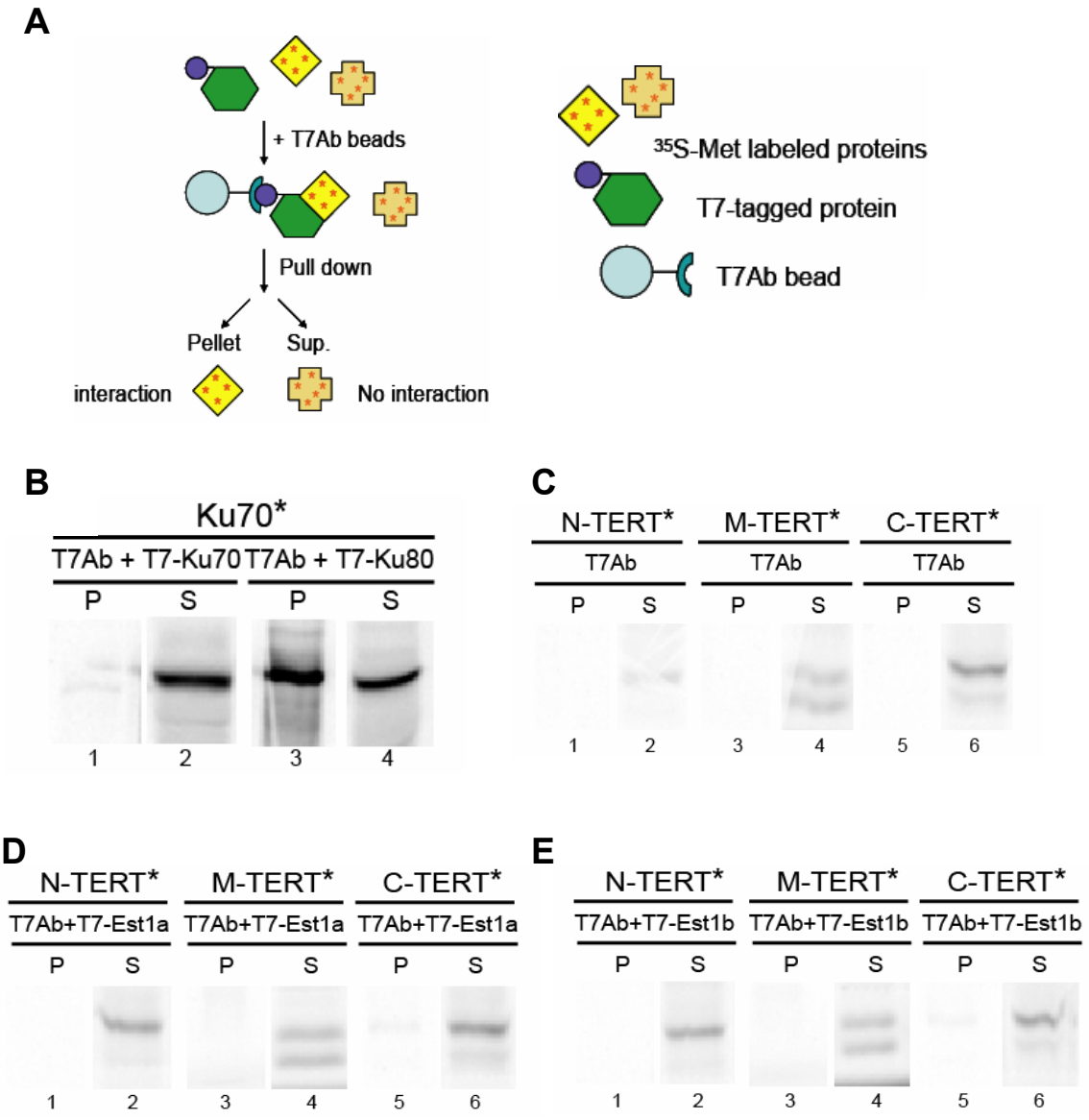

Fig. 24. *In vitro* interactions of AtEst1a and AtEst1b with AtTERT. (*A*) Schematic of coimmunoprecipitation. (*B*) Co-IP of T7-Ku70 with radiolabeled (asterisk) Ku70 and Ku80. P=pellet, S= sup. (*C*) Control pull down assays. Radio-labeled N, M and C-TERT (asterisk) do not interact with the beads. (*D*) Co-IP of T7-AtEst1a with radio-labeled N, M and C-TERT (asterisks). (*E*) Co-IP of T7-AtEst1b with radio-labeled N, M and C-TERT (asterisks). All products were run on 10% SDS-PAGE and visualized by autoradiography.

None of the three TERT constructs nor any of the other proteins interacted with the T7 antibody beads (Fig. 24C; and data not shown). To test for interactions between the Est1 proteins and TERT, T7-Est1a or T7-Est1b was incubated with one of the three TERT fragments (all TERT fragments were synthesized in the presence of ^{35}S-Met, asterisk), and subjected to coimmunoprecipitation using T7-antibody beads. As seen in Fig. 23D and 23E, we detected no interactions between AtEst1a, AtEst1b and N-, M- or C-TERT. Although there appears to be a weak interaction between C-TERT and both Est1a (Figure 24D, lanes 5 and 6) and Est1b (Figure 24E, lanes 5 and 6), this interaction was not reliably reproducible.

Identification and Characterization of T-DNA insertions in *AtEST1a* and *AtEST1b*

To examine the role of AtEst1a and AtEst1b *in vivo*, we obtained *Arabidopsis* lines harboring T-DNA insertions in each gene (Figs. 25-29). *Agrobacterium tumefaciens* will integrate T-DNAs randomly into the *Arabidopsis* genome using sequences located at either end of the T-DNA. Plants heterozygous for each T-DNA insertion were identified by PCR and self-pollinated to produce wild type, heterozygous and homozygous mutant lines.

To establish the genotype of the mutant plants, PCR was employed using a primer directed at the left border of the T-DNA and a gene specific primer. For *AtEST1a*, two lines were identified, *est1a-1* and *est1a-2*. The *est1a-1* line was identified from a screen of 60,480 lines established by University of Wisconsin (176) and is in the WS ecotype of *Arabidopsis* (Fig. 25A). The insertions site

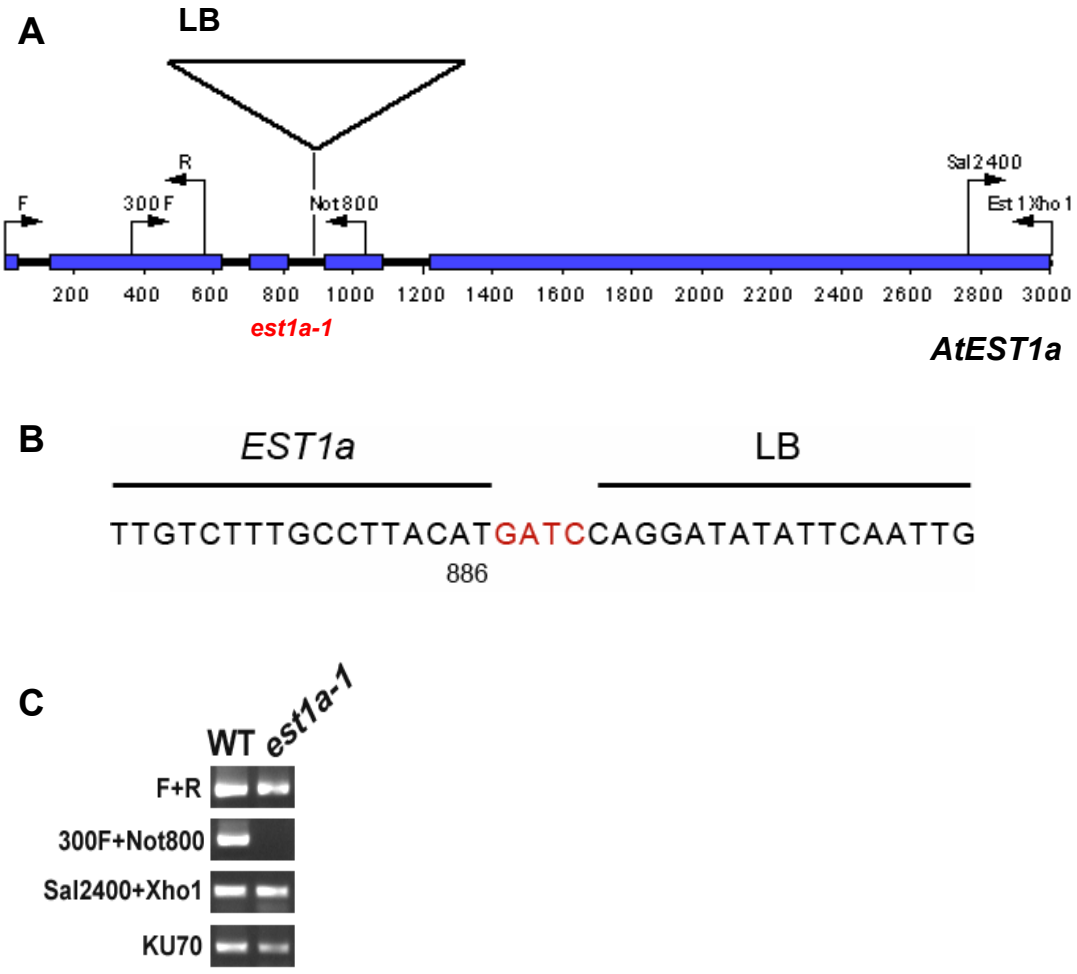

Fig. 25. Mapping and characterization of the insertion site in *est1a-1*. (*A*) *AtEST1a* gene structure, exons are in shown in blue. The T-DNA insertion site and position of left borders are indicated. (*B*) Sequence analysis of the junction between the T-DNA and *AtEST1a*, filler DNA is shown in red. Number indicates the first nucleotide of *AtEST1a* at the junction. We were unable to amplify a product using RB or LB primers for the other side of the insertion in *est1a-1*. (*C*) Analysis of *AtEST1a* expression by RT-PCR. Total RNA was prepared from flowers and subjected to cDNA synthesis by reverse transcription. Transcripts were amplified by 40 cycles of PCR with indicated sets of primers. Control RT-PCR was done using primers that were specific for *AtKU70*, and 40 cycles of PCR.

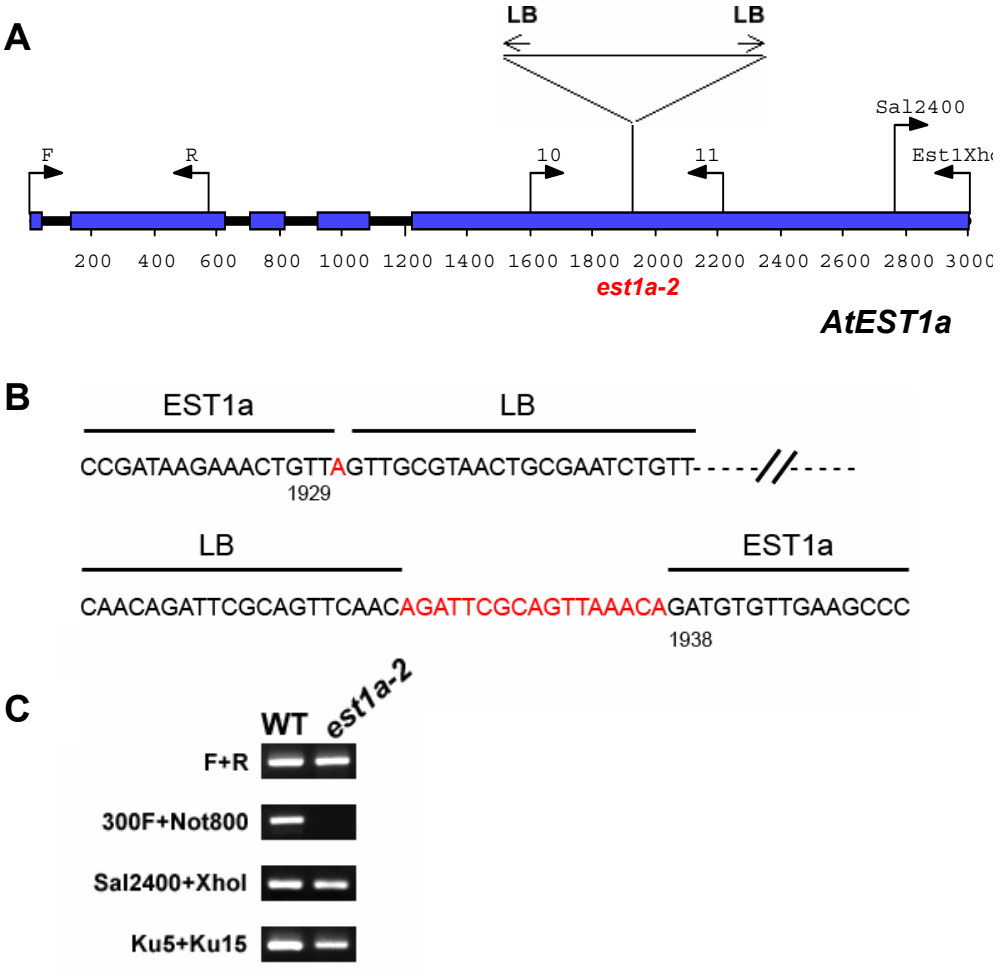

Fig. 26. Mapping and characterization of the insertion site in *est1a-2*. (*A*) *AtEST1a* gene structure, exons are in shown in blue. The T-DNA insertion site and position of left borders are indicated. (*B*) Sequence analysis of the junctions between the T-DNA and *AtEST1a*, filler DNA is shown in red. Numbers indicate the first nucleotide of *AtEST1a* at each junction. (*C*) Analysis of *AtEST1a* expression by RT-PCR. RT-PCR was performed as in Fig. 25C.

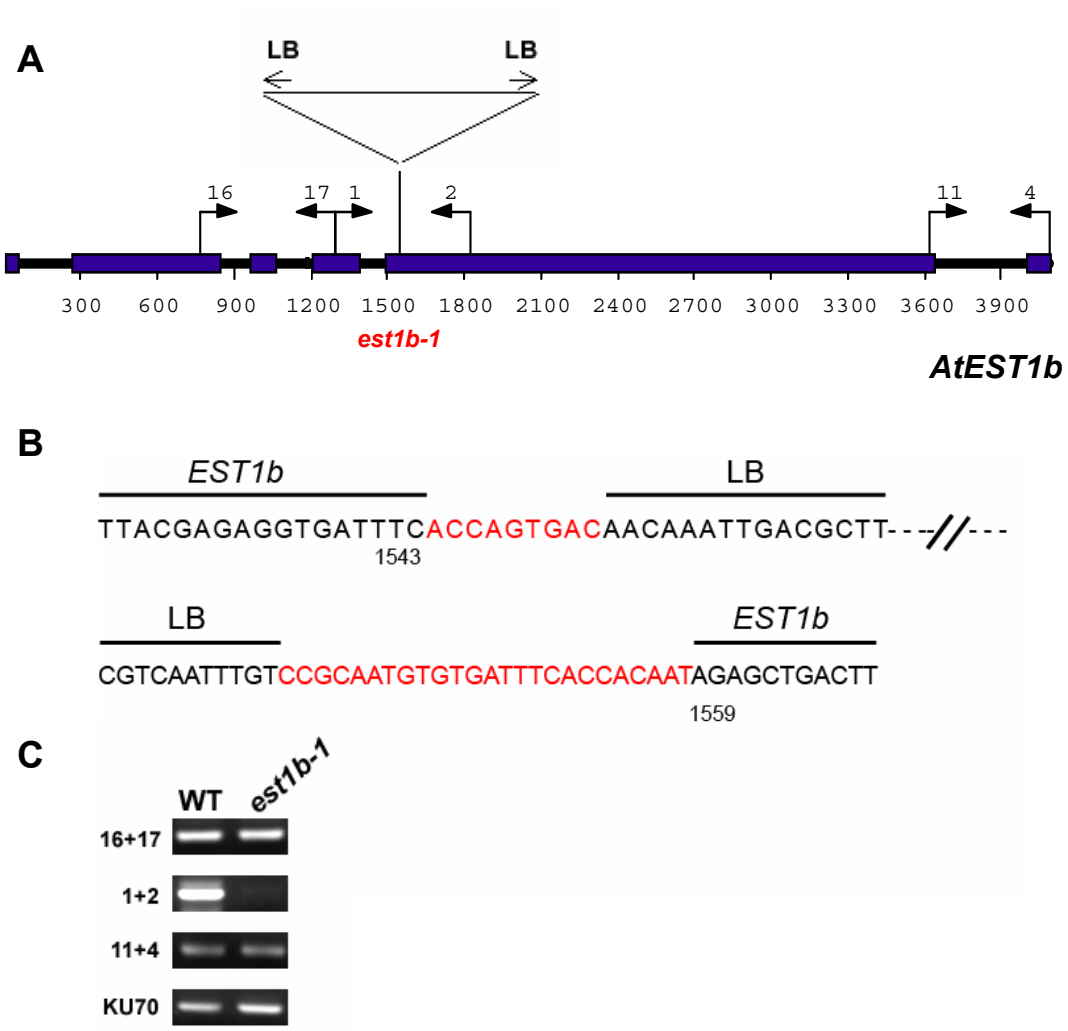

Fig. 27. Mapping and characterization of the insertion site in *est1b-1*. (*A*) *AtEST1b* gene structure, exons are in shown in blue. The T-DNA insertion site and position of left borders are indicated. (*B*) Sequence analysis of the junctions between the T-DNA and AtEST1b: filler DNA is shown in red. Numbers indicate the first nucleotide of *AtEST1b* at each junction. (*C*) Analysis of *AtESTb* expression by RT-PCR. RT-PCR was performed as in Fig. 25C.

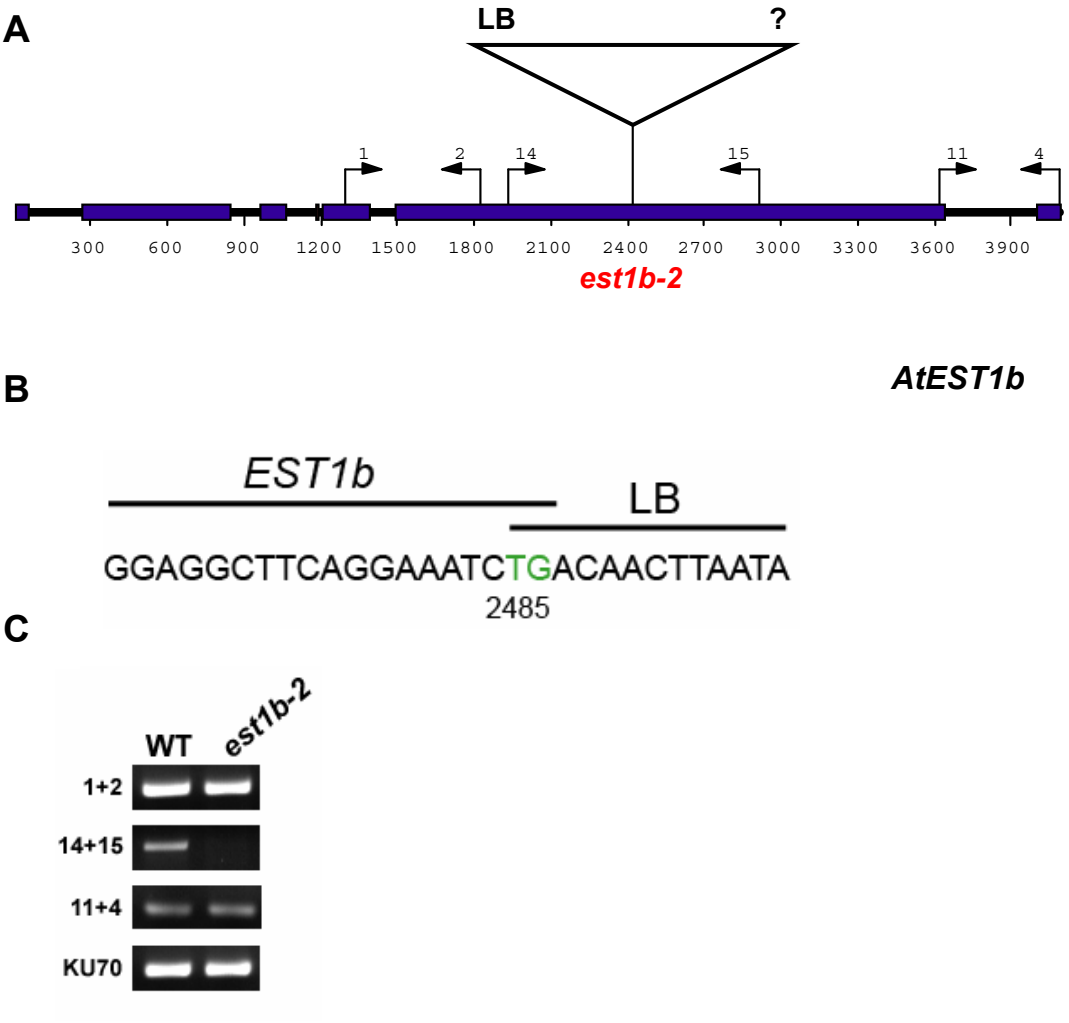

Fig. 28. Mapping and characterization of the insertion site in *est1b-2*. (*A*) *AtEST1b* gene structure, exons are in shown in blue. The T-DNA insertion site and position of left borders are indicated. (*B*) Sequence analysis of the junctions between the T-DNA and *AtEST1b.* Regions of microhomology are shown in green. Numbers indicates the first nucleotide of *AtEST1b* at the junction. We were unable to amplify a product using RB or LB primers for the other side of the insertion. (*C*) Analysis of *AtEST1b* expression by RT-PCR. RT-PCR was performed as in Fig. 25C.

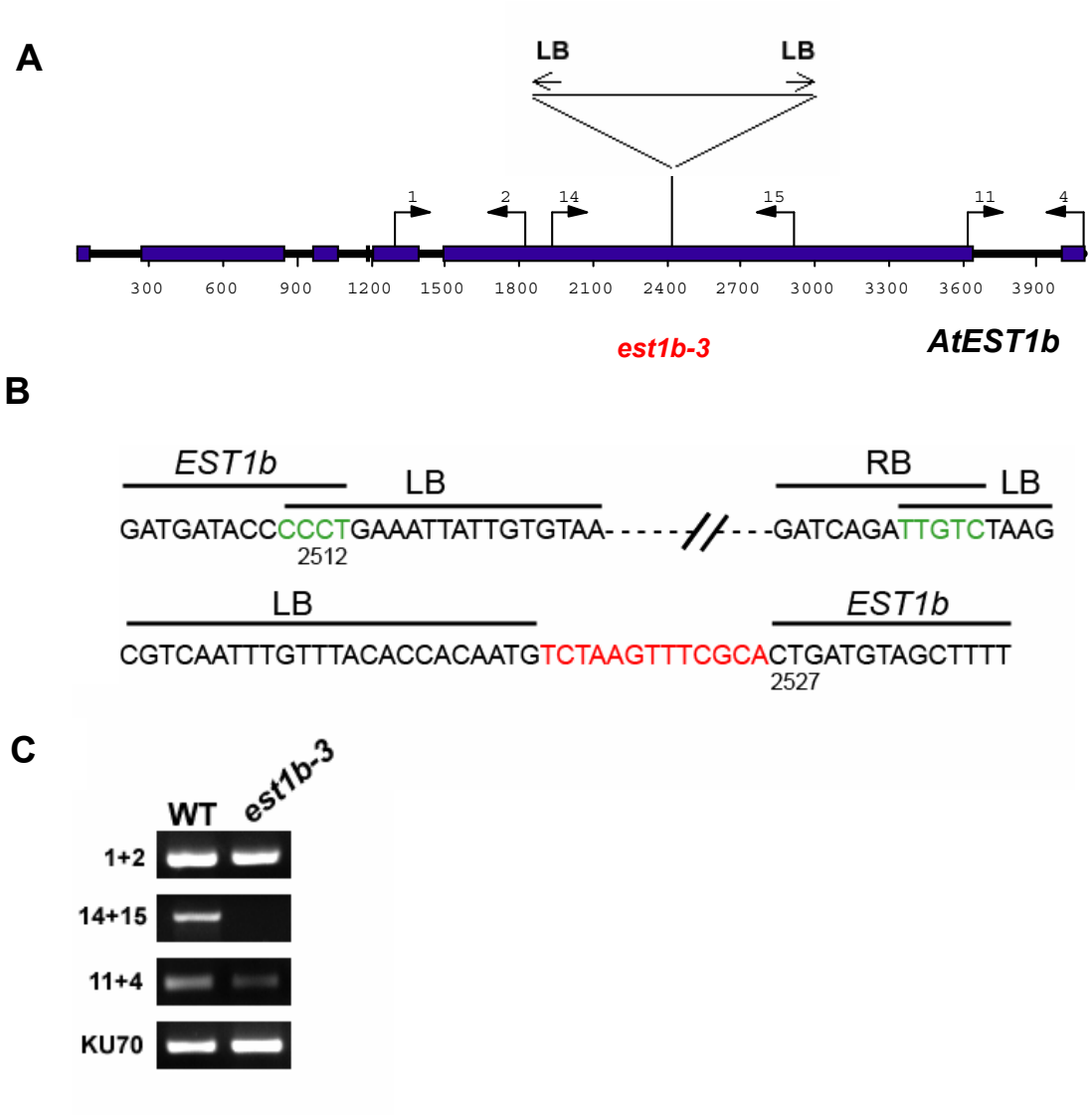

Fig. 29. Mapping and characterization of the insertion site in *est1b-3*. (*A*) *AtEST1b* gene structure, exons are in shown in blue. The T-DNA insertion site and position of left borders are indicated. (*B*) Sequence analysis of the junctions between the T-DNA and *AtEST1b.* Regions of microhomology are shown in green, and filler DNA is shown in red. Numbers indicate the first nucleotide of *AtEST1b* at each junction. (*C*) Analysis of *AtEST1b* expression by RT-PCR. RT-PCR was performed as in Fig. 25C.

in *est1a-1* was mapped to the second intron of *AtEST1a* (Fig. 25A and 25B). The *est1a-2* line was identified from the SALK collection of T-DNA inserts (http://signal.salk.edu/cgi-bin/tdnaexpress) (177) and is in the Columbia ecotype of *Arabidopsis*. The insertion site in *est1a-2* was mapped to exon five of *AtEST1a* (Fig. 26A and 26B). RT-PCR of each line showed expression of the *EST1a* mRNA both 5' and 3' to the insertion, but no products could be amplified across the T-DNA insertion (Fig. 25C and 26C). Thus, these alleles of *EST1a* are null.

Three lines containing T-DNA insertions in *AtEST1b* (Figs. 27A, 28A and 29A) were identified from the SALK collection of T-DNA inserts (http://signal.salk.edu/cgi-bin/tdnaexpress) (177), also in the Columbia ecotype. The exact position of each insertion site was mapped (Figs. 27B, 28B and 29B) by sequence analysis of the junctions. RT-PCR analysis of each line demonstrated that *EST1b* RNA could be amplified both 5' and 3' to the insertion site, but no products could be amplified spanning the insertion sites (Figs. 27C, 28C and 29C). Thus, these three alleles of *EST1b* are null.

Phenotypic and cytogenetic analysis of *AtEst1a* and *AtEst1b* mutants

Plants homozygous for the T-DNA insertions in *est1a-1* and *est1a-2* lines were cultivated. Both lines were wild type in appearance, and could be propagated for successive generations. In contrast, plants from all three *est1b* lines had severe vegetative defects (Fig. 30, B-E). *est1b* plants displayed a lack

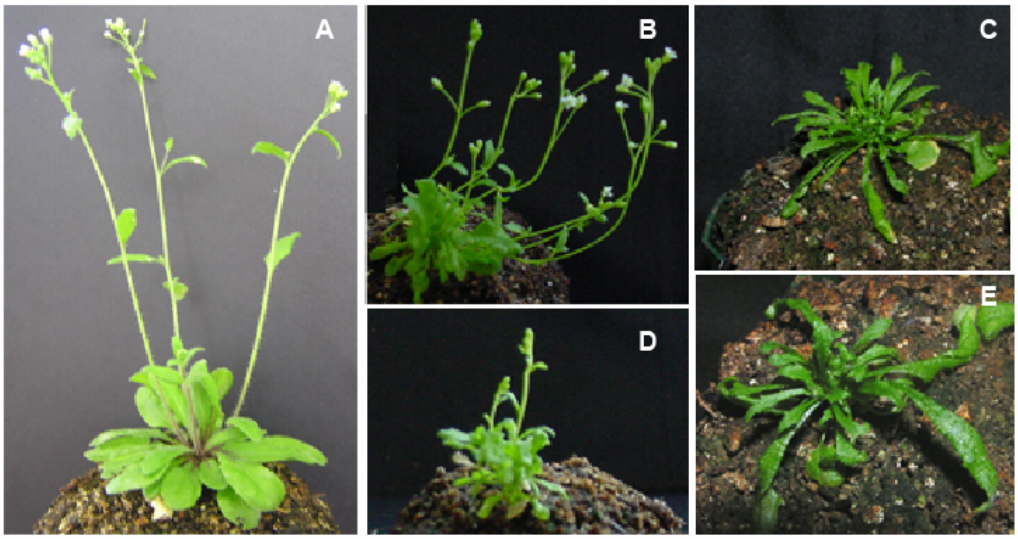

Fig. 30. Vegetative defects in *est1b* plants. (*A*) Wild type *Arabidopsis* plant. (*B*) *est1b* mutant plants display a lack of apical dominance. Inflorescence bolts are thin and weak. (*C* and *E*) Rosette leaves in the *est1b* plants are long, thin and occasionally curl under. (*D*) Some *est1b* plants also have a dwarf phenotype, as well as a lack of apical dominance and long, thin leaves.

of apical dominance, producing multiple inflorescence bolts (Fig. 30, B and D) and thin, often curled leaves (Fig. 30, C and E). In addition to the vegetative defects, *est1b* plants were male sterile and produced no viable pollen (Riha *et. al.* unpublished data). Flowers from *est1b* lines occasionally showed alterations similar to what is seen in meristic mutations (178-180), such as increases in floral organ number (carpel and stamen) (Fig. 31, B and C) or fusion of two or more organs (sepal and carpel) (Fig. 31, C).

Over-expression of hEst1a caused immediate fusion of human telomeres, implicating hEst1a in telomere end protection. To determine whether disruption of *AtEST1a* or *AtEST1b* causes telomere fusions, we used cytogenetics to assay for the presence of anaphase bridges. All three *est1b* mutant lines displayed a low level of anaphase bridges (Table 2 and Fig. 32; data not shown), approximately 5-7%, while neither *est1a* line nor wild type showed evidence for genome instability (Table 2 and Fig. 32A; data not shown).

To further investigate the nature of bridged chromosomes, we used a PCR based assay called Fusion-PCR (Fig. 32B) (161) to look for telomere fusions in the *AtEST1a* and *AtEST1b* mutant lines. In this assay, sub-telomeric DNA primers directed towards the chromosome terminus are used in PCR (Fig. 32B). PCR products are generated only when chromosome ends have been covalently joined. As expected, abundant fusion PCR products were obtained with DNA isolated from late generation *tert* mutants that display profound genome instability (Fig. 32C, lanes 2 and 6), however, we were unable to amplify fusion products in *est1b* or *est1a* lines (Fig. 32C). It is possible that

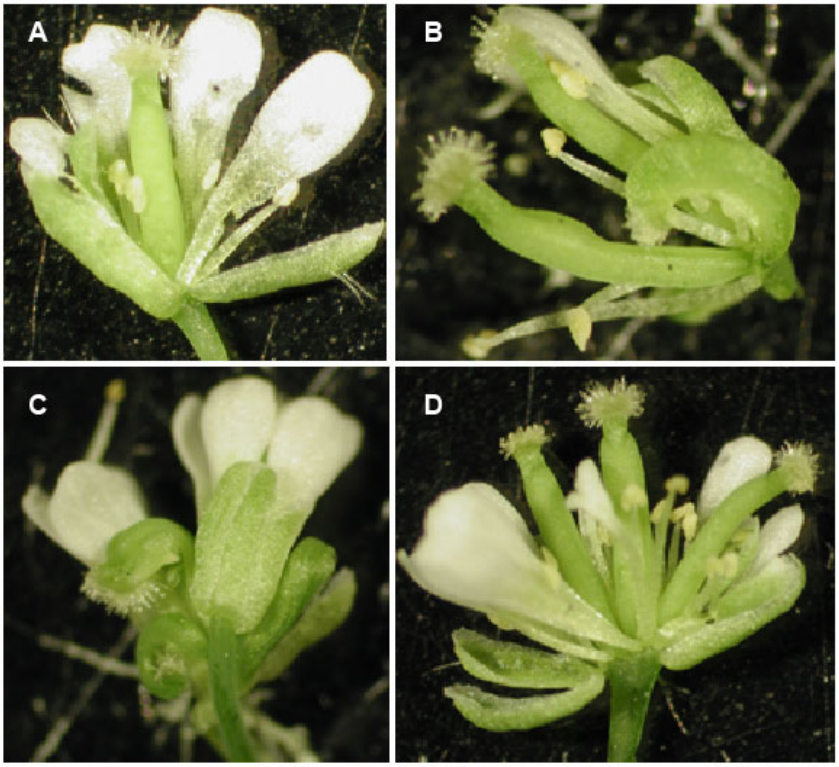

Fig. 31. Defects in flower morphology in *est1b* mutants. (*A*) Wild type flower, with four sepals, four petals, six stamen and one pistil. (*B*) *est1b* flower. This flower has two pistils and one sepal has been fused with a carpel. (*C*) Two examples of the fusion of sepals and carpels in *est1b* plants. These flowers have no petals, but do have very small, clear stamen inside. (*D*) This *est1b* flower has three pistils and 12 stamen, but the normal number of petals, pistils and sepals.

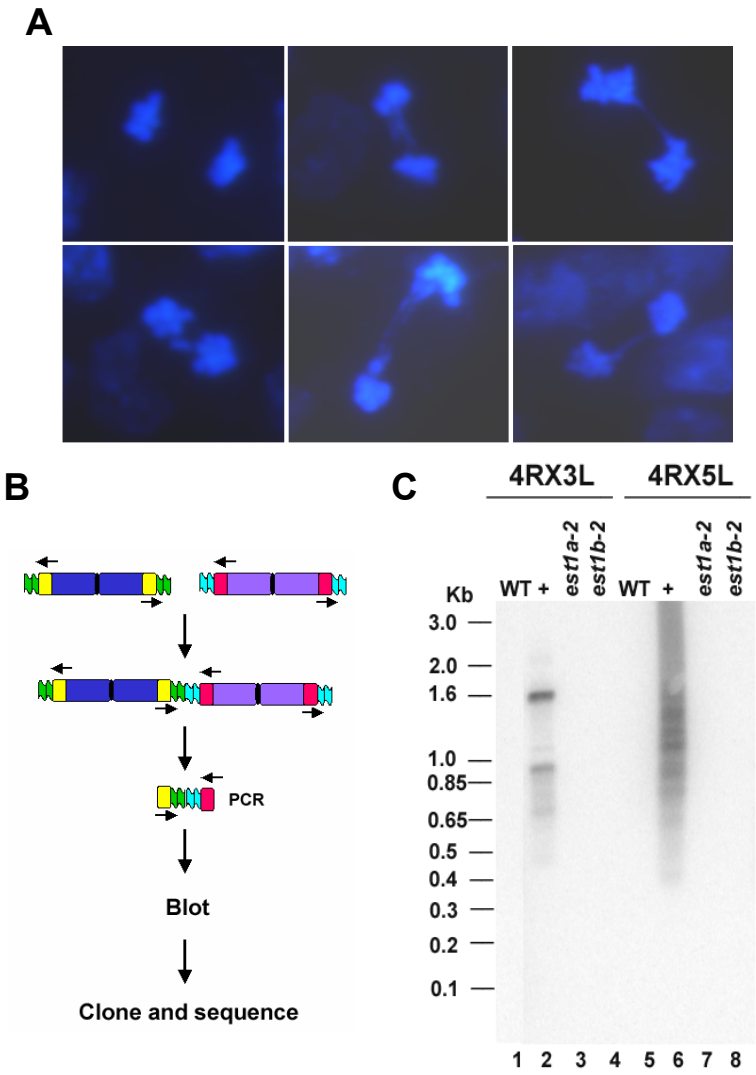

Fig. 32. Genome instability in *est1b* mutants. (*A*) Anaphase bridges were observed in actively dividing mitotic tissues of pistils. Wild type anaphase, and examples of anaphase bridges seen in *est1b* mutants are shown. In some instances, more than one bridge can be seen. In the lower left panel an example of a lagging chromosome is shown. (*B*) Schematic of fusion PCR. (*C*) Fusion PCR on one *est1a-2* plant and one *est1b-2* plant. Two primer pairs were tested, 4RX3L (lanes 1-4) and 4RX5L (lanes 5-8). Wild type DNA (WT, lanes 1 and 5) was used as a negative control, and DNA from a G_8 *tert* mutant (+, lanes 2 and 6) was used as a positive control.

Table 2. Genome instability in *est1b* mutants

	Anaphases Scored	Number with Bridges	Percentage with Bridges
Wild type	213	0	0
est1a-2	200	0	0
est1b-2	315	17	5.4

telomeres are fusing in the est1b mutants, but we are unable to amplify them with our PCR technique because the telomeres involved are very long (2-5kb). Similarly, the fusion of sister chromatids, or the fusion of telomeres to double strand DNA breaks, would not be detected by this technique. Thus, although there appears to be a low level of genome instability in the *AtEST1b* mutant plants, we cannot determine whether telomere de-protection is a contributing factor.

Telomere length analysis of *est1a* and *est1b* plants

To address the role of *EST1a* and *EST1b* in telomere maintenance, terminal restriction length (TRF) analysis was performed on DNA isolated from *AtEST1a* and *AtEST1b* mutant lines. Relative to wild type, no changes in telomere length were associated with any *est1a* or *est1b* line (Fig. 33; data not shown). All telomeres for the *est1b* lines were within the normal 2-5kb size range for telomeres in plants of the Columbia ecotype (Fig. 33A, lanes 5-12 and data not shown) (3). In the *est1a-2* line, telomeres were also within the wild type Columbia telomere range (Fig. 33B). The *est1a-1* line is in a Wassilewskija (WS) background, which is known to have two distinct groups of telomere length (3). Telomeres in WS plants can be 2-5kb, or slightly longer, ranging from 3-8kb. Telomeres in the *est1a-1* line are within the 3-8kb long WS telomere range (Fig. 33, lanes 1-4). These data indicate that Est1a and Est1b do not contribute to telomere length homeostasis in *Arabidopsis*.

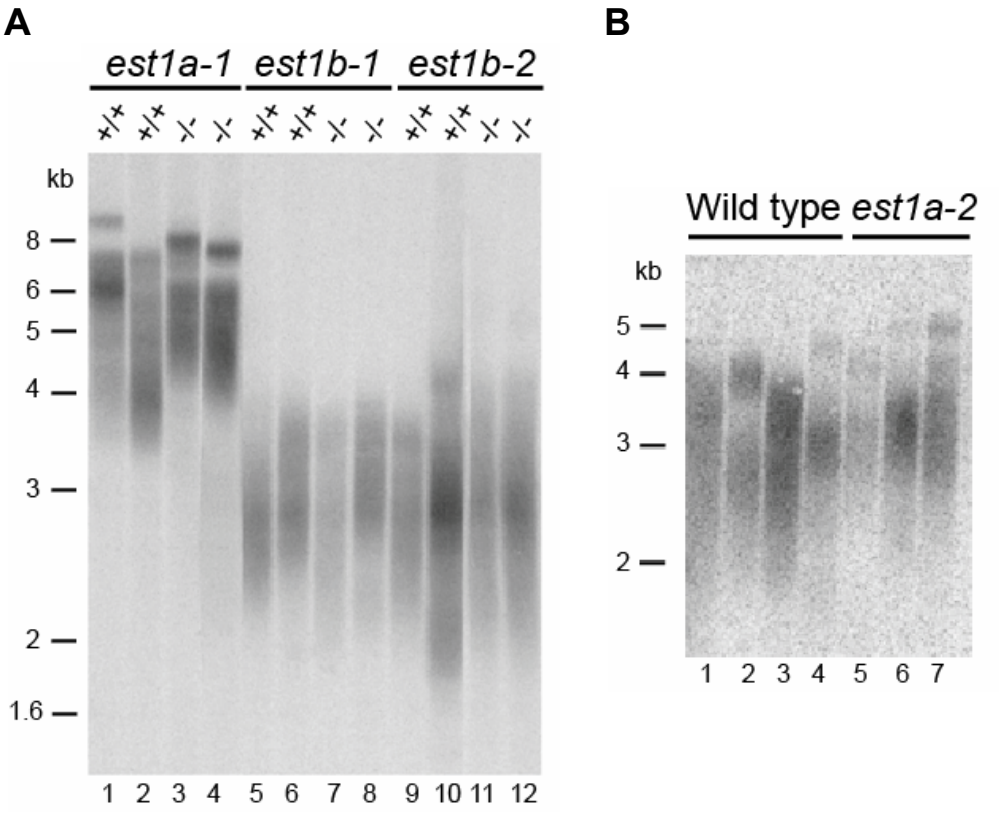

Fig. 33. Terminal restriction fragment analysis of *est1a-1, est1a-2 est1b-1* and *est1b-2*. (*A*) For each line, two wild type and two mutant plants were analyzed. The *est1a*-1 line is in the WS ecotype, and telomeres are within the 3-8kb range for long WS telomeres, lanes 1-4. All *est1b-1* and *est1b*-2 plants had telomeres in the wild type range for Columbia lanes 5-12. (*B*) TRF analysis of *est1a-2*. Four wild type and three *est1a-2* mutant plants were analyzed. All plants had telomere lengths within the normal Columbia range.

It was possible that *AtEST1a* and *AtEST1b* are functionally redundant with respect to telomere biology. Therefore, a mutant deficient in both *EST1a* and *EST1b* was established to investigate this possibility. Plants homozygous for the *est1a-2* or *est1b-2* T-DNA insertion were crossed, and an individual plant heterozygous for each insertion was identified in the F1 population and allowed to self-pollinate. Wild type, *est1a-2*, *est1b-2* and *est1a-2 est1b-2* plants were identified in G_1, and TRF analysis was performed. No changes in telomere length were seen in the *est1a-2 est1b-2* double mutant (Fig. 34).

It was also possible that *AtEST1a* and *AtEST1b* play only a minor role in recruitment of telomerase to the telomere, and that any defects caused by loss of *EST1a* or *EST1b* would not be observed when telomere tracts are within the wild type range. In this case, a telomerase recruitment function for Est1a or Est1b might be revealed in a plant where telomeres become extremely long. To test this idea, we examined the consequences of combining an *AtEST1b* deficiency with a mutant lacking *KU70* (Fig. 35). In *KU70* mutants, telomeres become extremely long expanding to more than double the size of wild type telomeres in a single generation (146). Plants heterozygous for *ku70* and *est1b-2* were

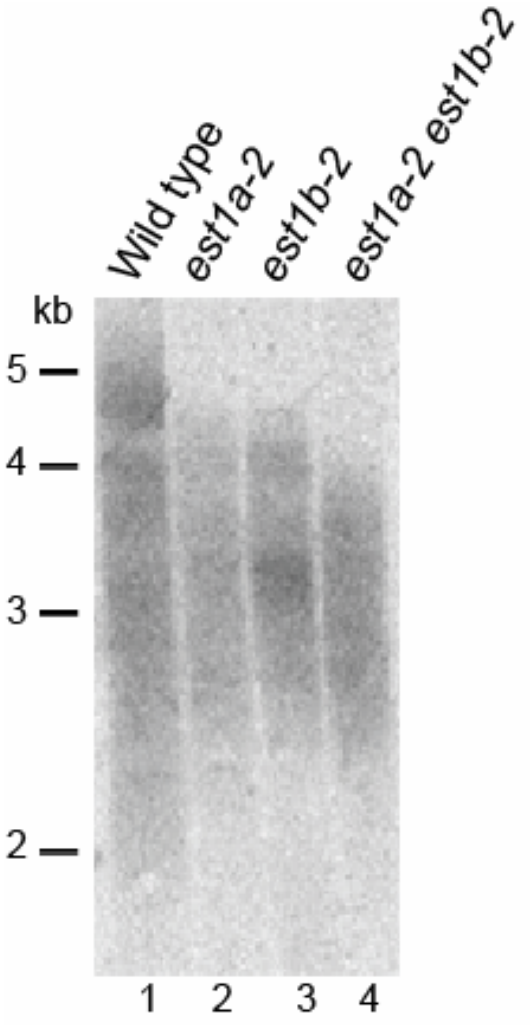

Fig. 34. TRF analysis of *est1a-2 est1b-2* double mutants. All mutants have telomeres within the wild type range.

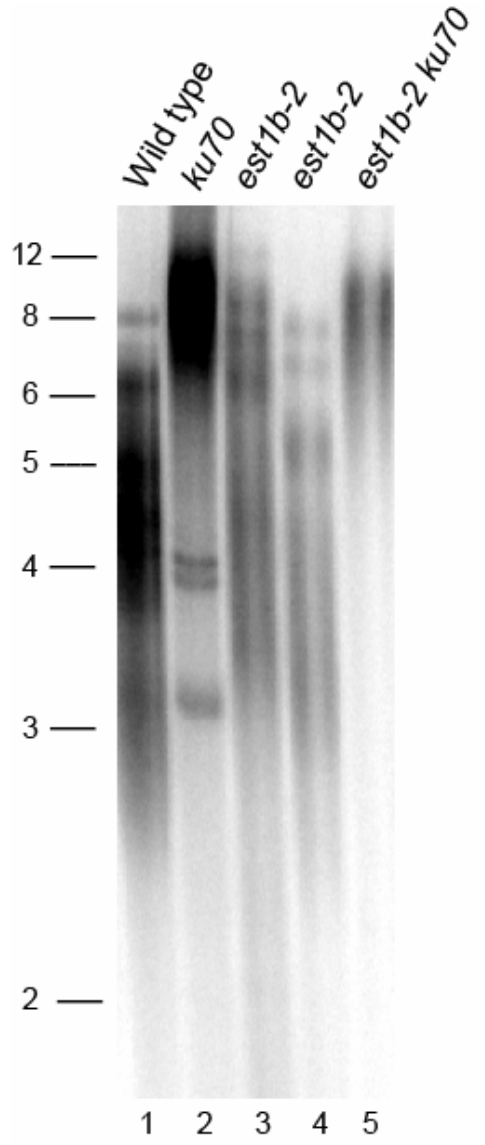

Fig. 35. Terminal restriction length analysis of the *est1b-2 ku70* double mutant. No change in telomere length can be detected between the *ku70* single (lane 2) and the *est1b-2 ku70* double mutant (lane 5).

crossed, and a plant heterozygous for both *ku70* and *est1b-2* was identified in F1. This plant was allowed to self-pollinate, and wild type, *ku70*, *est1b-2* and *est1b-2 ku70* double mutants were identified, and analyzed by TRF (Fig. 35). The *ku70* line comes from the WS ecotype, and has long telomeres (3-8Kb), while the *est1b-2* line is in the Columbia background and has telomeres in the 2-5Kb range. When crosses are made between two ecotypes with different telomere lengths, the resulting plants have telomeres that span the range of both ecotypes (3). As expected, *ku70* mutants had telomeres much longer than their wild type and *est1b-2* counterparts. No change in telomere length was detected between the *ku70* single mutant and the *est1b-2 ku70* double mutants (Fig. 35). Thus, neither AtEst1a nor AtEst1b appear to play any role in telomerase recruitment.

DISCUSSION

Most of our understanding about the recruitment of telomerase comes from work in *S. cerevisiae*, where Est1p plays an integral but as of yet poorly defined role in this process. With the identification of Est1 sequence homologues in other organisms, it may be possible to clarify the role of this Est1 protein.

Arabidopsis has two Est1-like genes

As sequenced genomes became available for higher eukaryotes, Est1p-like proteins were identified in many organisms, including humans, *C. elegans* *Drosophila* and *Arabidopsis* (37, 38). Many of these higher eukaryotes have more than one obvious Est1-like homologue, humans have three, while *Arabidopsis* and *Drosophila* each have two (37, 38).

To further our understanding of Est1 in telomere biology, we have identified and characterized two Est1-like proteins in the model plant, *Arabidopsis thaliana*. Although the predicted proteins of *AtEST1a* and *AtEST1b* genes have very weak sequence similarity to ScEst1p, both *Arabidopsis* proteins have the EST1 and TPR domain found in all Est1-like proteins, suggesting that AtEst1a and AtEst1b are the *Arabidopsis* sequence homologues of ScEst1p. The constitutive expression profile of the *Arabidopsis EST1a* and *EST1b* is similar to what is seen for the human *EST1a* mRNA (37, 38).

Like Est1p from *S. cerevisiae*, AtEst1a binds *Arabidopsis* single-stranded telomeric DNA as well as small RNA oligos and large RNAs *in vitro*. AtEst1a-Cterm was able to bind both *Arabidopsis* telomeric DNA and human telomeric

DNA. This flexibility in sequence recognition is not unique to AtEst1a, both ScEst1p and hEst1a are able to bind telomeric DNA from other organisms (34, 38). ScEst1p binds yeast telomeric DNA $(TGTGTGGG)_3$ and *Oxytricha nova* telomeric DNA $(TTGGGG)_3$ equally well, and to a much lesser extent, human telomeric DNA $(TTAGGG)_4$ (34). Interestingly, human Est1a preferentially binds Sc telomeric DNA, binding human telomeric DNA to a much lesser extent (38). Neither AtEst1a, ScEst1p or hEst1a bind double-stranded telomeric DNA (34, 38)(R. Idol and D. Shippen unpublished data).

AtEst1a-Cterm bound both large RNAs and small RNA oligonucleotides *in vitro*. In contrast, ScEst1p binds only large RNAs (34), and hEst1a does not show specificity for the human telomerase RNA subunit *in vitro*, although it's binding to small RNA oligos was not tested (38). Thus, AtEst1a shows both similarities and differences in its nucleic acid binding properties relative to human and yeast Est1 proteins.

The human Est1a directly interacts with TERT (38), however we failed to observe an interaction between AtEst1a or AtEst1b with *Arabidopsis* TERT. It is possible that the *Arabidopsis* Est1 proteins bind the *Arabidopsis* telomerase RNA subunit, much in the same way as ScEst1p binds *TLC1* (35). However, the *Arabidopsis* telomerase RNA subunit has not yet been identified, so this hypothesis cannot be tested.

Est1a and Est1b do not play a role in telomere length regulation in *Arabidopsis*

Est1 proteins in *S. cerevisiae* and humans are important in telomere length regulation and in humans, telomere capping (30, 37). Surprisingly, our data indicate that AtEst1a and AtEst1b do not play an analogous role in *Arabidopsis*. We failed to observe changes in telomere length in any single *est1a* or *est1b* line or the *est1a-2 est1b-2* double mutant. Moreover, in the *est1b-2 ku70* double mutant, telomeres were elongated to the same extent as in the *ku70* single mutant. It will be interesting to determine whether human Est1c, the closest relative of the *Arabidopsis* Est1 proteins functions in telomere biology. Perhaps like the Est1-like proteins in plants, hEst1c has evolved new functions outside of telomere length maintenance and end protection.

***Arabidopsis EST1b* is an essential gene**

Disruption of *AtEST1a* had no effect on plant growth or development and these plants could be propagated for multiple generations. By contrast, T-DNA insertions in *AtEST1b* had severe consequences for both vegetative and reproductive tissues. *est1b* mutants are sterile and recent studies have shown a novel role for AtEst1b in meiosis, apparently unrelated to telomere function (Riha et. al. in preparation).

One possible role for Est1b is in the nonsense-mediated-decay (NMD) pathway. NMD is responsible for eliminating aberrant mRNAs that prematurely terminate translation. Human Est1a was independently identified as a

component of the human NMD pathway (181), and in yeast, NMD regulates expression levels of several telomere components (182, 183). Additional support for this link between Est1-like proteins and NMD comes from sequence analysis of proteins known to be important for NMD in *C. elegans* (SMG 1, 2, 5, 6 and 7; suppressor with morphogenetic effect on genitalia). Both Smg5 and Smg7 have N-terminal TPR domains, and Smg5 has a C-terminal PIN domain (184). When Smg5 and Smg7 are used as a query against the *Arabidopsis* non-redundant database, the only proteins identified are AtEst1a and AtEst1b, suggesting a link between *Arabidopsis* Est1 proteins and NMD. If AtEst1b was involved in NMD in *Arabidopsis*, knocking out other genes in the NMD pathway may cause similar growth and reproductive phenotypes like those observed in the *est1b* mutants. Besides the *C. elegans* Smg proteins, three other NMD proteins have been identified in *S. cerevisiae*, UPF 1-3 (up-frameshift). We identified a sequence homologue of UPF1 in *Arabidopsis* (At5g47010) and obtained a line harboring a T-DNA insertion in this gene; however, these mutants had none of the vegetative or reproductive defects associated with a deficiency in *AtEst1b*. While this result does not rule out a role in NMD for the *Arabidopsis* Est1-like proteins, it deepens the mystery surrounding this class of genes in plants.

MATERIALS AND METHODS

Plant materials and growth conditions

Arabidopsis seeds were treated overnight at 4°C, then placed in an environmental growth chamber and grown under a 16/18-hour light/dark photoperiod at 23°C. The *est1a-1* line was obtained by screening the Wisconsin T-DNA collection. All other lines were obtained from the SIGNAL SALK database (http://signal.salk.edu/cgi-bin/tdnaexpress). *est1a-2, est1b-1, est1b-2* and *est1b-3* are SALK_071725, SALK_073354, SALK_025699 and SALK_112476 respectively. Insertion sites were mapped using gene specific primers that flanked the insertion site, and primers specific to the left or right border region. PCR products were cloned into the pCR2.1-TOPO vector (Invitrogen) and sequenced using M13 forward and reverse primers.

cDNA synthesis and RT-PCR analysis

Total mRNA was extracted from 100-500mg of plant tissue using Tri-Reagent (Sigma). AtEst1a and AtEst1b were synthesized from flower RNA using SuperScript III reverse transcriptase (Invitrogen). Oligo dT was incubated with 1μg total RNA in the supplied buffer at 65°C for 5 min. Reverse transcription was carried out with 200 units of SuperScript III at 55°C for 1hr. RNA was degraded with RNase H (USB). The coding regions of *AtEST1a* and *AtEST1b* were then amplified with Ex-Taq (Takara). The PCR products were cloned into pet28b (Novagen). For expression analysis of *AtEST1a* and *AtEST1b*, RNA was made as above for each tissue (rosette leaves, cauline leaves, stem, flowers and

callus) and subjected to RT-PCR. First strand was made with oligo dT as above, and primers specific to *EST1a* and *EST1b* were used to amplify a portion of each mRNA.

Expression and purification of recombinant Est1a-Cterm

A region of the AtEst1a cDNA corresponding to nucleotides 1600-2623 (amino acids 533-880) was PCR-amplified and cloned into the *Sal*1 and *Not*1 sites of pet28b. This construct, designated AtEst1a-Cterm, was transformed into bacteria strain er2566 (New England Biolabs) for over-expression. Western blotting with T7-tag antibodies was used to monitor expression of AtEst1a-Cterm. Cells were grown at 37°C to $O.D._{600}$ 0.5, induced with IPTG (0.7 mM) and harvest after 4hr. Cells were re-suspended in binding buffer (50mM $NaHPO_4$, 300mM NaCl, 10mM imidazole, and 1% NP-40), sonicated on ice, and the supernatant was taken for affinity purification. AtEst1a-Cterm was purified as a soluble recombinant protein using a 6X His tag present at the C-terminus, and immobilized metal affinity chromatography purification with Ni-NTA His-Bind Resin (Novagen). Fractions were analyzed by SDS-PAGE, and the fractions containing AtEst1a-Cterm were combined and dialyzed against 50mM Tris-Cl pH 7.9, 100mM KCl, 1mM DTT and 50% glycerol. The dialyzed sample was then concentrated against solid PEG, 3hr at 4°C. Protein concentrations were determined using Bradford analysis.

The appropriate coding regions of N (nucleotides 1-1539), M (nucleotides 984-2010) and C-TERT (nucleotides 1557-3372) were cloned into the pCITE

vector (no T7 tag added). The full-length coding region of *KU70* was cloned into pet28, plus and minus the T7 tag. The full-length coding region of *KU80* was cloned in pet28a without the T7 tag.

Electrophoretic mobility shift assays

EMSA was performed in 10mM HEPES (pH 7.8), 75mM KCl, 2.5mM $MgCl_2$, 0.1mM EDTA, 1mM DTT, 3% Ficoll. Incubations were performed in 10μL reaction volumes with 4.4ng of AtEst1a-Cterm, 200μg/mL *E. coli* digested DNA as a nonspecific competitor, end-labeled single-stranded oligonucleotides (boiled 2min and snap-cooled on ice just prior to use), and competitors (when added). Oligonucleotides used in this study were: 6Telo $(TTTAGGG)_6$, 6Human $(TTAGGG)_6$, 5RNA $(UUUAGGG)_5$ and non-specific (TTCCTCGAAGAAGC CTCT AAAGATGTGTCTTCTAAAGAATGCAGT). Protein ($3.3x10^{-4}$ μM per reaction) and unlabeled competitors were mixed in the above gel shift buffer and incubated for 10min at room temperature after the addition of the labeled oligonucleotide. The reactions were subjected to electrophoresis through a 7.5% non-denaturing polyacrylamide gel in 1X TBE (pH 7.5) at 150 volts for 4hr. RNA binding was done under the same conditions. After the gels were run, they were dried and subjected to a phosphorimager screen overnight. Data was analyzed using ImageQuant software.

Purified DNA and RNA oligonucleotides were obtained from Integrated DNA Technologies. Single-strand oligonucleotides were 5'end labeled with γ-^{32}P- ATP and T4 polynucleotide kinase (NEB). For each reaction, $5.5X10^{-4}$ ρM

oligonucleotide was used, and the molar fold excess of each unlabeled competitor was calculated based on this number.

Co-immunoprecipitation

Full-length T7-Ku70, Ku70, Ku80, T7-Est1a, T7-Est1b, N-TERT, M-TERT and C-TERT were expressed in separate rabbit reticulocyte lysate reactions (25μL reaction volume) following the manufacturer directions and using 500ηg DNA of each template. The Ku70, Ku80, N, M and C-TERT reactions contained 0.5μL of [^{35}S] methionine to label the product. The reactions were stopped by the addition of 1.5μL cyclohexamide (2mg/mL stock in water) per reaction. Co-immunoprecipitations were carried out as described previously (Wang *et. al.* 2002) using anti-T7 monoclonal antibody (Novagen). After immunoprecipitation, the bound and unbound fractions were resolved by SDS-PAGE. The dried gels were subjected to a phosphorimager analysis, and the data was analyzed using ImageQuant software.

Cytogenetics

Mitotic anaphases were prepared as previously described (Riha et. al., 2001) with the following modification: floral buds were digested in 20% (v/v) pectinase (Sigma), 2% (w/v) cellulase (Sigma) for 1hr at 37°C. Slides were stained with 2μg/mL DAPI and mounted in 50% glycerol. Anaphase spreads were visualized as described previously (Riha *et. al.* 2001).

Fusion PCR

Unique subtelomeric primers directed 5' to 3' toward the telomeric repeat were designed for each chromosome: 1L (5' ACAAGGATAG AAATAGAGCATCGTC 3'); 3L (5'AGACGAGGAGACTAGGAACG 3'), 3R (5' GTATGGATGCC GGGAAAGTTGCAGACAA 3), 5R (5' TCGGTTGTC GTCTTCAAG 3'). PCR samples were prepared as previously described (161). A 10μL aliquot of the PCR products was separated by electrophoresis through a 1% agarose gel, and transferred to a nylon membrane. Membranes were hybridized with a ^{32}P end-labeled $(T_3AG_3)_4$ probe. Hybridization signals were detected using a STORM Phosphor Imager (Molecular Dynamics) and the data were analyzed using IMAGEQUANT software (Molecular Dynamics).

Terminal restriction fragment length analysis

DNA from individual plants was extracted as previously described (66). TRF analysis was performed with *Tru*1I restriction enzyme (Fermentas) and ^{32}P 5’ end-labeled $(T_3AG_3)_4$ oligonucleotide as a probe (68).

CHAPTER IV

Arabidopsis LIGASE IV IS REQUIRED FOR TELOMERE MAINTENANCE, BUT NOT FOR FUSION OF DYSFUNCTIONAL TELOMERES

INTRODUCTION

It is essential that cells are able to maintain genome integrity. To protect against genome instability, a cell must differentiate between un-repaired DNA double strand breaks (DSBs) and the natural ends of the chromosomes. Telomeres provide this protection by their unusual architecture and composition. Telomeres are comprised of repetitive G-rich DNA sequences that end with a 3' single strand overhang, which loops back and invades the double strand portion of the telomere forming a t-loop (10). Current models suggest that through much of the cell cycle, the t-loop hides the 3' overhang, but during S-phase telomerase is permitted access (96). Telomerase, a specialized reverse transcriptase, uses its integral RNA subunit as a template to synthesize telomeric repeats, and hence maintains telomeric DNA. The chromosome terminus is coated by proteins that recognize and associate with the telomeric DNA either through binding directly to the DNA or through protein-protein interactions (89).

When a telomere becomes dysfunctional, the cell is no longer able to distinguish it from a DSB. The telomere is treated as such, resulting in end-to-end chromosome fusions. Telomere dysfunction can arise through depletion of telomeric repeats or by loss of telomeric proteins essential to maintaining the

protective cap (28, 65, 66, 68, 84, 149, 151, 185). In mammals, plants and yeast, the fusion of dysfunctional telomeres requires components of the non-homologous end-joining (NHEJ) pathway (84, 99, 161, 185, 186).

The major components of the NHEJ pathway are the Ku70/80 heterodimer, DNA ligase IV (Lig4), XRCC4, and in mammals, the catalytic subunit of DNA-dependent protein kinase (DNA-PK_{cs}) (133). Once detected, a DSB is bound at each end by the Ku heterodimer, which subsequently recruits DNA-PK_{cs}. The broken ends are then processed by a complex consisting of DNA-PK_{cs} and Artemis, whose latent exonucleolytic function becomes activated by DNA-PK_{cs} (187). Finally, the processed ends are ligated by the DNA ligase IV/XRCC4 complex (133).

Several of the NHEJ components have been shown to be required for the fusion of dysfunctional telomeres. In fission yeast, Ku and Lig4 are required for end-to-end chromosome fusions in the absence of Taz1p (84). Ku and Lig4 are also required for chromosome fusions in *atm* or *atr* single mutants, *atm atr* double mutants, *tlc1 atm* mutants, and *est2 nhej1* mutants in budding yeast (186, 188, 189). Similarly, fusion of uncapped mammalian telomeres requires Ku (185) and DNA ligase IV (99). However, there are several examples of alternate NHEJ pathways for telomere fusions. Ku-independent pathways for telomere joining have been documented in yeast, plants and mammals (139, 145, 147, 149, 161, 186). In addition, end fusions also occur in mice lacking DNA-PK_{cs} (149-151). Thus, many organisms have backup NHEJ pathways to repair DSBs.

Elucidating the functions of NHEJ components at telomeres is complicated by the fact that several of these proteins are associated with telomeres and are required for length regulation and end protection. In fission and budding yeast, deletion of Ku leads to telomere shortening and extension of the 3' overhang (139-141, 143, 144). This data implicates Ku in telomere end protection. In addition, Ku acts syngerstically with telomerase in telomere maintenance. Deletion of Ku in budding yeast and fission yeast leads to an increased rate of telomere shortening (139, 190). For mammals, both telomere lengthening (147) and shortening (148) have been reported in the absence of Ku. Additionally, deletion of Ku in mice leads to chromosome fusions, demonstrating a role in telomere capping (147, 148). However, telomeres in mice deficient for Ku and telomerase shorten at the same rate as telomeres in telomerase deficient mice (185).

DNA-PK_{cs} also plays a role in telomere maintenance and end protection. Deletion of DNA-PKcs leads to gradual telomere shortening and chromosome fusions in mice (149-151) and interestingly, the kinase activity of DNA-PK_{cs} is required to prevent the end-to-end fusions (152). By contrast, DNA ligase IV and its binding partner XRCC4 have not been linked to telomere maintenance or end protection (148, 153, 155).

Arabidopsis thaliana has emerged as a useful model for telomere biology in higher eukaryotes. This small weed shows extreme tolerance to genome instability (66), and perhaps because of this, deletion of several DSB repair genes, including *MRE11*, *ATR* and *LIG4* that are lethal in mammals are not in

Arabidopsis (154, 155, 162, 191, 192). In telomerase mutants, progressive telomere shortening eventually leads to sterility and massive genome instability, although plants in the terminal generation remain viable despite more than half of their chromosomes being involved in end-to-end fusions (66). Deletion of *KU70* causes telomerase dependent telomere lengthening (145) but no telomere fusions (146). However, plants doubly deficient for both Ku70 and TERT display an advanced onset of genome instability, caused by a two-to-three fold in the rate of telomere shortening (145). The fusion of critically shortened telomeres occurs in the absence of Ku70 (145) via a more microhomology driven pathway that appears to be mediated in part by Mre11 (161). Remarkably, telomeres in telomerase mutants deficient in Ku and Mre11 are still subject to chromosome fusion, arguing that *Arabidopsis* has robust and redundant NHEJ capacities (161).

Although deletion of Lig4 or XRCC4 leads to embryonic lethality in mice (156, 158, 193), *LIG4* is not an essential gene in yeast or *Arabidopsis* (139, 153, 155, 158). Therefore, we examined the role of DNA ligase IV in the fusion of critically shortened telomeres in *Arabidopsis*. Here we show that Lig4 is not required for chromosome fusions, but unexpectedly is required for telomere maintenance in *Arabidopsis*. This is the first evidence for a role for Lig4 outside of NHEJ.

RESULTS

Identification and characterization of *lig4-3*

We obtained an *Arabidopsis* line with a T-DNA insertion in *AtLIG4* from the SIGnAL collection of *Arabidopsis* T-DNA insertion lines (http://signal.salk.edu/cgi-bin/tdnaexpress) (177). The insertion, SALK_044027, is located within exon 6 of *AtLIG4* (Fig. 36A), and we refer to this mutant as *lig4-3*. A plant heterozygous for the insertion in *AtLIG4* was identified by PCR and self-pollinated to produce progeny that were wild type or homozygous for the T-DNA insertion. To pinpoint the site of insertion, the junction between each LB and *LIG4* was sequenced (Fig. 36B). The disruption in *lig4-3* contains two tandem T-DNA insertions, each with the left border (LB) pointing out into *LIG4* (Fig. 36A). RT-PCR analysis of the homozygous mutants indicated that insertion abolished production of full-length *Lig4* mRNA. Although PCR products could be amplified both 5' and 3' of the T-DNA insertion, no product was obtained using primers flanking this site (Fig. 36C). Consistent with results for *lig4-1* and *lig4-2* *Arabidopsis* mutants (154, 155), plants homozygous for the *lig4-3* mutation displayed no defects in growth or development (data not shown).

Mutants lacking components of a DNA repair pathway are typically hypersensitive to DNA damaging agents. As previously reported, both *ku70*$^{-/-}$ (Fig. 37) and *lig4-1* and *lig4-2* (146, 154, 155) mutants were sensitive to DNA damaging agents. Therefore, we examined the response of *lig4-3* by comparing its growth on methyl methanesulfonate (MMS) relative to wild-type and *ku70*$^{-/-}$

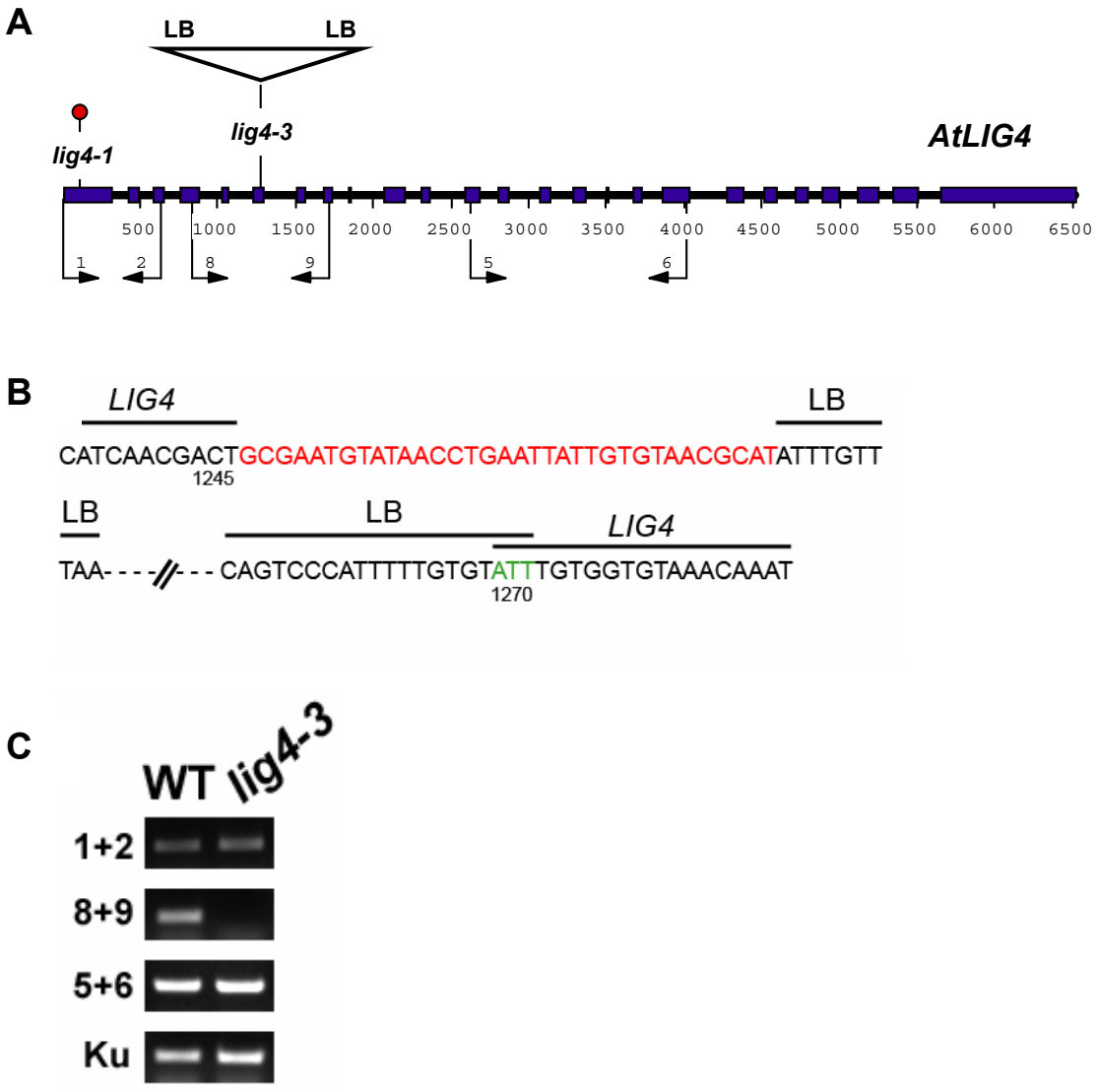

Fig. 36. Characterization of the T-DNA insertion in *lig4-3*. (*A*) *AtLIG4* gene structure, exons are in blue. The positions of *lig4-1* and *lig4-3* are shown. (*B*) Sequence analysis of the T-DNA-*LIG4* junctions. Filler DNA is in red, and regions of microhomology are in green. Numbers indicate the first nucleotide of *AtLIG4* adjacent to the T-DNA. (*C*) Expression of *AtLIG4* in the *lig4-3* line.

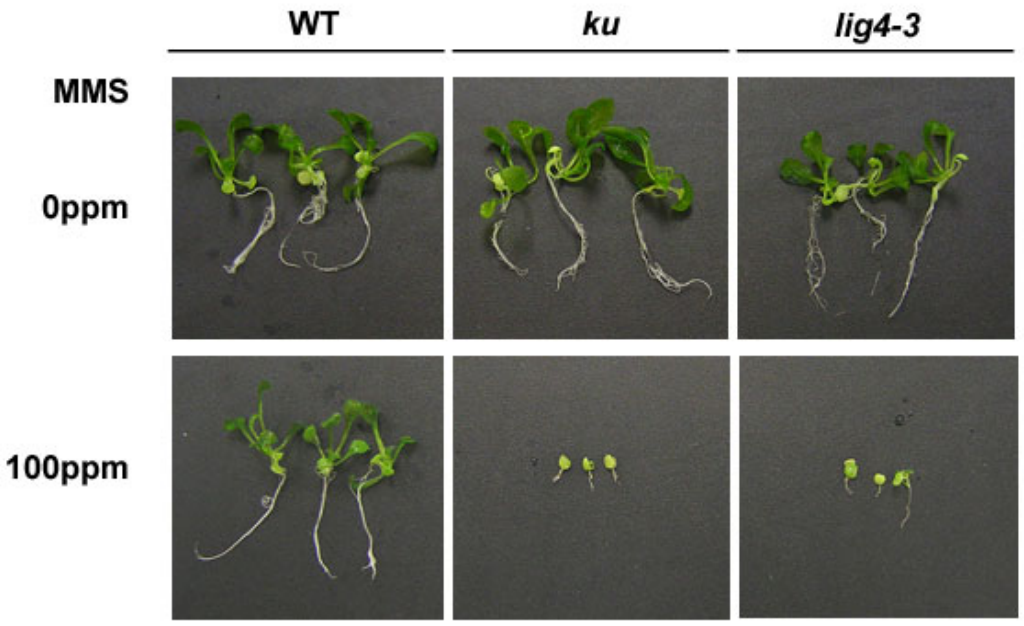

Fig. 37. *lig4-3* plants are hypersensitive to DNA damage. Four-day old seedlings were transferred to liquid MS media containing 0ppm or 100ppm methyl methanesulfonate (MMS). Seedlings were scored after 10 days in MMS containing media.

plants as expected, the *lig4-3 line* was hypersensitive to MMS (Fig. 37), indicating it is a null allele.

lig4-3 plants have wild type telomere length

Previous characterization of *lig4* deficient lines have shown no defects in telomere length maintenance (154, 155). To verify that is was true for *lig4-3*, we performed terminal restriction fragment (TRF) analysis on the second generation (G_2) of the *lig4-3* line. Nine wild type and ten G_2 *lig4-3* plants were selected randomly and telomere length was examined by TRF. Although we noted slight variability in telomere lengths, this is not uncommon in *Arabidopsis* (3). All telomeres in *lig4-3* mutants were within the 2-5kb range for Columbia ecotype (Fig. 38).

Creation of the *ku70 tert lig4-3* triple mutant

To determine whether *LIG4* is required for the fusion of dysfunctional telomeres in *Arabidopsis*, we examined the fate of mutant combinations lacking *TERT*, the telomerase catalytic subunit, *KU70* or *LIG4*. A plant heterozygous for T-DNA insertions in both *KU70* and *TERT* (145) was crossed with a *lig4-3* heterozygote (Fig. 39A). A single F1 plant heterozygous for T-DNA insertions in all three genes was identified by PCR and self-pollinated to produce all possible mutant combinations. From this cross, two lines (line 1 and line 2) were created (Fig. 39A), which were then propagated for three consecutive generations. For

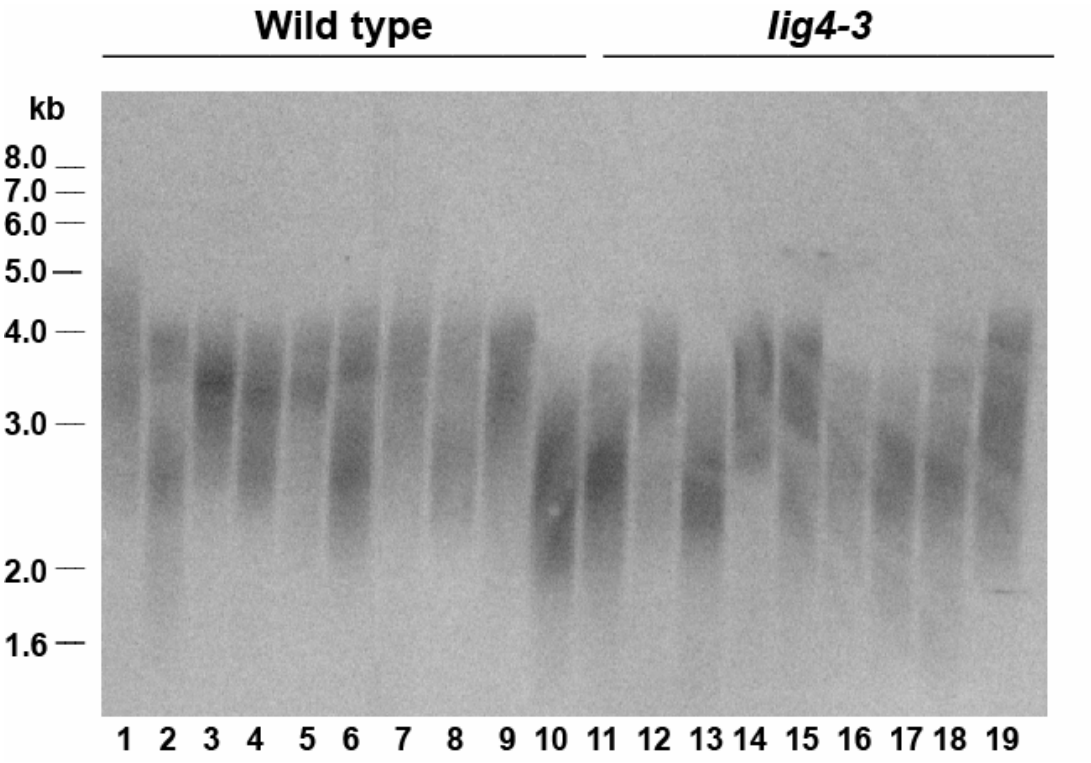

Fig. 38. TRF analysis of the *lig4-3* line. Plants were segregated from one plant heterozygous for the *lig4-3* insertion. Nine second generation (G_2) wild type plants and ten G_2 *lig4-3* plants were analyzed. All plants have telomeres within the wild type telomere range for the Columbia ecotype (2-5kb).

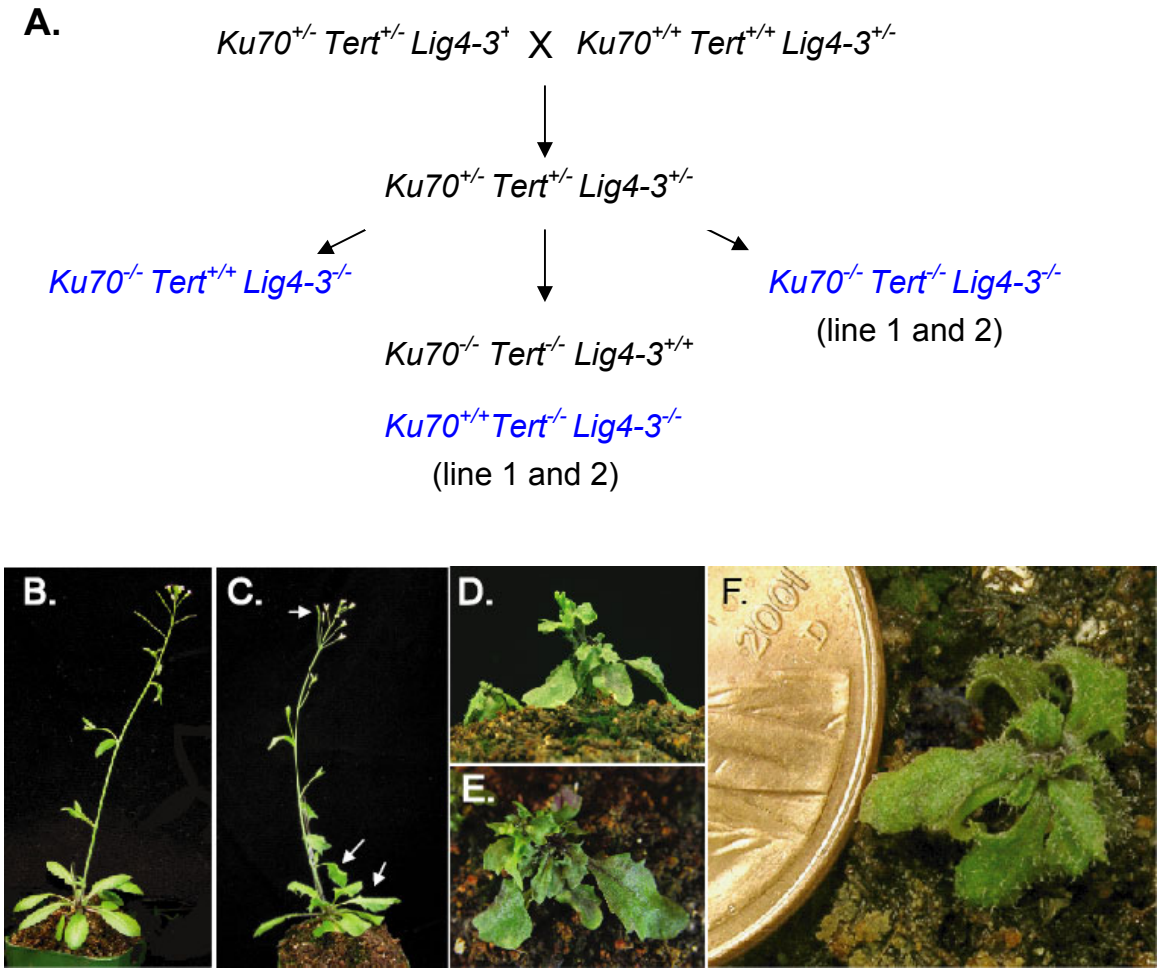

Fig. 39. Creation of *ku70 tert lig4* mutants and phenotypes of terminal *ku70 tert lig4-3* mutants. (*A*) Scheme for creation of *ku70 tert lig4-3* mutants. (*B-F*) Phenotype of G_4 plants. Wild type (*B*), *ku70 tert* (*C*) and two *ku70 tert lig4-3* (*D*) plants in G_4. A top view of the larger *ku70 tert lig4-3* plant from (*D*) is shown in (*E*). The smaller plant from (*D*) is pictured from the top (*F*) with a penny to demonstrate scale.

the first two generations (G_1 and G_2), all the single and double mutants exhibited a wild type phenotype. However, in G_1 the *ku70 tert lig4* mutants were smaller and produced a smaller seed-set (data not shown). In G_3, the *ku70 tert* mutants began to exhibit mild growth defects consistent with the accelerated rate of shortening previously documented for this background (145) (Fig. 39C). All other double and single mutant combinations appeared wild type. Strikingly, by G_3, *ku70 tert lig4-3* mutants were sterile, displaying a terminal phenotype (Fig. 39D and 39E), with rough, misshapen leaves and either no inflorescence bolt, or an inflorescence bolt bearing infertile flowers. The phenotypes seen in terminal *ku70 tert lig4-3* mutants is reminiscent of the phenotypes observed in late generation *tert* mutants (66).

DNA ligase IV is not required for fusion of critically shortened telomeres in *Arabidopsis*

We next asked whether *LIG4* is necessary for the fusion of dysfunctional telomeres in *Arabidopsis* by monitoring anaphase figures for the presence of bridged, and presumably covalently fused, chromosomes. In G_2, the incidence of anaphase bridges in the single and double mutants was extremely low and mirrored that of wild type plants. In contrast, 21% of the anaphases examined in G_2 triple *ku70 tert lig4* mutants contained bridged chromosomes (Fig. 40 and Table 3) and in G_3 the incidence rose to 54% (Table 4). To determine whether the cytogenetic abnormalities we observed correlated with telomere joining

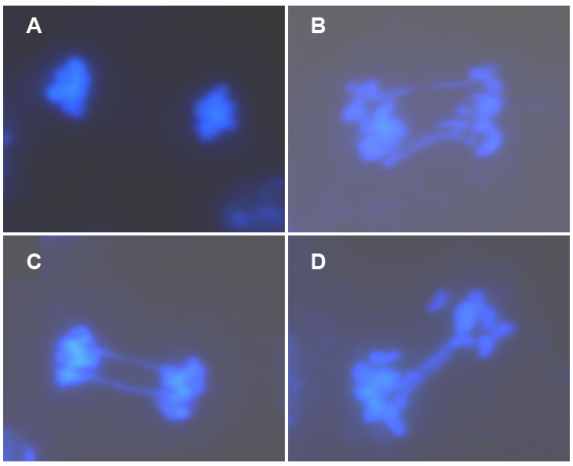

Fig. 40. Anaphase bridges in *ku70 tert lig4-3* mutants. Anaphase figures were prepared from pistils stained with 4'6-diamidino-2-phenylinodle (DAPI). (*A*) Wild type anaphase. (*B-D*) Examples of anaphase figures from *ku70 tert lig4-3* mutants.

Table 3. Genome instability in G_2 *ku70 tert lig4-3*

	Anaphases Scored	Number of Anaphases with Bridges	Percentage with Anaphase Bridges
Wild type	227	0	0
ku70 tert	254	1	0.4
tert lig4-3	243	1	0.4
ku70 lig4-3	269	1	0.37
ku70 tert lig4-3	210	44	21

Table 4. Genome instability in G_3 *ku70 tert lig4-3*

	Anaphases Scored	Number of Anaphases with Bridges	Percentage with Anaphase Bridges
Wild type	210	0	0
ku70 tert	205	13	6
tert lig4-3	203	0	0
ku70 lig4-3	197	1	0.5
ku70 tert lig4-3	299	160	54

events, we employed fusion PCR (161) using sub- telomeric DNA primers directed towards the chromosome terminus (Fig. 41A). In this technique, PCR products are generated only when chromosome ends have been covalently joined.

Although no fusion products were detected with any DNA samples from G_1 single or double mutants, products were obtained with $G_1$and G_2 *ku70 tert lig4* triple mutants (Fig. 41B). Fusion products were also associated with G_2 *ku70 tert* mutants (161). The failure to detect chromosome fusion events by cytogenetics in these G_2 *ku70 tert* double mutants likely reflects the decreased sensitivity of cytogenetic analysis relative to PCR.

To examine the architecture of chromosome fusion junctions formed in the absence of *LIG4*, we cloned and sequenced fusion PCR products obtained from a G_3 *ku70 tert lig4* triple mutant. PCR primer combinations were for three chromosome pairs (1R-3L, 3R-3L. 3L-5R). A total of 22 clones were evaluated. Overall, these clones were similar to those obtained from *ku70 tert* mutants (161). The majority of the clones contained telomeric DNA and sequences from both chromosome arms, consistent with fusion of heterologous chromosomes. All but one had a structure consistent with primary end-to-end chromosome fusion (Fig. 40B). Forty-five percent of the clones represented telomere-telomere fusions, while 45% were telomere- subtelomere fusions. One subtelomere-subtelomere clone was identified, and one additional clone showed a complex structure at the fusion junction suggestive of a secondary fusion (Fig. 41C). As

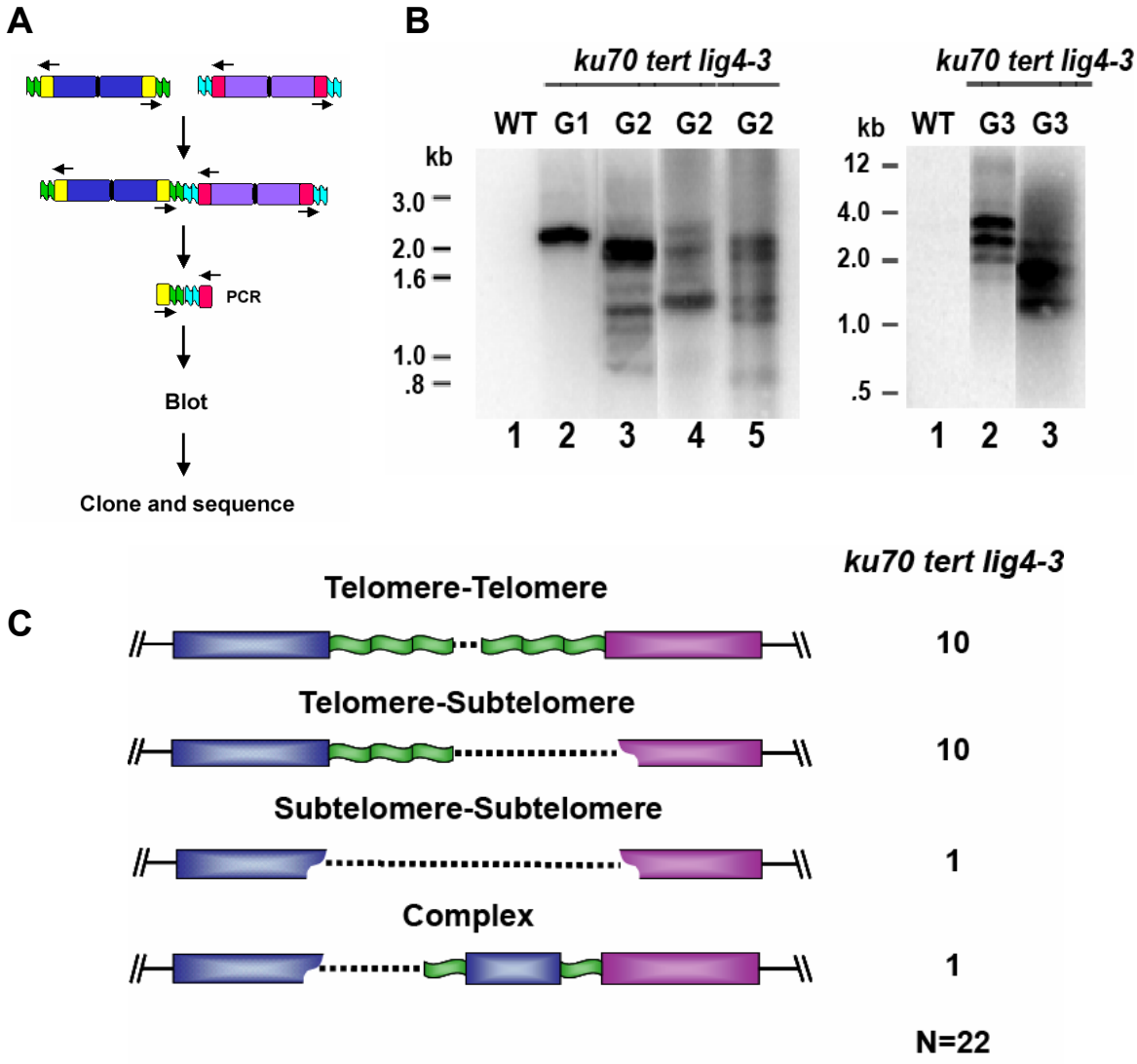

Fig. 41. Analysis of telomere fusions in *ku70 tert lig4-3* mutants. (*A*) Schematic of fusion PCR. (*B*) Fusion PCR results for G_1, G_2, and G_3 *ku70 tert lig4-3* plants. In the panel on the left, DNA from individual plants was used with the primer pair 4RX3L. In the panel on the right, DNA from one wild type plant and one *ku70 tert lig4-3* plant were analyzed using two different primer pairs (4RX3L, lanes 1-2; 4RX5L, lane 3). (*C*) Summary of chromosome fusion junctions in Fusion PCR clones obtained from *ku70 tert lig4-3* mutants.

with fusions formed in the *ku70 tert* background (161), the amount of telomeric DNA captured in the fusions varied, ranging from 52-1085bp. The average amount of telomeric DNA in the fusions (345bp) correlated roughly with the minimum functional telomere length previously defined for *Arabidopsis* (161). For telomere-subtelomere fusions the extent of deletion of subtelomeric sequences varied from 61 bp to 479 bp, and in all but one of those clones there was a short region of overlapping microhomology between the sequences at the fusion junction. The insertion of novel DNA sequence at the fusion junction was not a prominent feature of these clones. From these data, we conclude that fusion of dysfunctional telomeres can proceed in the absence of *LIG4*.

LIG4 contributes to telomere maintenance in *Arabidopsis*

In contrast to the situation with Ku and DNA-PK_{CS}, previous studies have failed to implicate *LIG4* in telomere biology (139, 148, 150, 152, 153). Nevertheless, our data indicate that *ku70 tert lig4-3* mutants display a precocious onset of growth and developmental defects. To investigate the molecular basis for the phenotypes associated with *ku70 tert lig4-3* mutants, TRF analysis was performed on DNA from G_2 and G_3 mutants.

As discussed earlier, the *lig4-3* mutation had no affect on telomere length on its own (Fig. 38). Telomeres are extended in mutants lacking *KU70* (66), Fig. 42, lanes 1-5 and Fig. 43A, lane 3. This is also the case in *ku70 lig4* mutants (Fig. 42, lanes 6-10 and Fig. 43A, lane 5). Although the data shown indicates that telomere tracts may be slightly shorter in *ku70 lig4-3* mutants, further

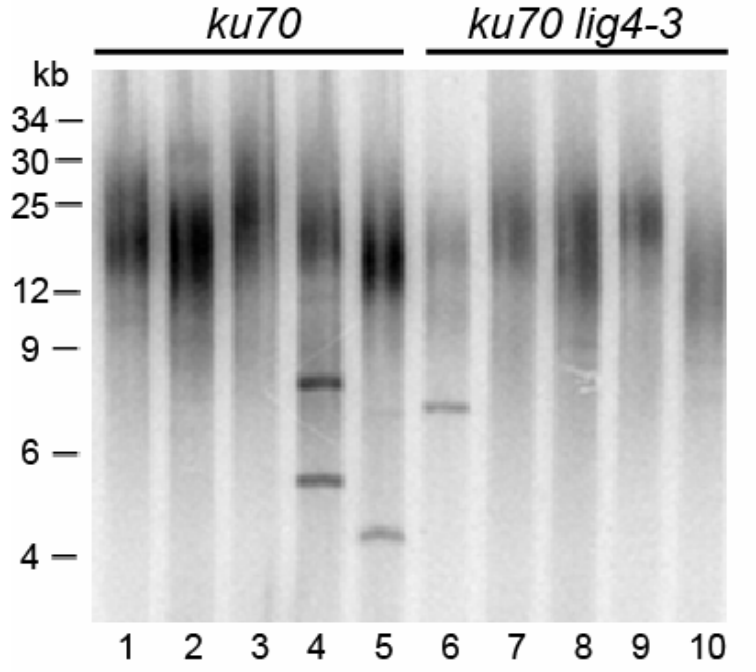

Fig. 42. Comparison of telomere length between *ku70* and *ku70 lig4-3* mutants in G_2. DNA from five *ku70* mutants and five *ku70 lig4-3* mutants was digested with *Tru*I1 and subjected to pulse-field gel electrophoresis to separate DNA in the 4-30Kb range. The gel was blotted onto nitrocellulose and probed with a 5' end labeled $(TTTAGGG)_4$ probe.

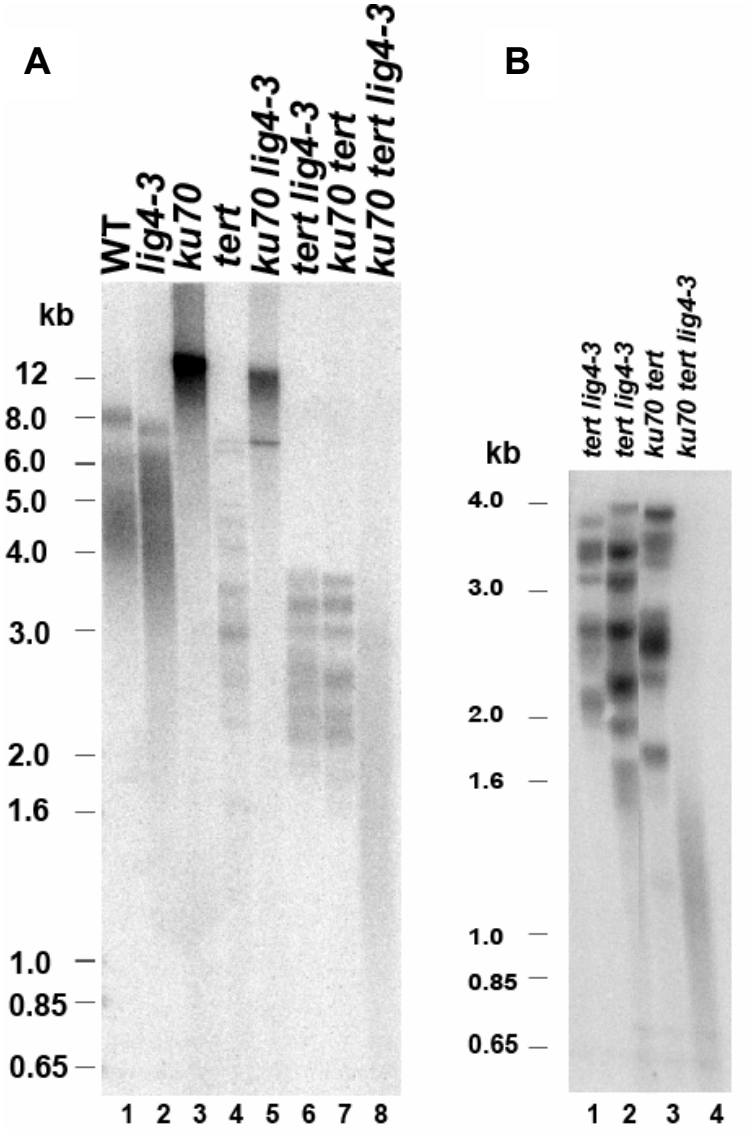

Fig. 43. TRF analysis of G_2 *ku70 tert lig4* mutants. Genomic DNA was isolated from one plant of each genotype and digested with *Tru*1I. DNA was transferred onto nitrocellulose and hybridized with a ^{32}P-labeled $(TTTAGGG)_4$ probe. (*A* and *B*) G_2 population blot. Examples of *ku70 tert lig4-3* line 1 (*A*, lane 8) and *ku70 tert lig4-3* line 2 (*B*, lane 4).

analysis of TRF length on a pulse field gel revealed no significant difference relative to *ku70* mutants (Fig. 42).

A different result was obtained when *lig4-3* was combined with a *tert* mutation. *Tert* mutants lose telomeric DNA at a rate of approximately 200-500 bp per generation (66). Accordingly, in G_2 telomeres in *tert* mutants ranged from 2.3 to 7kb. In contrast, telomeres were markedly shorter in *tert lig4-3* mutants, spanning only 2-3.5 kb (Fig. 43A, lane 6) in line 1, and 1.6-4kB in line 2 (Fig. 43B, lanes 1 and 2). This accelerated rate of telomere erosion mimicked that of G_2 *ku70 tert* mutants (Fig. 43A, lane 7; Fig. 43B, lane 3). Furthermore, in both *tert lig4* and *ku70 tert* mutants, TRFs formed a discrete banding profile bearing significantly less heterogeneity than wild type telomere tracts (Fig. 43A, compare lane 1 with lanes 6 and 7). These data suggest that Lig4 and Ku70 make similar contributions to telomere maintenance.

Further support that Lig4 contributes to telomere maintenance came from TRF analysis of G_2 *ku70 tert lig4-3* triple mutants. The TRF profile in these plants differed dramatically from the other mutants we examined. Instead of a discrete banding profile, telomeres in the *ku70 tert lig4-3* mutants consisted of a broad homogenous smear with products ranging in size from approximately 1-3kb in line 1 (Fig. 43A, lane 8) and only 0.65-1.6Kb in line 2 (Fig. 43B, lane 4). The more accelerated rate of telomere shortening in line 2 versus line 1 *ku70 tert lig4-3* mutants correlates with the earlier onset of the terminal phenotype in this line (data not shown). The dramatic shortening of telomere tracts in the triple mutants is also consistent with the early onset of genome instability in these plants and strongly argues that Lig4 contributes to telomere maintenance in *Arabidopsis*.

DISCUSSION

The interaction of NHEJ components with functional and dysfunctional telomeres is enigmatic. While such proteins are required for repair of double strand breaks, their presence at telomeres somehow precludes this process. The data presented here uncovers two unexpected characteristics of Lig4; the protein is not required for fusion of dysfunctional telomeres, but is necessary for telomere maintenance.

Fusion of critically shortened telomeres can proceed in the absence of *LIG4*

Data from mammals that suggests that Lig4 is required for the fusion of telomeres in cells over-expressing a dominant negative TRF2 (99). Yet in *Arabidopsis* telomeres fuse in the absence of Lig4. Approximately 90% of the chromosome fusion junctions we cloned from the *ku70 tert lig4-3* mutants had microhomology at the junction, suggesting that in the absence of Ku and Lig4 microhomology mediated end-joining is the mechanism for fusion. Although fusion junctions from *ku70 tert* and *ku70 tert lig4-3* were essentially indistinguishable, both display the hallmarks of NHEJ with deletions and microhomology at the fusion junctions. The similarity between fusions that

occurred in the absence of Ku or Ku and Lig4 was not surprising in light of the mechanism of NHEJ. Current models for NHEJ show Ku being recruited to the site of a DSB first, followed by DNA PK_{cs} and then Lig4/XRCC4 (194). In the absence of Ku, end-to-end fusions may be shuttled to a more micro-homology based pathway, such as one that utilizes the MRX complex (161). The absence of Lig4 apparently does not alter this choice. Although we cannot quantitate our Fusion PCR data, the large number of fusions observed by cytogenetics suggests that backup NHEJ pathways can efficiently fuse dysfunctional telomeres.

In plants, yeast and filamentous fungi, T-DNA integration occurs by NHEJ (195-199). Interestingly, *LIG4* is required for T-DNA integration in yeast (196, 200), but is not required in *Arabidopsis* (155). Sequence analysis of the T-DNA integration sites in Lig4 deficient plants showed no defects in the efficiency of integration or the features of T-DNA integration (155). These observations, combined with the data presented here argue that *Arabidopsis* harbors another ligase capable of functioning in NHEJ. While there are no obvious DNA ligase II and III homologues in *Arabidopsis*, one possible candidate for involvement in NHEJ is DNA Ligase I, which is an essential gene in *Arabidopsis* (201). The *Arabidopsis* DNA Ligase I is able to ligate nicks and double-stranded DNA with either blunt or cohesive ends (202). Hence, this enzyme could potentially substitute for Lig4 in DSB repair by NHEJ.

Lig4 contributes to telomere maintenance

Unexpectedly, our data point to a role for *LIG4* in telomere maintenance in *Arabidopsis*. We observed an accelerated rate of telomere shortening in *tert lig4* mutants, similar to that seen in *ku70 tert* mutants. Moreover, telomere tracts in both settings, telomeres displayed decreased heterogeneity, typical of a tert mutant. Ku is a negative regulator of telomerase and in its absence telomeres expand to two-to-three times their normal size (145). Telomeres are wild type length in *lig4-3* mutants, indicating that Lig4 does not modulate telomerase activity. Further support comes from TRF analysis of *ku70 tert lig4-3* mutants. In these plants, telomeres shorten even more dramatically than in either *ku70 tert* or *tert lig4-3* mutants, indicating that Ku and Lig4 make distinct contributions to telomere maintenance.

While interactions between Ku and telomerase in *Arabidopsis* are unknown, Ku has been shown to contact the telomerase RNP in yeast and mammals. In *S. cerevisiae*, Ku binds a 48-nt stem-loop region of TLC1 RNA *in vitro* (203, 204) and *in vivo* (174). While in mammals, Ku physically interacts with TERT, and this interaction does not require DNA (205). Interactions between Lig4 and other components of the telomere complex have not been explored (see below).

Interactions between Lig4 and telomeres

In addition to its interactions with telomerase, Ku plays an important role in maintenance of the telomeric C-strand. Deletion of Ku leads to long G-

overhangs in yeast and *Arabidopsis* (140-145) and recent studies argue that the extended G-overhang does not reflect increased telomere action, but rather failure to protect or fully replicate the C-strand of the telomere. Studies in yeast indicate that Exonuclease 1 is responsible for creating extended G-overhangs in Ku mutants (63, 206), implying that Ku is required to protect the telomere from shortening activities. Although the status of the G-overhang in the *ku70 tert lig4-3* mutants is unknown, preliminary data indicates that at least a subset of telomeres in the triple mutants possess G-overhangs (R. Idol and D. Shippen, unpublished results).

Our data argue that Ku and Lig4 may work together to protect telomeres in *Arabidopsis*. In the absence of TERT, deletion of either Ku or Lig4 leads to partial uncapping, allowing some exonucleolytic attack on these telomeres (model, Fig. 44). However, when a telomerase deficiency is combined with the loss of both Ku and Lig4, telomeres are dramatically shortened and extremely heterogeneous, arguing that the telomere capping function has been abolished leaving the ends susceptible to catastrophic exonuclease attack (model, Fig. 44).

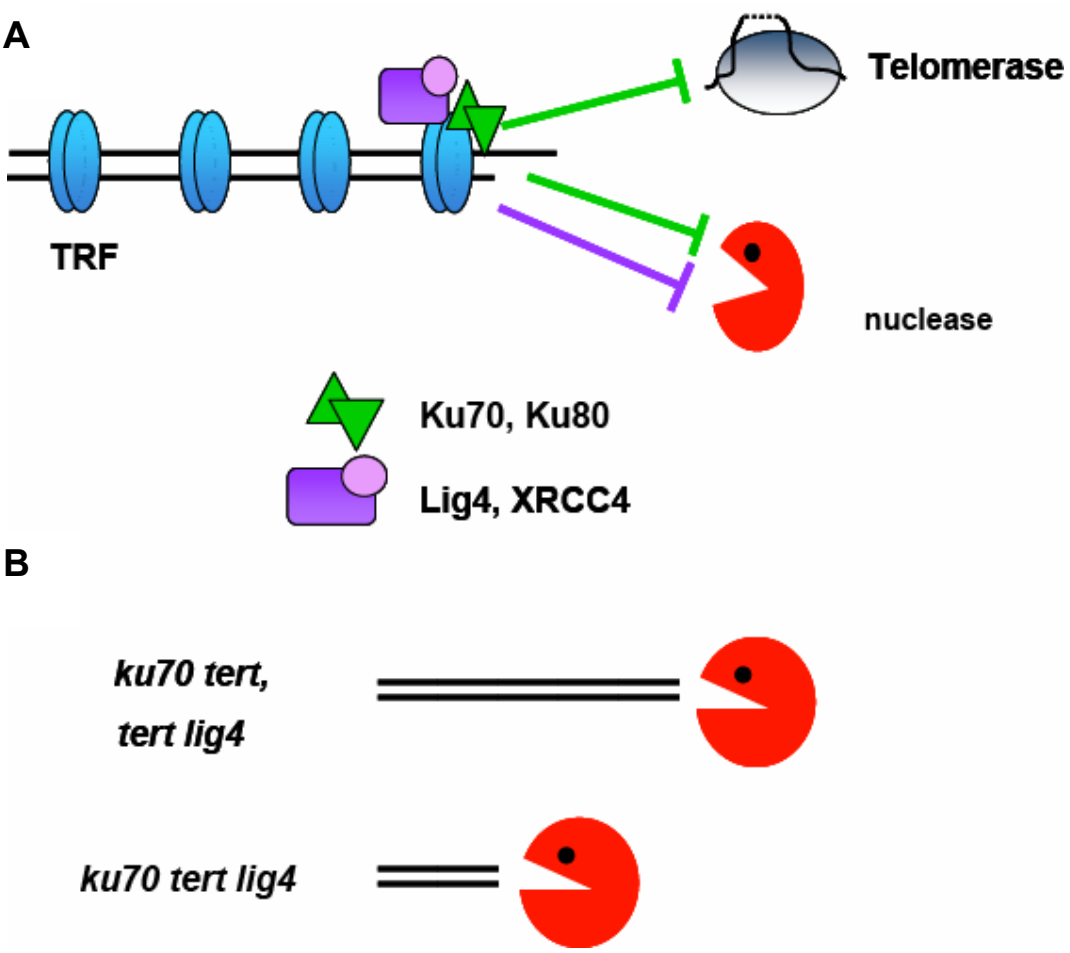

Fig. 44. Model for Lig4 action at telomeres. (*A*) Ku (green) and Lig4 (purple) are physically associated with the telomere. Ku is a negative regulator of telomerase, and helps protect against exonucleolytic attack. (*B*) In the absence of telomerase, deletion of either Ku or Lig4 leads to partial telomere uncapping, and this allows some exonucleolytic activity on these telomeres. In *ku70 tert* mutants, the C-strand appears to be more exposed to attack. The status of the G- and C-strands in *lig4-3* mutants is unknown. However, telomerase mutants that lack both Ku and Lig4 chromosome ends become even more susceptible to attack, resulting in catastrophic telomere shortening.

Our genetic data are consistent with the idea that Lig4 is a stable component of the telomere in *Arabidopsis*. While not yet addressed in plants, Ku is physically associated with telomeres in mammals and yeast through interactions with TRF1 or Sir4p, respectively (143, 148, 207, 208). Although current models of NHEJ show Lig4 being recruited to a DSB after both Ku and DNA-PK_{cs} (209), perhaps Lig4 normally resides at *Arabidopsis* telomeres through interactions similar to those made with Ku.

Recent work has shown the catalytic activity of DNA-PK_{CS} is required to prevent end-to-end fusions (152). It is unknown whether the catalytic activity is *LIG4* is required to protect chromosome ends. Blackburn and colleagues showed more than twenty years ago that yeast and *Tetrahymena* telomeres carry discontinuities within the C-strand (210, 211). Perhaps Lig4 is involved in sealing these nicks to help maintain C-strand continuity.

MATERIALS AND METHODS

Plant materials

Arabidopsis thaliana plants with a T-DNA insertion in *AtLIG4* were obtained from the SALK collection (SALK_04427) (177). Heterozygous plants were identified using PCR with primers Lig4-8 (5’ GTGATTTGAA ACTAGTCTGTG 3’), Lig4-9 (5’ CAGCAAACCGATTCAGAGATG 3’) and Lba-1 (5' TGGTTCACGTAGTGGGCCATCG 3') (177). Plants heterozygous for T-DNA insertions in *KU70* and *TERT* (145) were crossed to heterozygous *lig4-3* plants. PCR was used to identify a single triple heterozygous plant in F1, and this plant was self-pollinated to produce a segregating F2 population. Two lines (line 1 and line2) were established for *ku70 tert*, *tert lig4-3* and *ku70 tert lig4-3* mutants. All single, double, and triple mutants along with WT plants were identified by PCR from this population. Plants were grown at 23°C in an environmental chamber under a 16/18-hr light/dark photoperiod.

RNA extraction and RT-PCR

Total RNA was extracted from flowers using the Tri-Reagent solution (Sigma, St. Louis, MO). Reverse transcription was performed using 1μg of total RNA with SuperScript III (Invitrogen) and oligo dT at 55°C. The following primers were used: Lig4-p1 (5’ ATGACGGAGGAGATCAAATTCAGCG 3’), Lig4-p2R (5’ TGACCCACTTCATCTCCTGAGC 3’), Lig4-8 (5’ GTGATTTGAAA CTAGTCTGTG 3’), Lig4-9 (5’ CAGCAAACCGATTCAGAGATG 3’), Lig4-p5F (5’ GGGAACCTGGAGATCGTAGTGG 3’), Lig4-p6 (5’ TGCCCTTGATATCCG

ATACATCAG 3'). PCR conditions were as follows: 94°C for 2 min., followed by 40 cycles of 94°C for 45 sec, 55°C for 45 sec and 72°C for 1 min, with a final incubation at 72°C for 10 min.

Assay for sensitivity to MMS

Seeds of wild type, *ku70* and *lig4-3* were sterilized in 50% bleach and plated on solid 0.5 MS media. Four-day-old seedlings were transferred to separate wells of a 24-well plate containing liquid 0.5 MS medium containing 0, 60, 80 or 100ppm (v/v) MMS (Aldrich) and incubated in a shaker with constant light. Seedlings were scored after ten days.

Analysis of mitotic chromosomes

Mitotic anaphases were prepared as described previously (66) with the following modifications. Buds were digested with an enzyme mixture containing 2% cellulase w/v (Sigma) and 20% v/v pectinase (Sigma) in 0.01M citrate buffer pH 4.6 at 37°C for 1 hr. Squashes were then analyzed as described (66).

PCR amplification, cloning and sequence analysis of fusion junctions

Unique subtelomeric primers directed 5' to 3' toward the telomeric repeat were designed for each: 1L (5' ACAAGGATAG AAATAGAGCATCGTC 3'); 3L (5'AGACGAGGAGACTAGGAACG 3'); 3R (5' GTATGGATGCCGGGAAA GTTGCAGACAA 3); and 5R (5' TCGGTTGTC GTCTTCAAG 3'). PCR was performed as previously described (161). A 10μL aliquot of the PCR products

was separated by electrophoresis through a 1% agarose gel, and transferred to a nylon membrane. Membranes were hybridized as previously described (161). Hybridization signals were detected using a STORM PhosphorImager (Molecular Dynamics) and the data were analyzed using IMAGEQUANT software (Molecular Dynamics).

For cloning of PCR products, unincorporated primers were removed using the QIAquick PCR Purification Kit (Qiagen). Products were then ligated into the pDRIVE vector (Qiagen) and transformed into SURE® competent cells (Stratagene). Fusion clones were detected by colony hybridization as described previously (161). DNA was prepared from clones of interest using a QIAprep Spin Miniprep Kit (Qiagen). DNA sequence reactions were performed using the BigDye Reaction Mix (Perkin Elmer-ABI), and products were evaluated using an ABI PRISM 377 DNA Sequencer.

Terminal restriction fragment length analysis

DNA was extracted from whole plants three to five weeks after germination (212). TRF analysis was performed as follows: 1µg genomic DNA was digested with *Tru*I1 (Fermentas) restriction enzyme, overnight at 65°C. DNA was separated by electrophoresis in a 1% agarose gel and blotted onto a nylon membrane. Membranes were probed with a ^{32}P end-labeled telomeric oligonucleotide $(T_3AG_3)_4$ as above. Hybridization signals were detected using a STORM PhosphorImager (Molecular Dynamics) and the data were analyzed using IMAGEQUANT software (Molecular Dynamics).

CHAPTER V

SUMMARY AND FUTURE DIRECTIONS

Telomere biology has its roots in experiments carried out in the 1930s by two geneticists: Barbara McClintock and Hermann J. Muller. Working separately and with different organisms (maize and *Drosophila*, respectively), both realized that chromosomes contained specialized ends that were required for stability. Muller coined the term "telomere," from the Greek for "end" (telos) and "part" (meros) (213). Although much of the information known about telomeres has come from other organisms, plant telomere biology is moving to the forefront of telomere research.

This renewed interest in plant telomeres is due in a large part to the small weed, *Arabidopsis thaliana*. The sequencing of the *Arabidopsis* genome and the availability of gene knockout lines has allowed the identification and characterization of many telomere-related genes. Additional features that make *Arabidopsis* an excellent model system for telomere biology include its extreme tolerance to genome instability and major stresses. Many genes involved in sensing and repairing genome instability are non-essential. Moreover, *Arabidopsis* is genetically tractable and multiple mutant combinations can be created by simple genetic crosses. I have exploited these features to address fundamental questions about telomeres and telomerase in plants.

TELOMERE DYNAMICS IN *Arabidopsis*

Telomere length varies between different eukaryotes, but telomeres are strictly maintained at a species-specific set point. Regulation of this set point involves a large number of different genes (Askreee et. al., 2004). The regulation and strict maintenance of the telomere length set point is not fully understood in any model system. Telomeric DNA is subjected to both lengthening and shortening activities (60). The combined contributions of both types of activities maintain telomere length homeostasis.

In wild type cells, the primary mode for telomere shortening is thought to occur as a result of the end replication problem. Recently, more active processes have been identified that can lead to rapid loss of telomeric DNA, including Telomere Rapid Deletion (TRD) (61), deficiencies in proteins important for protection of the extreme terminus of the telomere (62), and exonuclease activity on uncapped telomeres (63). These telomere-shortening activities are circumvented through the action of telomerase.

Despite the fact that telomere length is maintained at an equilibrium length for each species, this “set point” can vary within species of the same genus. In mice, telomeres in the established inbred mice strains are approximately 40kb, while in wild-derived mice the length is much shorter, around 10-15kb (64). In the model plant, *Arabidopsis thaliana*, telomere length varies amongst different ecotypes, which can be divided into two distinct groups based on telomere length (3). In one group, telomeres range from 2-5kb while in the other group telomeres

span 3.5-8kb. Thus, telomeres that range from 2-8kb are acceptable for *Arabidopsis* (3).

Telomere length can also vary within an organism. In barley embryos, telomeres are 80kb, but in leaves are shortened to 23kb (214). This rapid shortening is reminiscent of TRD described for budding yeast (61). Barley telomeres also undergo dramatic elongation in cell culture, expanding from 10kb to over 150kb (214).

When crosses are made between mice with long telomeres and mice with short telomeres, a new telomere length set point is established in the F1 progeny (163). The new telomere length is intermediate relative to the short and long telomere parents. Telomeres from the short telomere parent are lengthened, but the long telomeres from the long parent are not acted upon and may shorten slightly (163). This observation suggests that telomere elongation by telomerase is limited to the shortest telomeres. Similar to what is seen in mice, crosses between plants with long and short telomeres result in an intermediate telomere length in the F1 progeny (3). This species-specific telomere length is dependent on telomerase; in the absence of telomerase telomere length is no longer maintained at the set point.

How is the optimal telomere length size determined in each organism and what are the sensing mechanisms each organism has developed to monitor telomere length? Some organisms have short telomeres while others have very long telomeres, yet very similar lengthening and shortening activities function in all systems studied to date. The coordination of these activities must be

regulated in each system, but factors governing this coordination are unknown. It will be very interesting to see common machinery is used to regulate the length altering activities at telomeres, or if telomere length is set by species-specific factors.

Disruption of telomerase activity leads to progressive telomere shortening, defects in cellular proliferation, and an increase in genetic instability and infertility (65-70, 164). Although telomeric DNA is lost over successive generations in mice, phenotypic defects are not observed until the fourth generation (G_4) of mice (65, 164) and the sixth generation (G_6) of *Arabidopsis* (66). Nevertheless, these telomerase-deficient eukaryotes ultimately reach a terminal phenotype, characterized by severe genome instability and sterility, which occurs by G_6 in mice and G_9 in plants (65, 66).

When the telomere length set point is disrupted, how do different organisms reestablish their set point? The disruption of telomere length set point in telomerase-deficient mice is reversible. By re-introducing one copy of the TR, telomeres are elongated and progeny show no defects in growth or proliferation (163, 165). In this dissertation, I investigated the dynamics of reestablishing the telomere length set point in *Arabidopsis*.

The first strategy we used to examine reestablishing telomere length set point was to over-express TERT in different generations of *tert* mutants (66). I was able to recover transformants, and named these plants “Tert backs”. Plants expressing telomerase activity in the leaves were selected for further analysis. Terminal restriction fragment analysis of the Tert back plants gave surprising

results, telomeres were not lengthened in these plants. Fusion PCR on the Tert back plants demonstrated that telomere fusion events had occurred, signifying that the presence of telomerase activity was not sufficient to prevent or stop genome instability in these plants. Moreover, telomeres not lengthened when Tac1 is over-expressed in plants (213), suggesting that plants are unable to utilize telomerase in vegetative tissues.

Another approach to examine the consequence of reintroducing telomerase into telomerase mutants was through classical genetic crosses. Wild type plants were crossed to different generations of *tert* mutants, and analyze the resulting F1 progeny. This proved to be more successful than the over-expression approach used earlier. Progeny plants had telomerase activity and were able to lengthen short telomeres.

As discussed in Chapter II, in *Arabidopsis*, although the shortest telomeres were lengthened in the F1 progeny, one generation of *TERT* heterozygosity was not enough to return all telomeres to the wild type set point of 2-5kb. Perhaps in the presence of very short telomeres, telomerase cannot lengthen telomeres to the extent necessary to restore the set point. Data from yeast and human cells suggests that multiple cell divisions (30-50 population doublings) are required to restore shortened telomeres to the species specific set point (169, 171). Therefore, it is conceivable that the number of cellular divisions in one plant generation, and thus the length of time telomeres are exposed to telomerase is not sufficient to fully restore all the telomeres to the wild type set point. This hypothesis would explain why mice are also unable to return all

telomeres to the set point in one generation after reinstating telomerase activity (165).

Future directions

To investigate our hypothesis that more cellular divisions in the presence of telomerase are necessary to return all telomeres to the set point, plants can be propagated for additional generations. This will allow the wild type *TERT* allele to segregate, and the resulting wild type and heterozygous *tert* mutants will have additional cellular divisions in the presence of telomerase activity. Repeating the TRF analysis on the F2 plants could reveal the number of plant generations needed to reestablish the telomere length set point. It is possible that two generations may not be enough to return all short telomeres to the *Arabidopsis* set point. If so, these plants will be propagated until all telomeres are within the wild type range of 2-5kb.

In this study I did not examine the F1 progeny for the presence or absence of chromosome instability. It would be very interesting to ask whether these F1 plants have ongoing genome instability, even in the presence of telomerase activity. Telomerase action should reestablish the proactive cap on the chromosome terminus by giving telomere binding proteins adequate sites to bind. *Arabidopsis* telomeres have unique sequences adjacent to the telomeric repeats (sub-telomeric sequences), thereby allowing the capture of fusion events by PCR (fusion PCR) and sequence analysis of the fusion junctions (161). A careful parent-progeny analysis using fusion PCR should identify any fusion

events in the F1 progeny, and allow us to ask several interesting questions. First, are there telomere fusions in the F1 progeny, and secondly, if there are fusions in the F1 progeny, do they persist in the F2 population? Finally, have any fusion events been "healed" by the addition of telomeric DNA, and are they propagated in successive generations.

One remaining question is at what point they cannot be rescued by telomerase. To address this, I have attempted crosses with G_8 *tert* mutants that have severe vegetative and reproductive defects, and would be categorized as a Type II phenotype (66). Although the majority of these crosses were unsuccessful, I was able to generate progeny from a cross using a G_8 plant as a mother, and progeny from two crosses using a G_8 plant as the father. If the seeds produced are viable, following the F1 progeny from these crosses will allow us to test whether re-activating telomerase is sufficient to prevent the phenotypic changes associated with telomerase deficiency. TRF analysis could be performed to check the telomere length in the progeny. Of special interest will be the length of the longest telomeres in the F1 progeny as compared to those from the wild type parent. It will also be intriguing to look for telomere fusion events that may have been "healed" by telomerase and propagated to the progeny. The work shown here demonstrates the plasticity of telomere dynamics in *Arabidopsis.* It is possible to reestablish the wild type telomere length set point in plants, although multiple generations may be needed to fully restore all telomeres to the set point.

IDENTIFICATION AND ANALYSIS OF TWO *EST1* HOMOLOGUES FROM *Arabidopsis thaliana*

One major arena of investigation in the telomerase field is characterization of the telomerase ribonucleoprotein (RNP). Although the two core components of telomerase, TERT and TR have been identified in many model organisms, very little is known about other components of the telomerase holoenzyme. Non-catalytic telomerase components have been isolated from yeast and humans, yet our understanding of these proteins is limited. The recruitment of telomerase to the telomere in higher eukaryotes has also remained enigmatic.

Currently, there is very little biochemical data available concerning the telomerase RNP from plants. Partial purification of the telomerase holoenzyme from cauliflower indicates a molecular mass of approximately 670kD (M. Fitzgerald and D. Shippen, unpublished). Tobacco telomerase appears to be of similar size, although a minor portion of the telomerase activity associates with a smaller, 250kD complex (103). While TERT has been cloned from *Arabidopsis* and rice (68, 215, 216), TR has remained elusive in plants. To gain a better understanding of the telomerase RNP in *Arabidopsis*, I identified and characterized two putative components of the telomerase RNP, AtEst1a and AtEst1b.

There is currently no information regarding the protein interactions necessary to bring telomerase to the telomere in higher eukaryotes. Therefore, we hypothesized that the *Arabidopsis* Est1 proteins might interact with the ScCdc13p functional homologues, Pot1 and Pot2 (Shakirov et. al. unpublished

data). In experiments not discussed in Chapter III, we were unable to detect any interactions between Est1a, Est1b, Pot1 and Pot2 by coimmunoprecipitation (R. Idol, E. Shakirov, Y. Surovtseva and D. Shipppen, unpublished data).

Interestingly, *AtEST1b* is an essential gene. The *est1b* mutants are sterile, and must be segregated from a plant heterozygous for the T-DNA insertion. Recent studies have shown a novel role for AtEst1b in meiosis (Riha in preparation). Taken together, these phenotypes suggested to us that AtEst1b must be involved in a pathway or mechanism essential for plant development.

I tested whether AtEst1b was involved in the DNA damage response. If so, est1b mutants would be more sensitive to DNA damaging agents than wild type plants. This experiment was complicated as est1b mutants are sterile and have to be segregated from heterozygous plants. To address the DNA damage sensitivity of *est1b* mutants, I plated seeds from an *est1b-2* heterozygote on plain MS media. After four days, seedlings were transferred to liquid media containing 0ppm or 100ppm MMS. After 6 days, surviving plants were harvested and genotyped. While all possible mutant combinations were identified at 0ppm MMS, no *est1b* mutants were isolated from the survivors of the 100ppm MMS treatment, suggesting that est1b mutants may be sensitive to DNA damage (R. Idol and D. Shippen, unpublished data). However, we cannot determine if this is a direct or indirect effect of AtEst1b.

Besides their similarity to Est1-like proteins from other organisms, AtEst1a and AtEst1b display similarity to proteins in the nonsense-mediated decay pathway (NMD). NMD is a RNA surveillance mechanism that safeguards cells

from potentially deleterious proteins produced as a consequence of routine mistakes in gene expression. These mistakes generally result in mRNAs having frame-shift mutations that generate nonsense mutations. Approximately one third of human genetic diseases are due to frame-shift and nonsense mutations that result in the premature termination of translation, which demonstrates the importance of this pathway.

Many of the proteins known to be important for NMD were isolated from *C. elegans* (SMG 1, 2, 5, 6 and 7; suppressor with morphogenetic effect on genitalia) and *S. cerevisiae*, UPF 1-3 (up-frameshift). Both Smg5 and Smg7 have N-terminal TPR domains, and Smg5 has a C-terminal PIN domain (184). Interestingly, when Smg5 and Smg7 are used as a query against the *Arabidopsis* non-redundant database the only proteins identified are AtEst1a and AtEst1b, suggesting a link between *Arabidopsis* Est1 proteins and NMD.

If AtEst1b was involved in NMD in *Arabidopsis*, knocking out other genes in the NMD pathway may cause similar growth and reproductive phenotypes like those observed in the *est1b* mutants. I identified a sequence homologue of UPF1 in *Arabidopsis* and obtained a line harboring a T-DNA insertion in this gene; however, these mutants had none of the vegetative or reproductive defects associated with a deficiency in *AtEst1b* (R. Idol and D. Shippen, unpublished data). The T-DNA insertion in *UPF1* was at the 3' end of the gene, and would allow the majority of the transcript to be expressed. If this partial *UPF1* transcript was able to produce a functional protein, NMD may not be altered in this mutant and would explain why I was unable to recapitulate the *est1b* phenotypes.

Future directions

Several questions remain concerning the biochemical characterization of Est1a and Est1b. Is the N-term of AtEst1a or any portion of AtEst1b capable of binding nucleic acids? Characterization of nucleic acid binding properties of AtEst1b and the N-terminal domain of AtEst1a are currently underway. Do either Est1a or Est1b physically interact with the *Arabidopsis* telomerase RNA subunit? Efforts are currently underway in the Shippen lab to identify the *Arabidopsis* telomerase RNA subunit, and once it has been identified, the RNA subunit could be used in coimmunoprecipitation experiments with the Est1-like proteins and TERT to assess the interaction status of all three. Finally, do the Est1 proteins in plants play any role in the recruitment of telomerase? It is possible that another bridging protein is required to bring telomerase to the telomere in plants, and yeast two hybrid screens with either the Pot proteins or Est1 proteins may help identify this protein.

The intriguing question of Est1b's function in plants remains unanswered. One possible role for Est1b is in the nonsense-mediated-decay (NMD) pathway. Human Est1a was identified as a component of the human NMD pathway (181), and in yeast, NMD regulates expression levels of several telomere components (182, 183). It is certainly possible that the effects seen by disruption of AtEst1b are not direct effects, but are a result of defects in NMD.

There has been little work done on NMD in plants, but recent reports from rice and barely have identified mutations in genes that cause the aberrant

mRNAs to undergo NMD (217, 218). Identification of similar aberrant mRNAs in *Arabidopsis*, and characterizations of these mRNAs in an *est1b* null background could address if *AtEST1b* plays any role in NMD. Additionally, micro-array analysis of *est1b* mutants may help identify transcripts that are improperly processed in the mutants and thereby help us to elucidate the role of AtEst1b in *Arabidopsis*. Moreover, yeast two-hybrid screens could identify Est1b interacting proteins and give us an indication of Est1b function in plants.

Recently, a role in meiosis was established for *AtEST1b* (Riha et al., in preparation). In *est1b* mutants, meiosis is normal through metaphase II. However, in anaphase II, chromatids are randomly distributed over the entire cell, and the cells arrest at the anaphase II/telophase II transition (Riha et al., in preparation). This suggests that est1b mutants fail to exit meiosis due to an insufficient degradation of mitotic cyclins (Riha et al, in preparation). Whether this is caused indirectly by a failure to shut down the spindle checkpoint due to premature chromatid separation, or by a more direct involvement of Est1b in assisting cyclin degradation will require further study. The possibility of Est1b participating in cyclin degradation provides another intriguing link between Est1b and NMD.

THE ROLE OF NHEJ COMPONENTS IN TELOMERE MAINTENANCE

Consolidating the seemingly antagonizing functions of DSB repair proteins at and on telomeres is one of the major enigmas in the telomere field today. If dysfunctional telomeres are fused by the NHEJ pathway, why are many of the

key NHEJ factors components of the wild type telomere? Which of the NHEJ proteins are required for the fusion of dysfunctional telomeres, and of those, how many play separate roles in telomere maintenance? Dissecting the interactions of NHEJ proteins at the telomere and elucidating mechanism of telomere fusion events is crucial to fully characterize the telomere itself. To this end, I characterized the role of DNA Ligase IV at Arabidopsis telomeres (Chapter IV).

To address the role of Lig4 in the fusion of critically shortened telomeres, I created a *ku70 tert lig4-3* triple mutant. Using both a cytogenetic approach, and a PCR based assay, I detected telomere fusions in the *ku70 tert lig4-3* triple mutant. Although these plants are deficient for *KU70* and *LIG4*, analysis of the fusion junctions showed the presence of deletions, insertions and micro-homology at the fusion junctions, clearly demonstrating that the fusions arose through a NHEJ pathway. Our finding that telomeres can fuse in the absence of *LIG4* was surprising based on data from mammals, which clearly demonstrates that Lig4 is required for the fusion of telomeres in cells over-expressing a dominant negative TRF2 (99).

This is not the first evidence for NHEJ function in the absence of Lig4. T-DNA integration occurs by NHEJ in plants, yeast and filamentous fungi (195-199). Lig4 is required for T-DNA integration in yeast (196, 200) but is not required in *Arabidopsis* (155). Sequence analysis of the T-DNA integration sites in Lig4 deficient plants showed no defects in the efficiency of integration or the features of T-DNA integration (155), demonstrating the presence of a Lig4 independent pathway for NHEJ.

Moreover, a Lig4-null human cell line was able to rejoin *Eco*RV and *Eco*RI cut plasmids *in vivo*, albeit with a much lower efficiency and accuracy than Lig4 proficient cells (219). Interestingly, microhomology (6-9bp) was observed at the majority of the junctions (219). However, in XRCC4-null murine cells were able to efficiently rejoin *Bam*HI or *Sal*1 cut plasmids *in vivo* (220). Sequence analysis of junctions derived from XRCC4-deficient cells revealed a strong preference for a junction containing a 7bp of microhomology (220). The difference in efficiency of end-joining in the absence of Lig4 could be explained by rodent cells having higher levels of an alternative end-joining pathway relative to human cells; this theory is supported by analysis of end joining using cell-free extracts (221). These findings demonstrate the existence of a DNA Ligase IV-independent rejoining mechanism in mammalian cells.

Surprisingly, while Lig4 is not required for the fusion of dysfunctional telomeres, it is required for telomere maintenance in *Arabidopsis*. I observed an accelerated rate of telomere shortening in *tert lig4* mutants, similar to the amount of shortening seen in *ku70 tert* mutants (145). In addition telomeres in both mutants showed the decrease in heterogeneity typical of a Tert mutant (68). Furthermore, telomeres in the triple mutants shortened even more dramatically than in either double mutant, implying that the function of Lig4 is distinct from Ku. Telomeres in the *ku70 tert lig4-3* plants are extremely heterogeneous, suggesting that they have been exposed to a catastrophic nucleolytic attack. My data provide the first evidence for a role for Lig4 outside of NHEJ, and in telomere biology.

The role of Lig4 in telomere length regulation was only uncovered in combination with a telomerase deficiency. Mutants deficient in telomerase (TERT) and Lig4 have been created in *S. pombe* (188), however these strains senesced at the same rate as *trt1⊿* single mutants (139). In *S. cerevisiae*, many mutant combinations of Lig4 and telomerase deficient strains have been generated; however, telomere length was not addressed in any of the mutant combinations. These strains were all generated for studying the mechanism of telomere fusions, and depending on the assay used, the fusions are dependent or partially dependent on Lig4 (186, 188, 189). The best explanation for the lack of telomere length analysis in these mutants stems from the single Lig4 mutant having wild type telomere length. Hence, these strains were generated for experiments to examine double strand break repair, not to uncover Lig4 telomere length regulation. Thus, it is possible that Lig4 functions at telomeres in yeast. A more careful study of the yeast telomerase and Lig4 mutants is worthwhile.

Future directions

There is more work to be done on Lig4 in *Arabidopsis*. Our genetic data suggest that Lig4 is a stable component of the *Arabidopsis* telomere. Both chromatin immunoprecipitation and coimmunoprecipitation experiments should be performed to determine if Lig4 is present at the telomere and what proteins it interacts with. Also of interest is the status of the G-overhang in Lig4 mutants. We know that in the absence of *KU70* G-overhangs become greatly elongated (145), but what about in Lig4 mutants? Similarly, what has happened to the G-

overhang in the *ku70 tert lig4* triple mutants? Can we detect G-overhangs, and if so, are they lengthened reminiscent of G-overhangs in the *ku70 tert* double? Finally, is the catalytic activity is Lig4 is required to protect chromosome ends? Recent work has shown the catalytic activity of DNA-PK_{CS} is required to prevent end-to-end fusions (152). Work done in yeast and *Tetrahymena* in the early 1980's demonstrated the presence of discontinuities within in the C-strand (210, 211). One possible role for Lig4 would be in sealing these nicks to help maintain C-strand continuity. Work is currently in progress to address these questions and increase our understanding of Lig4's role in telomere length maintenance.

Over the past several years, tantalizing evidence has been accumulating suggesting that homologous and non-homologous repair of DSB are overlapping pathways (222-225). In *Drosophila*, *lig4* and *rad54* mutants are sensitive to DSBs, but the double *lig4 rad54* mutants show a synergistic increase in DSB sensitivity (223). In comparison to *LIG4* deletion, deletion of *RAD54* results in only mild phenotypes in mice, sensitivity to ionizing radiation and a mild susceptibility to genomic instability (226). However, in *lig4 rad54* double mutant mice, severe proliferation defects, high levels of un-repaired DSBs, and increased chromatid instability was observed in comparison to either single mutant (227). These findings demonstrate overlapping functions for NHEJ and Rad54-dependent HR in the repair of DSBs. Moreover, deletion of *RAD54* in mice causes telomere shortening (137). In light of the overlapping functions of HR and NHEJ, it would be interesting to address telomere length in *rad54* single mutants, and *rad54 lig4* double mutants in *Arabidopsis*.

CONCLUSIONS

The research presented here significantly adds to the knowledge previously gathered from *Arabidopsis* telomere biology and these results illustrate the value of studying telomere biology in many model systems. This small weed's amazing tolerance to genome instability allowed novel functions of previously characterized proteins to be elucidated. Further characterization of Lig4's role in telomere biology may also help us to understand the intriguing relationship between telomeres and DNA damage response proteins.

REFERENCES

1. Blackburn, E. H. (2001) *Cell* **106,** 661-673.

2. Kipling, D. & Cooke, H. J. (1990) *Nature* **347,** 400-402.

3. Shakirov, E. V. & Shippen, D. E. (2004) *Plant Cell* **16,** 1959-1967.

4. Shampay, J. & Blackburn, E. H. (1988) *Proc. Natl. Acad. Sci. USA* **85,** 534-538.

5. Klobutcher, L. A., Swanton, M. T., Donini, P. & Prescott, D. M. (1981) *Proc. Natl. Acad. Sci. USA* **78,** 3015-3019.

6. Makarov, V. L., Hirose, Y. & Langmore, J. P. (1997) *Cell* **88,** 657-666.

7. Riha, K., McKnight, T. D., Fajkus, J., Vyskot, B. & Shippen, D. E. (2000) *Plant J.* **23,** 633-641.

8. van Steensel, B., Smogorzewska, A. & de Lange, T. (1998) *Cell* **92,** 401-413.

9. Cesare, A. J., Quinney, N., Willcox, S., Subramanian, D. & Griffith, J. D. (2003) *Plant J.* **36,** 271-279.

10. Griffith, J. D., Comeau, L., Rosenfield, S., Stansel, R. M., Bianchi, A., Moss, H. & de Lange, T. (1999) *Cell* **97,** 503-514.

11. Munoz-Jordan, J. L., Cross, G. A., de Lange, T. & Griffith, J. D. (2001) *EMBO J.* **20,** 579-588.

12. Murti, K. G. & Prescott, D. M. (1999) *Proc. Natl. Acad. Sci. USA* **96,** 14436-14439.

13. Olovnikov, A. M. (1973) *J. Theor. Biol.* **41,** 181-190.

14. Watson, J. D. (1972) *Nat. New Biol.* **239,** 197-201.

15. Greider, C. W. & Blackburn, E. H. (1985) *Cell* **43,** 405-413.

16. Feng, J., Funk, W. D., Wang, S. S., Weinrich, S. L., Avilion, A. A., Chiu, C. P., Adams, R. R., Chang, E., Allsopp, R. C., Yu, J. & et al. (1995) *Science* **269,** 1236-1241.

17. Blackburn, E. H. (2000) *Keio. J. Med.* **49,** 59-65.

18. O'Reilly, M., Teichmann, S. A. & Rhodes, D. (1999) *Curr. Opin. Struct. Biol.* **9,** 56-65.

19. Armbruster, B. N., Banik, S. S., Guo, C., Smith, A. C. & Counter, C. M. (2001) *Mol. Cell. Biol.* **21,** 7775-7786.

20. Bachand, F. & Autexier, C. (2001) *Mol. Cell. Biol.* **21,** 1888-1897.

21. Bryan, T. M., Goodrich, K. J. & Cech, T. R. (2000) *J. Biol. Chem.* **275,** 24199-24207.

22. Friedman, K. L. & Cech, T. R. (1999) *Genes Dev.* **13,** 2863-2874.

23. Chen, J. L., Blasco, M. A. & Greider, C. W. (2000) *Cell* **100,** 503-514.

24. Collins, K. (2000) *Curr. Opin. Cell Biol.* **12,** 378-383.

25. Collins, K. & Mitchell, J. R. (2002) *Oncogene* **21,** 564-579.

26. Lingner, J., Cech, T. R., Hughes, T. R. & Lundblad, V. (1997) *Proc. Natl. Acad. Sci. USA* **94,** 11190-1195.

27. Evans, S. K. & Lundblad, V. (1999) *Science* **286,** 117-120.

28. Lendvay, T. S., Morris, D. K., Sah, J., Balasubramanian, B. & Lundblad, V. (1996) *Genetics* **144,** 1399-1412.

29. Singer, M. S. & Gottschling, D. E. (1994) *Science* **266,** 404-449.

30. Lundblad, V. & Szostak, J. W. (1989) *Cell* **57,** 633-643.

31. Nugent, C. I. & Lundblad, V. (1998) *Genes Dev.* **12,** 1073-1085.

32. Hughes, T. R., Evans, S. K., Weilbaecher, R. G. & Lundblad, V. (2000) *Curr. Biol.* **10,** 809-812.

33. Zhou, J., Hidaka, K. & Futcher, B. (2000) *Mol. Cell. Biol.* **20,** 1947-1955.

34. Virta-Pearlman, V., Morris, D. K. & Lundblad, V. (1996) *Genes Dev.* **10,** 3094-3104.

35. Qi, H. & Zakian, V. A. (2000) *Genes Dev.* **14,** 1777-1788.

36. Nugent, C. I., Hughes, T. R., Lue, N. F. & Lundblad, V. (1996) *Science* **274,** 249-252.

37. Reichenbach, P., Hoss, M., Azzalin, C. M., Nabholz, M., Bucher, P. & Lingner, J. (2003) *Curr. Biol.* **13,** 568-574.

38. Snow, B. E., Erdmann, N., Cruickshank, J., Goldman, H., Gill, R. M., Robinson, M. O. & Harrington, L. (2003) *Curr. Biol.* **13,** 698-704.

39. Ford, L. P., Wright, W. E. & Shay, J. W. (2002) *Oncogene* **21,** 580-583.

40. Holt, S. E., Aisner, D. L., Baur, J., Tesmer, V. M., Dy, M., Ouellette, M., Trager, J. B., Morin, G. B., Toft, D. O., Shay, J. W., Wright, W. E. & White, M. A. (1999) *Genes Dev.* **13,** 817-826.

41. Harrington, L., McPhail, T., Mar, V., Zhou, W., Oulton, R., Bass, M. B., Arruda, I. & Robinson, M. O. (1997) *Science* **275,** 973-977.

42. Greene, E. C. & Shippen, D. E. (1998) *Genes Dev.***12,** 2921-2931.

43. Karamysheva, Z., Wang, L., Shrode, T., Bednenko, J., Hurley, L. A. & Shippen, D. E. (2003) *Cell* **113,** 565-576.

44. Wright, W. E., Piatyszek, M. A., Rainey, W. E., Byrd, W. & Shay, J. W. (1996) *Dev. Genet.***18,** 173-179.

45. Cong, Y. S., Wright, W. E. & Shay, J. W. (2002) *Microbiol. Mol. Biol.Rev.* **66,** 407-425.

46. Fitzgerald, M. S., McKnight, T. D. & Shippen, D. E. (1996) *Proc. Natl. Acad. Sci. USA* **93,** 14422-14427.

47. Heller, K., Kilian, A., Piatyszek, M. A. & Kleinhofs, A. (1996) *Mol. Gen. Genet.* **252,** 342-345.

48. Riha, K., Fajkus, J., Siroky, J. & Vyskot, B. (1998) *Plant Cell* **10,** 1691-1698.

49. Pardue, M. L. & DeBaryshe, P. G. (1999) *Genetica* **107,** 189-196.

50. Henson, J. D., Neumann, A. A., Yeager, T. R. & Reddel, R. R. (2002) *Oncogene* **21,** 598-610.

51. Chen, Q., Ijpma, A. & Greider, C. W. (2001) *Mol. Cell. Biol.* **21,** 1819-1827.

52. Le, S., Moore, J. K., Haber, J. E. & Greider, C. W. (1999) *Genetics* **152,** 143-152.

53. Lundblad, V. & Blackburn, E. H. (1993) *Cell* **73,** 347-360.

54. Nakamura, T. M., Cooper, J. P. & Cech, T. R. (1998) *Science* **282,** 493-496.

55. Teng, S. C. & Zakian, V. A. (1999) *Mol. Cell. Biol.* **19,** 8083-8093.

56. Lundblad, V. (2002) *Oncogene* **21,** 522-531.

57. Kim, N. W., Piatyszek, M. A., Prowse, K. R., Harley, C. B., West, M. D., Ho, P. L., Coviello, G. M., Wright, W. E., Weinrich, S. L. & Shay, J. W. (1994) *Science* **266,** 2011-2015.

58. Saldanha, S. N., Andrews, L. G. & Tollefsbol, T. O. (2003) *Anal. Biochem*. **315,** 1-21.

59. Askree, S. H., Yehuda, T., Smolikov, S., Gurevich, R., Hawk, J., Coker, C., Krauskopf, A., Kupiec, M. & McEachern, M. J. (2004) *Proc. Natl. Acad. Sci. USA* **101,** 8658-8663.

60. McEachern, M. J., Krauskopf, A. & Blackburn, E. H. (2000) *Annu. Rev. Genet.* **34,** 331-358.

61. Lustig, A. J. (2003) *Nat. Rev. Genet.* **4,** 916-923.

62. Baumann, P., Podell, E. & Cech, T. R. (2002) *Mol. Cell. Biol.* **22,** 8079-8087.

63. Maringele, L. & Lydall, D. (2002) *Genes Dev.* **16,** 1919-1933.

64. Hemann, M. T. & Greider, C. W. (2000) *Nucleic Acids Res.* **28,** 4474-4478.

65. Blasco, M. A., Lee, H. W., Hande, M. P., Samper, E., Lansdorp, P. M., DePinho, R. A. & Greider, C. W. (1997) *Cell* **91,** 25-34.

66. Riha, K., McKnight, T. D., Griffing, L. R. & Shippen, D. E. (2001) *Science* **291,** 1797-1800.

67. Chin, L., Artandi, S. E., Shen, Q., Tam, A., Lee, S. L., Gottlieb, G. J., Greider, C. W. & DePinho, R. A. (1999) *Cell* **97,** 527-538.

68. Fitzgerald, M. S., Riha, K., Gao, F., Ren, S., McKnight, T. D. & Shippen, D. E. (1999) *Proc. Natl.Acad. Sci. USA* **96,** 14813-14818.

69. Greenberg, R. A., Chin, L., Femino, A., Lee, K. H., Gottlieb, G. J., Singer, R. H., Greider, C. W. & DePinho, R. A. (1999) *Cell* **97,** 515-525.

70. Rudolph, K. L., Chang, S., Lee, H. W., Blasco, M., Gottlieb, G. J., Greider, C. & DePinho, R. A. (1999) *Cell* **96,** 701-712.

71. Shore, D. (1994) *Trends Genet.* **10,** 408-412.

72. Evans, S. K. & Lundblad, V. (2000) *J. Cell Sci.* **113,** 3357-3364.

73. Cooper, J. P., Nimmo, E. R., Allshire, R. C. & Cech, T. R. (1997) *Nature* **385,** 744-747.

74. Broccoli, D., Smogorzewska, A., Chong, L. & de Lange, T. (1997) *Nat. Genet.* **17,** 231-235.

75. Marcand, S., Gilson, E. & Shore, D. (1997) *Science* **275,** 986-990.

76. Kyrion, G., Boakye, K. A. & Lustig, A. J. (1992) *Mol. Cell. Biol*. **12,** 5159-5173.

77. Wotton, D. & Shore, D. (1997) *Genes Dev.* **11,** 748-760.

78. Hardy, C. F., Sussel, L. & Shore, D. (1992) *Genes Dev.* **6,** 801-814.

79. Moretti, P., Freeman, K., Coodly, L. & Shore, D. (1994) *Genes Dev.* **8,** 2257-2269.

80. Spink, K. G., Evans, R. J. & Chambers, A. (2000) *Nucleic Acids Res.* **28,** 527-533.

81. Kanoh, J. & Ishikawa, F. (2001) *Curr. Biol.* **11,** 1624-1630.

82. Tomita, K., Matsuura, A., Caspari, T., Carr, A. M., Akamatsu, Y., Iwasaki, H., Mizuno, K., Ohta, K., Uritani, M., Ushimaru, T., Yoshinaga, K. & Ueno, M. (2003) *Mol. Cell. Biol.* **23,** 5186-5197.

83. Miller, K. M. & Cooper, J. P. (2003) *Mol. Cell* **11,** 303-313.

84. Ferreira, M. G. & Cooper, J. P. (2001) *Mol. Cell* **7,** 55-63.

85. Chong, L., van Steensel, B., Broccoli, D., Erdjument-Bromage, H., Hanish, J., Tempst, P. & de Lange, T. (1995) *Science* **270,** 1663-1667.

86. Bilaud, T., Brun, C., Ancelin, K., Koering, C. E., Laroche, T. & Gilson, E. (1997) *Nat. Genet.* **17,** 236-239.

87. van Steensel, B. & de Lange, T. (1997) *Nature* **385,** 740-743.

88. Smith, S., Giriat, I., Schmitt, A. & de Lange, T. (1998) *Science* **282,** 1484-1487.

89. Smogorzewska, A. & de Lange, T. (2004) *Annu. Rev. Biochem.* **73,** 177-208.

90. Kim, S. H., Kaminker, P. & Campisi, J. (1999) *Nat. Genet.* **23,** 405-412.

91. Ye, J. Z., Hockemeyer, D., Krutchinsky, A. N., Loayza, D., Hooper, S. M., Chait, B. T. & de Lange, T. (2004) *Genes Dev.* **18,** 1649-1654.

92. Zhou, X. Z. & Lu, K. P. (2001) *Cell* **107,** 347-359.

93. Lin, J. & Blackburn, E. H. (2004) *Genes Dev.* **18,** 387-396.

94. Smogorzewska, A., van Steensel, B., Bianchi, A., Oelmann, S., Schaefer, M. R., Schnapp, G. & de Lange, T. (2000) *Mol. Cell. Biol.* **20,** 1659-1668.

95. Stansel, R. M., de Lange, T. & Griffith, J. D. (2001) *EMBO J.* **20,** 5532-5540.

96. de Lange, T. (2004) *Nat Rev Mol Cell Biol* **5,** 323-329.

97. Karlseder, J., Broccoli, D., Dai, Y., Hardy, S. & de Lange, T. (1999) *Science* **283,** 1321-1325.

98. Zhu, X. D., Niedernhofer, L., Kuster, B., Mann, M., Hoeijmakers, J. H. & de Lange, T. (2003) *Mol. Cell* **12,** 1489-1498.

99. Smogorzewska, A., Karlseder, J., Holtgreve-Grez, H., Jauch, A. & de Lange, T. (2002) *Curr. Biol*.**12,** 1635-1644.

100. Li, B., Oestreich, S. & de Lange, T. (2000) *Cell* **101,** 471-483.

101. Karamysheva, Z. N., Surovtseva, Y. V., Vespa, L., Shakirov, E. V. & Shippen, D. E. (2004) *J. Biol. Chem.* **279,** 47799-47807.

102. Yang, S. W., Kim, D. H., Lee, J. J., Chun, Y. J., Lee, J. H., Kim, Y. J., Chung, I. K. & Kim, W. T. (2003) *J. Biol. Chem.* **278,** 21395-21407.

103. Yang, S. W., Kim, S. K. & Kim, W. T. (2004) *Plant Cell* **16,** 3370-3385.

104. Wei, C. & Price, M. (2003) *Cell. Mol. Life Sci.* **60,** 2283-2294.

105. Gray, J. T., Celander, D. W., Price, C. M. & Cech, T. R. (1991) *Cell* **67,** 807-814.

106. Hicke, B. J., Celander, D. W., MacDonald, G. H., Price, C. M. & Cech, T. R. (1990) *Proc. Natl. Acad. Sci. USA* **87,** 1481-1485.

107. Prescott, J. D., DuBois, M. L. & Prescott, D. M. (1998) *Chromosoma* **107,** 293-303.

108. Price, C. M. (1990) *Mol. Cell. Biol.* **10,** 3421-3431.

109. Murzin, A. G. (1993) *EMBO J.* **12,** 861-867.

110. Theobald, D. L. & Wuttke, D. S. (2004) *Structure (Camb.)* **12,** 1877-1879.

111. Mitton-Fry, R. M., Anderson, E. M., Theobald, D. L., Glustrom, L. W. & Wuttke, D. S. (2004) *J. Mol. Biol.* **338,** 241-255.

112. Vega, L. R., Mateyak, M. K. & Zakian, V. A. (2003) *Nat. Rev. Mol. Cell. Biol.* **4,** 948-959.

113. Garvik, B., Carson, M. & Hartwell, L. (1995) *Mol. Cell. Biol.* **15,** 6128-6138.

114. Pennock, E., Buckley, K. & Lundblad, V. (2001) *Cell* **104,** 387-396.

115. Grandin, N., Reed, S. I. & Charbonneau, M. (1997) *Genes Dev.* **11,** 512-527.

116. Grandin, N., Damon, C. & Charbonneau, M. (2001) *EMBO J.* **20,** 1173-1183.

117. Adams Martin, A., Dionne, I., Wellinger, R. J. & Holm, C. (2000) *Mol. Cell. Biol.* **20,** 786-796.

118. Baumann, P. & Cech, T. R. (2001) *Science* **292,** 1171-1175.

119. Lei, M., Podell, E. R. & Cech, T. R. (2004) *Nat. Struct. Mol. Biol.* **11,** 1223-1229.

120. d'Adda di Fagagna, F., Teo, S. H. & Jackson, S. P. (2004) *Genes Dev.* **18,** 1781-1799.

121. Dahlen, M., Olsson, T., Kanter-Smoler, G., Ramne, A. & Sunnerhagen, P. (1998) *Mol. Biol. Cell* **9,** 611-621.

122. Greenwell, P. W., Kronmal, S. L., Porter, S. E., Gassenhuber, J., Obermaier, B. & Petes, T. D. (1995) *Cell* **82,** 823-829.

123. Hande, M. P., Balajee, A. S., Tchirkov, A., Wynshaw-Boris, A. & Lansdorp, P. M. (2001) *Hum. Mol. Genet.* **10,** 519-528.

124. Lustig, A. J. & Petes, T. D. (1986) *Proc. Natl. Acad. Sci. USA* **83,** 1398-1402.

125. Matsuura, A., Naito, T. & Ishikawa, F. (1999) *Genetics* **152,** 1501-1512.

126. Metcalfe, J. A., Parkhill, J., Campbell, L., Stacey, M., Biggs, P., Byrd, P. J. & Taylor, A. M. (1996) *Nat. Genet.* **13,** 350-353.

127. Naito, T., Matsuura, A. & Ishikawa, F. (1998) *Nat. Genet.* **20,** 203-206.

128. Robertson, D. M., Li, L., Fisher, S., Pearce, V. P., Shay, J. W., Wright, W. E., Cavanagh, H. D. & Jester, J. V. (2005) *Invest. Ophthalmol. Vis. Sci.* **46,** 470-478.

129. Ritchie, K. B., Mallory, J. C. & Petes, T. D. (1999) *Mol. Cell. Biol.* **19,** 6065-6075.

130. de Klein, A., Muijtjens, M., van Os, R., Verhoeven, Y., Smit, B., Carr, A. M., Lehmann, A. R. & Hoeijmakers, J. H. (2000) *Curr. Biol.* **10,** 479-482.

131. Takata, H., Kanoh, Y., Gunge, N., Shirahige, K. & Matsuura, A. (2004) *Mol. Cell* **14,** 515-522.

132. Qi, L., Strong, M. A., Karim, B. O., Armanios, M., Huso, D. L. & Greider, C. W. (2003) *Cancer Res.* **63,** 8188-8196.

133. Lieber, M. R., Ma, Y., Pannicke, U. & Schwarz, K. (2003) *Nat. Rev. Mol. Cell Biol.* **4,** 712-720.

134. Lieber, M. R., Ma, Y., Pannicke, U. & Schwarz, K. (2004) *DNA Repair (Amst.)* **3,** 817-826.

135. Shin, D. S., Chahwan, C., Huffman, J. L. & Tainer, J. A. (2004) *DNA Repair (Amst.)* **3,** 863-873.

136. Wei, C., Skopp, R., Takata, M., Takeda, S. & Price, C. M. (2002) *Nucleic Acids Res.* **30,** 2862-2870.

137. Jaco, I., Munoz, P., Goytisolo, F., Wesoly, J., Bailey, S., Taccioli, G. & Blasco, M. A. (2003) *Mol. Cell. Biol.* **23,** 5572-5580.

138. Wang, R. C., Smogorzewska, A. & de Lange, T. (2004) *Cell* **119,** 355-368.

139. Baumann, P. & Cech, T. R. (2000) *Mol. Biol. Cell* **11,** 3265-3275.

140. Fellerhoff, B., Eckardt-Schupp, F. & Friedl, A. A. (2000) *Genetics* **154,** 1039-1051.

141. Grandin, N. & Charbonneau, M. (2003) *Mol. Cell. Biol.* **23,** 3721-3734.

142. Gravel, S., Larrivee, M., Labrecque, P. & Wellinger, R. J. (1998) *Science* **280,** 741-744.

143. Laroche, T., Martin, S. G., Gotta, M., Gorham, H. C., Pryde, F. E., Louis, E. J. & Gasser, S. M. (1998) *Curr. Biol.* **8,** 653-656.

144. Polotnianka, R. M., Li, J. & Lustig, A. J. (1998) *Curr. Biol.* **8,** 831-834.

145. Riha, K. & Shippen, D. E. (2003) *Proc. Natl. Acad. Sci. USA* **100,** 611-615.

146. Riha, K., Watson, J. M., Parkey, J. & Shippen, D. E. (2002) *EMBO J.* **21,** 2819-2826.

147. Samper, E., Goytisolo, F. A., Slijepcevic, P., van Buul, P. P. & Blasco, M. A. (2000) *EMBO Rep.* **1,** 244-252.

148. d'Adda di Fagagna, F., Hande, M. P., Tong, W. M., Roth, D., Lansdorp, P. M., Wang, Z. Q. & Jackson, S. P. (2001) *Curr. Biol.* **11,** 1192-1196.

149. Bailey, S. M., Meyne, J., Chen, D. J., Kurimasa, A., Li, G. C., Lehnert, B. E. & Goodwin, E. H. (1999) *Proc. Natl. Acad. Sci. U S A* **96,** 14899-14904.

150. Espejel, S., Martin, M., Klatt, P., Martin-Caballero, J., Flores, J. M. & Blasco, M. A. (2004) *EMBO Rep.* **5,** 503-509.

151. Goytisolo, F. A., Samper, E., Edmonson, S., Taccioli, G. E. & Blasco, M. A. (2001) *Mol. Cell. Biol.* **21,** 3642-3651.

152. Bailey, S. M., Brenneman, M. A., Halbrook, J., Nickoloff, J. A., Ullrich, R. L. & Goodwin, E. H. (2004) *DNA Repair (Amst.)* **3,** 225-233.

153. Teo, S. H. & Jackson, S. P. (1997) *EMBO J.* **16,** 4788-4795.

154. Friesner, J. & Britt, A. B. (2003) *Plant J.* **34,** 427-440.

155. van Attikum, H., Bundock, P., Overmeer, R. M., Lee, L. Y., Gelvin, S. B. & Hooykaas, P. J. (2003) *Nucleic Acids Res*. **31,** 4247-4255.

156. Barnes, D. E., Stamp, G., Rosewell, I., Denzel, A. & Lindahl, T. (1998) *Curr. Biol.* **8,** 1395-1398.

157. Frank, K. M., Sharpless, N. E., Gao, Y., Sekiguchi, J. M., Ferguson, D. O., Zhu, C., Manis, J. P., Horner, J., DePinho, R. A. & Alt, F. W. (2000) *Mol. Cell* **5,** 993-1002.

158. Gao, Y., Sun, Y., Frank, K. M., Dikkes, P., Fujiwara, Y., Seidl, K. J., Sekiguchi, J. M., Rathbun, G. A., Swat, W., Wang, J., Bronson, R. T., Malynn, B. A., Bryans, M., Zhu, C., Chaudhuri, J., Davidson, L., Ferrini, R., Stamato, T., Orkin, S. H., Greenberg, M. E. & Alt, F. W. (1998) *Cell* **95,** 891-902.

159. Zentgraf, U., Hinderhofer, K. & Kolb, D. (2000) *Plant Mol. Biol.* **42,** 429-438.

160. Copenhaver, G. P. & Pikaard, C. S. (1996) *Plant J.* **9,** 259-272.

161. Heacock, M., Spangler, E., Riha, K., Puizina, J. & Shippen, D. E. (2004) *EMBO J.* **23,** 2304-2313.

162. Culligan, K., Tissier, A. & Britt, A. (2004) *Plant Cell* **16,** 1091-1104.

163. Hathcock, K. S., Hemann, M. T., Opperman, K. K., Strong, M. A., Greider, C. W. & Hodes, R. J. (2002) *Proc. Natl. Acad. Sci. USA* **99,** 3591-3596.

164. Lee, H. W., Blasco, M. A., Gottlieb, G. J., Horner, J. W., 2nd, Greider, C. W. & DePinho, R. A. (1998) *Nature* **392,** 569-574.

165. Samper, E., Flores, J. M. & Blasco, M. A. (2001) *EMBO Rep.* **2,** 800-807.

166. Greider, C. W. (1996) *Annu. Rev. Biochem.* **65,** 337-365.

167. Marcand, S., Brevet, V., Mann, C. & Gilson, E. (2000) *Curr. Biol.* **10,** 487-490.

168. Teixeira, M. T., Arneric, M., Sperisen, P. & Lingner, J. (2004) *Cell* **117,** 323-335.

169. Marcand, S., Brevet, V. & Gilson, E. (1999) *EMBO J.* **18,** 3509-3519.

170. Nakamura, T. M., Morin, G. B., Chapman, K. B., Weinrich, S. L., Andrews, W. H., Lingner, J., Harley, C. B. & Cech, T. R. (1997) *Science* **277,** 955-959.

171. Vaziri, H. & Benchimol, S. (1998) *Curr. Biol.* **8,** 279-282.

172. Taggart, A. K., Teng, S. C. & Zakian, V. A. (2002) *Science* **297,** 1023-1026.

173. Bianchi, A., Negrini, S. & Shore, D. (2004) *Mol. Cell* **16,** 139-146.

174. Fisher, T. S., Taggart, A. K. & Zakian, V. A. (2004) *Nat. Struct. Mol. Biol.* **11,** 1198-1205.

175. Hsu, C. L., Chen, Y. S., Tsai, S. Y., Tu, P. J., Wang, M. J. & Lin, J. J. (2004) Nucleic Acids Res. **32,** 511-521

176. Krysan, P. J., Young, J. C. & Sussman, M. R. (1999) *Plant Cell* **11,** 2283-2290.

177. Alonso, J. M. & Stepanova, A. N. (2003) *Meth. Mol. Biol.* **236,** 177-188.

178. Clark, S. E., Jacobsen, S. E., Levin, J. Z. & Meyerowitz, E. M. (1996) *Development* **122,** 1567-1575.

179. Clark, S. E., Running, M. P. & Meyerowitz, E. M. (1993) *Development* **119,** 397-418.

180. Clark, S. E., Williams, R. W. & Meyerowitz, E. M. (1997) *Cell* **89,** 575-585.

181. Chiu, S. Y., Serin, G., Ohara, O. & Maquat, L. E. (2003) *RNA* **9,** 77-87.

182. Dahlseid, J. N., Lew-Smith, J., Lelivelt, M. J., Enomoto, S., Ford, A., Desruisseaux, M., McClellan, M., Lue, N., Culbertson, M. R. & Berman, J. (2003) *Eukaryotic Cell* **2,** 134-142.

183. Enomoto, S., Glowczewski, L., Lew-Smith, J. & Berman, J. G. (2004) *Mol. Cell. Biol.* **24,** 837-845.

184. Clissold, P. M. & Ponting, C. P. (2000) *Curr. Biol.* **10,** 888-890.

185. Espejel, S., Franco, S., Rodriguez-Perales, S., Bouffler, S. D., Cigudosa, J. C. & Blasco, M. A. (2002) *EMBO J.* **21,** 2207-2219.

186. Mieczkowski, P. A., Mieczkowska, J. O., Dominska, M. & Petes, T. D. (2003) *Proc. Natl. Acad. Sci. USA* **100,** 10854-10859.

187. Ma, Y., Pannicke, U., Schwarz, K. & Lieber, M. R. (2002) *Cell* **108,** 781-794.

188. Chan, S. W. & Blackburn, E. H. (2003) *Mol. Cell* **11,** 1379-1387.

189. Liti, G. & Louis, E. J. (2003) *Mol. Cell* **11,** 1373-1378.

190. Gravel, S. & Wellinger, R. J. (2002) *Mol. Cell. Biol*. **22,** 2182-2193.

191. Bundock, P. & Hooykaas, P. (2002) *Plant Cell* **14,** 2451-2462.

192. Puizina, J., Siroky, J., Mokros, P., Schweizer, D. & Riha, K. (2004) *Plant Cell* **16,** 1968-1678.

193. Frank, K. M., Sekiguchi, J. M., Seidl, K. J., Swat, W., Rathbun, G. A., Cheng, H. L., Davidson, L., Kangaloo, L. & Alt, F. W. (1998) *Nature* **396,** 173-177.

194. Lees-Miller, S. P. & Meek, K. (2003) *Biochimie* **85,** 1161-1173.

195. Bundock, P., den Dulk-Ras, A., Beijersbergen, A. & Hooykaas, P. J. (1995) *EMBO J.* **14,** 3206-3214.

196. Bundock, P. & Hooykaas, P. J. (1996) *Proc. Natl. Acad. Sci. USA* **93,** 15272-15275.

197. Gheysen, G., Villarroel, R. & Van Montagu, M. (1991) *Genes Dev.* **5,** 287-297.

198. Matsumoto, S., Ito, Y., Hosoi, T., Takahashi, Y. & Machida, Y. (1990) *Mol. Gen. Genet.* **224,** 309-316.

199. Mayerhofer, R., Koncz-Kalman, Z., Nawrath, C., Bakkeren, G., Crameri, A., Angelis, K., Redei, G. P., Schell, J., Hohn, B. & Koncz, C. (1991) *EMBO J.* **10,** 697-704.

200. van Attikum, H., Bundock, P. & Hooykaas, P. J. (2001) *EMBO J.* **20,** 6550-6558.

201. Babiychuk, E., Fuangthong, M., Van Montagu, M., Inze, D. & Kushnir, S. (1997) *Proc. Natl. Acad. Sci. USA* **94,** 12722-12727.

202. Wu, Y. Q., Hohn, B. & Ziemienowic, A. (2001) *Plant Mol. Biol.* **46,** 161-170.

203. Peterson, S. E., Stellwagen, A. E., Diede, S. J., Singer, M. S., Haimberger, Z. W., Johnson, C. O., Tzoneva, M. & Gottschling, D. E. (2001) *Nat. Genet.* **27,** 64-67.

204. Stellwagen, A. E., Haimberger, Z. W., Veatch, J. R. & Gottschling, D. E. (2003) *Genes Dev.* **17,** 2384-2395.

205. Chai, W., Ford, L. P., Lenertz, L., Wright, W. E. & Shay, J. W. (2002) *J. Biol. Chem*. **277,** 47242-47247.

206. Bertuch, A. A. & Lundblad, V. (2004) *Genetics* **166,** 1651-1659.

207. Hsu, H. L., Gilley, D., Blackburn, E. H. & Chen, D. J. (1999) *Proc. Natl. Acad. Sci. USA* **96,** 12454-12458.

208. Nakamura, T. M., Moser, B. A. & Russell, P. (2002) *Genetics* **161,** 1437-1452.

209. Downs, J. A. & Jackson, S. P. (2004) *Nat. Rev. Mol. Cell Biol.* **5,** 367-378.

210. Blackburn, E. H. & Gall, J. G. (1978) *J. Mol. Biol.* **120,** 33-53.

211. Szostak, J. W. & Blackburn, E. H. (1982) *Cell* **29,** 245-255.

212. Cocciolone, S. M. & Cone, K. C. (1993) *Genetics* **135,** 575-588.

213. McKnight, T. D. & Shippen, D. E. (2004) *Plant Cell* **16,** 794-803.

214. Kilian, A., Stiff, C. & Kleinhofs, A. (1995) *Proc. Natl. Acad. Sci. USA* **92,** 9555-9559.

215. Heller-Uszynska, K., Schnippenkoetter, W. & Kilian, A. (2002) *Plant J.* **31,** 75-86.

216. Oguchi, K., Tamura, K. & Takahashi, H. (2004) *Gene* **342,** 57-66.

217. Gadjieva, R., Axelsson, E., Olsson, U., Vallon-Christersson, J. & Hansson, M. (2004) *Plant. Physiol. Biochem.* **42,** 681-685.

218. Isshiki, M., Yamamoto, Y., Satoh, H. & Shimamoto, K. (2001) *Plant Physiol*. **125,** 1388-1395.

219. Smith, J., Riballo, E., Kysela, B., Baldeyron, C., Manolis, K., Masson, C., Lieber, M. R., Papadopoulo, D. & Jeggo, P. (2003) *Nucleic Acids Res*. **31,** 2157-2167.

220. Kabotyanski, E. B., Gomelsky, L., Han, J. O., Stamato, T. D. & Roth, D. B. (1998) *Nucleic Acids Res.* **26,** 5333-5342.

221. Baumann, P. & West, S. C. (1998) *Proc. Natl. Acad. Sci. USA* **95,** 14066-14070.

222. Couedel, C., Mills, K. D., Barchi, M., Shen, L., Olshen, A., Johnson, R. D., Nussenzweig, A., Essers, J., Kanaar, R., Li, G. C., Alt, F. W. & Jasin, M. (2004) *Genes Dev.* **18,** 1293-1304.

223. Gorski, M. M., Eeken, J. C., de Jong, A. W., Klink, I., Loos, M., Romeijn, R. J., van Veen, B. L., Mullenders, L. H., Ferro, W. & Pastink, A. (2003) *Genetics* **165,** 1929-1941.

224. Richardson, C. & Jasin, M. (2000) *Mol. Cell. Biol.* **20,** 9068-9075.

225. Takata, M., Sasaki, M. S., Sonoda, E., Morrison, C., Hashimoto, M., Utsumi, H., Yamaguchi-Iwai, Y., Shinohara, A. & Takeda, S. (1998) *EMBO J.* **17,** 5497-5508.

226. Dronkert, M. L., Beverloo, H. B., Johnson, R. D., Hoeijmakers, J. H., Jasin, M. & Kanaar, R. (2000) *Mol. Cell. Biol.* **20,** 3147-3156.

227. Mills, K. D., Ferguson, D. O., Essers, J., Eckersdorff, M., Kanaar, R. & Alt, F. W. (2004) *Genes Dev.* **18,** 1283-1292.

VITA

Rachel A. Idol
1815 320th Street
Hiawatha, KS, 66434

Education
Kansas State University, Manhattan, Kansas
1998, B.S. Biochemistry

Texas A&M University, College Station, Texas
2005, Ph.D. Biochemistry

Professional Experience
1995-1998 Undergraduate research assistant, Kansas State University, in the laboratory of Gerald R. Reeck, Department of Biochemistry
1998-1999 Technician I, Kansas State University, in the laboratory of Gerald R. Reeck, Department of Biochemistry
1999-2005 Graduate student, Texas A&M University, in the laboratory of Dorothy E. Shippen

Professional Activities and Honors
2000 TAMU Biochemistry Graduate Association Travel Grant
2001 Organized and hosted "The Ethel Tsutsui Memorial Lecture", TAMU Biochemistry Graduate Student Association Sponsored Speakers
2002 TAMU Biochemistry Graduate Association Travel Grant
2004 TAMU Biochemistry Graduate Association Travel Grant
2004 AACR Scholar-in-Training Award, The Ellison Medical Foundation
2004 Outstanding Presentation, AACR "Role of Telomeres and Telomerase in Cancer"

Conferences
2001 "Telomeres and Telomerase" Cold Spring Harbor
2003 "Telomeres and Telomerase" Cold Spring Harbor:
Poster presentation: "Identification and Analysis of Two Putative Est1 Homologues from *Arabidopsis thaliana*."
2004 AACR "Role of Telomeres and Telomerase in Cancer", San Francisco
Oral presentation: "A novel role for DNA Ligase IV in Telomere Maintenance and End Protection in *Arabidopsis thaliana*."